Mechanisms of invasion and metastasis in colorectal cancer

Xabier García de Albéniz

Mechanisms of invasion and metastasis in colorectal cancer

Xabier García de Albéniz

Institut Clínic de Malalties Hematològiques i Oncològiques. Oncología Médica.
Institut de Recerca Biomédica de Barcelona.

Universitat de Barcelona

Tesi presentada per optar al grau de

Doctor en Medicina

Abril 2015

Tesi dirigida per el Dr. Roger Gomis i el Dr. Antoni Castells

Abstract

The metastatic pattern of advanced CRC is somehow homogeneous. Liver is the most frequently affected organ, followed by the lung, peritoneum and bone. We studied the mechanisms driving the metastatic spread in CRC, focusing in the MAPK pathway. We developed *in vivo* a highly metastatic cell line using a KRAS-mutated cell line (SW620) in an ortothopic xenograft mouse model and used both *in vivo* and *in vitro* experiments to evaluate the mechanisms of metastasis. We also used data from two large prospective cohorts of incident CRC to evaluate the association of an intronic variant of *SMAD7* (rs4939827, 18q21) with the phenotype and molecular characterisitics of CRC. This variant is associated with a lower risk of developing CRC (odds ratio of 0.88, 95% confidence interval [CI] 0.85 - 0.93) and a poorer survival after diagnosis (hazards ratio of 1.16, 95% CI 1.06-1.27).

In the first project, where we evaluated the mechanisms of metastasis, we introduced in the SW620 cell line an expression vector for luciferase, which allowed us to monitor the kinetics of emergence of liver metastatic lesions by quantitative bioluminescence imaging. The SW620 luciferase-expressing cells were inoculated into portal circulation of immunodeficient mice via intrasplenic injection followed by splenectomy, in order to isolate cell populations that target the liver. Second, the SW620-derived liver metastases were expanded in culture and the resulting population (Liver Metastatic derivative, LiM1) was subjected to a second round of in vivo selection, producing the LiM2 cell population that showed a significant increase in liver and lung metastatic activity. Comparative transcriptomic analysis identified 194 genes differentially expressed between the parental and the highly metastatic cell line. This colon cancer metastatic gene set was contrasted against a cohort of 267 patients with stage I-III CRC and we investigated

the signaling pathways regulating the expression of a set of genes with increased metastatic capacity. We found pathways of nitrogen metabolism, cell adhesion molecules and mitogen-activated protein kinases (MAPKs). We focused on the MAPKs given the *KRAS*-mutated status of our cell line (and because patients harboring certain mutations in KRAS/BRAF have fewer therapeutic options that patients without them), finding that the activating phosphorylation of ERK1/ERK2 was increased, the p38 MAPKs was reduced and the phosphorylation of JNKs did not change. Downregulation of ERK2 (but not of ERK1) in the highly metastatic cell line reverted its metastatic capacity to the liver, but not to the lung in our mice model. We thus hypothesized that the ability to metastasize the lung by the highly metastatic derivative had to be driven by other mechanism.

The analysis of clinical samples evidenced that tumor biopsies with low phospho-38 MAPK were associated with metastasis to the lung but not to other organs. Treating mice harboring liver metastasis from the parental cell line with a p38 MAPK specific inhibitor produced an increase in the percentage of mice with lung metastasis. We validated this finding with a different cell line and different experimental setting. Conversely, activation of the p38 MAPK pathway by expression of $MKK6^{EE}$ (MKK6 is a MAP kinase-kinase that phosphorylates and activates p38 MAP kinase) diminished the lung metastatic capacity of the HCT116 cell line.

The expression of parathyroid hormone-like hormone (*PTHLH*) was upregulated (3.3 fold) in our highly metastatic derivative and was inversely correlated with the expression of *MKK6* in CRC primary tumors. Downregulation of *PHTLH* in the highly metastatic derivative decreased its capacity to colonize the lung without decreasing its capacity to colonize the liver after intra portal inoculation. Interestingly, tail vein (draining directly to the lungs) injections of the highly metastatic derivative did not yield any lung metastasis and silencing *PHTLH* in LiM2 cells did not affect its growth when injected directly into the lung. This suggested that the role of PTHLH in regulating lung metastasis did not depended on growth promotion but more probably on extravasation. This was supported by an experiment

where we injected in the tail vein LiM2 cells overexpressing or not PTHLH: mice injected with LiM2 cells overexpressing PTHLH presented a five-fold increase in the number of cells extravasated in the lungs. We finally evidenced that PTHLH induced apoptosis of human pulmonary endothelial cells (HPEC) by increasing Ca^{+} levels that in turn induces mobilization of the apoptosis-inducing factor mitochondrion-associated 1 (AIFM1), from the mitochondria to the cytosol, a caspase-independent cell death mechanism. This disrupts the lung vasculature increasing the permeability of the lung to metastatic cells.

In the second project, where we evaluate the association of the SMAD7 intronic variant with tumor phenotype and several CRC molecular characteristics, we used 1509 CRC cases and 2307 age-matched controls nested within the Nurses Health Study (NHS) and the Health Professionals Follow-up Study (HPFS). NHS and HPFS are cohorts of healthy individuals that record information biennially, with a follow-up greater than 90%. Samples for DNA extraction (blood or buccal cell specimens) from both cohorts were obtained in more than 90,000 individuals. Information on CRC is extracted from medical records from participants who reported CRC in the biennial questionnaires. We randomly selected between one and three controls (matched on ethnicity, year of birth and month/year of sampling) within the same cohort from participants who were free of CRC at the same time the CRC was diagnosed in the cases.

Among the 1509 cases with blood or buccal samples in this study, we were able to successfully obtain tissue suitable for molecular analyses in 658 cases. We genotyped rs4939827 (TaqMan®) successfully in 98% of the samples in NHS and 99.6% of the samples in HPFS. The phenotipic features evaluated were: TNM stage, grade of differentiation, location of the primary tumor (colon *vs.* rectum) and age at diagnosis. The evaluated molecular characteristics were DNA methylation of *RUNX3* and *LINE-1* (long interspersed nucleotide element-1), CpG island methylator phenotype (CIMP), microsatellite instability, TP53 expression by immunohistochemistry and the mutational status of BRAF, KRAS and PIK3CA.

We modeled each SNP using a log-additive approach, relating genotype dose (i.e. number of copies of the minor allele) to risk of CRC. We adjusted all analyses for age at sample collection, race, gender, aspirin use, non-steroidal anti-inflammatory drugs use, body mass index, physical activity, familial history of CRC, smoking, alcohol, meat consumption, energy-adjusted calcium and folate intake and type of sample (blood versus cheek). To assess heterogeneity in the association between rs4939827 and tumors according to clinical phenotype or molecular characteristics, we used a case-case design using logistic regression model comparing tumor subtypes.

We found that the minor allele (G) in rs4939827 was associated with a lower risk of developing tumor stage pT1 or pT2 CRC [multivariate odds ratio (OR), 0.73; 95% confidence interval (CI) 0.62-0.87] but not tumor stage pT3 or pT4 (multivariate OR, 1.07; 95% CI 0.93-1.23, P for heterogeneity = 1.2 x 10^{-4}). The association between rs4939827 and CRC also significantly differed by methylation of RUNX3 (P for heterogeneity = 0.005). Among those with CRC, the minor allele (G) in rs4939827 was significantly associated with poorer overall survival (hazards ratio, 1.20; 95% CI, 1.02-1.42).

We performed mediation analyses to decompose the total effect of the exposure (rs4939827) on the outcome (T3-T4 tumors) into a "direct effect" plus an "indirect effect" The "direct effect" can be interpreted as the OR comparing the risk of T3-T4 tumor stage with the genetic variant present *vs.* absent if the mediator (*e.g.* RUNX3) were what it would have been without the genetic variant. The "indirect effect" can be interpreted as the OR for T3-T4 tumor stage for those with the genetic variant present comparing the risk if the mediator were what it would have been with versus without the genetic variant.

The multivariate ORs that estimate the direct effect of rs4939827 were 1.96 (95% CI 1.18-3.25, P-value = 0.009) for one variant allele and 4.46 (95% CI 1.19-16.6, P-value = 0.038) for two variant alleles. The multivariate ORs estimating the indirect effect of rs4939827 on risk of pT3 and pT4 tumors was 1.05 (95% CI 0.96-1.15, P = 0.32) for one variant allele and 1.50 (95% CI 0.44-5.10, P = 0.51) for two variant alleles. We did not found evidence

of neither multiplicative nor additive interaction between rs4939827 and *RUNX3* methylation.

In conclusion, we provide clinical and molecular evidence showing that ERK2 activation provides colon cancer cells with the ability to seed and colonize the liver and reduced p38 MAPK signalling endows cancer cells with the ability to form lung metastasis from previously established liver lesions. Downregulation of p38 MAPK signalling results in increased expression of the cytokine PTHLH, which contributes to colon cancer cell extravasation to the lung by inducing caspase-independent death in endothelial cells of the lung microvasculature. We also show that patients with the rs4939827 CRC-susceptibility locus diagnosed with CRC tend to develop tumors with greater invasiveness (as measured by the pT stage). The variant rs4939827 is differentially associated with RUNX3 methylation status, supporting an effect of rs4939827 or causal variants tagged by this SNP on carcinogenesis mediated through the TGFβ pathway. Taken together, these results could explain, at least in part, the lower risk of CRC associated with the G allele of rs4939827 yet poorer survival.

Resumen

El patrón de metástasis de cáncer de colon y recto (CCR) avanzado es relativamente homogéneo. El hígado es el órgano más frecuentemente afectado, seguido del pulmón, el peritoneo y huesos. Parte de esta investigación consiste en explorar los mecanismos involucrados en el patrón metastático de CCR, focalizándonos en la vía biológica de MAPK. Para ello usamos una línea celular (SW620) con el gen *KRAS* mutado como punto de partida para crear un derivado con alta capacidad metastática mediante un modelo animal basado en la inyección de células tumorales en la circulación portal de ratones inmunodeprimidos. Además realizamos experimentos tanto *in vivo* como *in vitro* para desarrollar los hallazgos. Asimismo usamos datos procedentes de dos cohortes en las que se identificaron CCR incidentes, en los que se evaluó la asociación entre el polimorfismo intrónico de *SMAD7* (rs4939827, 18q21) con el genotipo y características tumorales. Este polimorfismo está asociado con un menor riesgo de desarrollar CCR (*odds ratio* 0.88, 95% confidence interval [CI] 0.85 - 0.93) y con peor pronóstico entre aquellos pacientes diagnosticados con CCR (*hazards ratio* of 1.16, 95% CI 1.06-1.27).

En el primer proyecto, donde evaluamos los mecanismos de metástasis, introdujimos en la línea celular SW620 un vector de expresión de luciferasa, lo cual permite monitorizar y cuantificar la emergencia de lesiones metastáticas *in vivo* mediante bioluminiscencia. Estas células marcadas son inoculadas en la circulación portal de los ratones inmunodeficientes mediante su inyección en el bazo, tras lo cual los esplenectomizamos. Cuando el ratón reproduce metástasis hepáticas, se recuperan éstas y se aíslan las células metastáticas (que las denominamos LiM1), sometiéndolas a otro ciclo idéntico de enriquecimiento de su capacidad metastática mediante una nueva inyección intraesplénica. Las células enriquecidas a partir de las metástasis resultantes (LiM2) muestran una alta capacidad metastática a hígado y a pulmón.

Mediante análisis de expresión de genes usando chips de transcripción identificamos 194 genes diferencialmente expresados entre las líneas parentales

(SW620) y las células altamente metastáticas (LiM2). Esta "firma" genética se contrastó con una cohorte clínica de 267 pacientes con CCR estadios I-III y asimismo investigamos las vías biológicas que podrían estar regulando el conjunto de genes que identificamos como asociados a mayor capacidad metastática. Encontramos que las siguientes vías biológicas estaban involucradas: metabolismo del nitrógeno, moléculas de adhesión celular y *mitogen-activated protein kinases (MAPKs)*. Decidimos centrarnos en la vía de MAPKs ya que las células con las que trabajamos tenían el gen *KRAS* mutado y además porque los pacientes que sufren un cancer de colon avanzado con *KRAS* mutado tienen menos opciones terapéuticas. Encontramos que la fosforilación de ERK1/ERK2 estaba aumentada, que las MAPKs p38 estaban disminuidas y que la fosforilación de JNKs no había cambiado. Evidenciamos además que, en nuestro modelo animal, el silenciamiento de ERK2 (pero no de ERK1) en la línea celular altamente metastática revierte su capacidad metastática al hígado, pero no al pulmón. Esto nos llevó a hipotetizar que la capacidad de metastatizar en el pulmón de la línea celular altamente metastática debía de estar mediado por algún otro mecanismo.

El análisis de muestras clínicas mostró que aquellos pacientes cuyo tumor presentaba bajos niveles de p38 sufrían una mayor frecuencia de metástasis al pulmón, pero no a otros órganos. Al tratar ratones que habían desarrollado metástasis hepáticas derivadas de la línea celular parental con un inhibidor específico de p38, vimos que se incrementaba la afinidad metastática al pulmón. Este hallazgo lo validamos con una línea celular diferente (HCT116) en un modelo animal también diferente. También evidenciamos que si activábamos la vía de p38 mediante la inducción de MKK6^{EE} (MKK6 es una *MAP kinase-kinase* que fosforila y activa la kinasa p38), la capacidad de metastatizar al pulmón de la línea celular HCT116 disminuía.

La expresión de *PTHLH* (*parathyroid hormone-like hormone*) presentaba un aumento relativo de 3,3 veces en la línea celular altamente metastática comparada con la línea parental. Asimismo, *PTHLH* se correlacionaba inversamente con la expresión de *MKK6* en tumores primarios de colon. Evidenciamos que el silenciamiento de *PTHLH* en el derivado celular altamente

metastático disminuía su capacidad de colonizar el pulmón, sin afectar su capacidad de colonizar el hígado tras su inyección en el sistema portal. La inyección el la vena de la cola del ratón (que drena directamente al pulmón) del derivado celular altamente metastático no producía metástasis pulmonares y el silenciamiento de *PTHLH* en estas células no afectaba su crecimiento si se inyectaban directamente en el pulmón. Esto nos llevó a pensar que el papel de *PTHLH* en la regulación de las metástasis hepáticas no era a través de un incremento de la proliferación, sino a través de un incremento en la capacidad de extravasarse. Para confirmar esto inyectamos células LiM2 que sobreexpresaban o no PTHLH en la cola de los ratones (drenando directamente al pulmón): encontramos que aquellos ratones a los que se les inyectaron células LiM2 que sobreexpresaban PTHLH presentaban cinco veces más células extravasadas que los ratones a los que se les inyectaron células LiM2 sin sobreexpresión de PTHLH. Finalmente pudimos demostrar que PTHLH induce la apoptosis de células humanas de endotelio pulmonar incrementando los niveles de calcio intracelulares, lo que causa la movilización del factor AIFM1(*apoptosis-inducing factor mitochondrion-associated 1*) de la mitocondria al citoplasma, induciendo la apoptosis celular mediante un mecanismo independiente de caspasas. Esto desestructura la vasculatura pulmonar, facilitando que las células metastáticas puedan extravasarse al pulmón.

En el segundo proyecto evaluamos la asociación de un polimorfismo intrónico del gen *SMAD7* con el fenotipo y varias características moleculares del tumor. Para ello empleamos 1509 casos de cáncer de colon y recto y 2307 controles emparejados anidados en las cohortes *Nurses Health Study* (NHS) y *Health Professionals Follow-up Study* (HPFS). NHS y HPFS son cohortes de individuos sanos cuando fueron reclutados y que han facilitado información sobre su salud y sus hábitos de vida cada dos aos, siendo el seguimiento superior al 90%. Las muestras para la extracción del DNA (sangre o frotis de mejilla) se obtuvieron en más de 90.000 individuos. En los casos, la información sobre el diagnóstico del tumor se extrajo de las historias médicas. Seleccionamos 1-3 controles emparejados en raza, ao de nacimiento y fecha

de muestreo por cada control, dentro de la cohorte de pacientes sin CCR cuando el caso fue diagnosticado.

De entre los 1509 casos con muestra de DNA, pudimos obtener tejido tumoral apropiado para realizar su análisis molecular en 658 casos. El genotipo del polimorfismo rs4939827 (TaqMan®) se realizó correctamente en el 98% de las muestras de la cohorte NHS y en el 99.6% de las muestras de la cohorte HPFS. Los rasgos fenotípicos que evaluamos fueron: el estadio TNM, grado de diferenciación, localización del tumor primario (colon *vs.* recto) y edad al diagnóstico. Las características moleculares que analizamos fueron la metilación de *RUNX3* y *LINE-1* (long interspersed nucleotide element-1), la metilación de las islas de CpG (CIMP), inestabilidad de microsatélites, la expresión por inmunohistoquímica de TP53 y el estado mutaciones de *BRAF*, *KRAS* y *PIK3CA*.

Para el análisis estadístico modelamos el polimorfismo usando un modelo log-aditivo que relacionaba la "dosis" de genotipo (*el número de copias del alelo de menor frecuencia* con el riesgo de CCR. Ajustamos los análisis por la edad en el momento de recogida de la muestra, raza, sexo, uso de aspirina, uso de antiinflamatorios no esteroideos, índice de masa corporal, actividad física, historia familiar de CCR, tabaquismo, alcohol, consumo de carne, consumo de calcio y folato y tipo de muestra para la obtención de DNA (sangre o frotis de mejilla). Para evaluar la heterogeneidad en la asociación entre el polimorfismo de rs4939827 y los tumores de acuerdo al fenotipo clínico o características moleculares, usamos un diseo "caso-caso" comparando los diferentes subgrupos tumorales usando regresión logística.

Encontramos que el alelo de menor frecuencia de rs4939827 (G) se asociaba con un menor riesgo de desarrollar un CCR con un estadio pT1 o pT2 [razón de *odds* (OR) ajustada, 0.73; intervalo de confianza al 95% (CI) 0.62-0.87] pero no con tumores con estadio pT3 o pT4 (OR ajustada, 1.07; 95% CI 0.93-1.23, valor p de heterogeneidad = 1.2 x 10^{-4}). La asociación entre el polimorfismo de rs4939827 y CCR también difería significativamente según la metilación de RUNX3 (valor p de heterogeneidad = 0.005). Entre aquellos pacientes diagnosticados con CCR, el alelo de menor frecuencia

de rs4939827 (G) estaba significativamente asociado con pero supervivencia (*hazards ratio*, 1.20; 95% CI, 1.02-1.42).

Realizamos además un análisis de mediación para descomponer el efecto total de la exposición de interés (rs4939827) en la variable dependiente (tumores pT3-pT4) en un efecto directo más un efecto indirecto. El efecto directo se puede interpretar como la razón de *odds* que compara el riesgo de presentar un tumor pT3-pT4 estando el polimorfismo de rs4939827 presente *vs.* ausente si el valor del mediador (RUNX3) fuera aquel que corresponde a la ausencia del polimorfismo de rs4939827. El efecto indirecto se puede interpretar como la razón de odds de presentar un tumor pT3-pT4 para aquellos pacientes con la presencia del polimorfismo de rs4939827 comparada con el riesgo si el mediador fuera el que corresponde a tener o no dicho polimorfismo.

La razón de *odds* ajustada que estima el efecto directo de rs4939827 fue 1.96 (95% CI 1.18-3.25, valor p = 0.009) para la presencia de un alelo y de 4.46 (95% CI 1.19-16.6, valor p = 0.038) para la presencia de dos alelos. La razón de *odds* ajustada que estima el efecto indirecto de rs4939827 en el riesgo de tumores pT3-pT4 fue 1.05 (95% CI 0.96-1.15, P = 0.32) para la presencia de un alelo y 1.50 (95% CI 0.44-5.10, P = 0.51) para la presencia de dos alelos. No encontramos evidencia de interacción en la escala multiplicativa o aditiva entre rs4939827 y la metilación de *RUNX3*.

Como conclusión, en el presente trabajo hemos hallado evidencia que muestra que la activación de ERK2 hace que las células de cáncer de colon tengan la habilidad de colonizar el hígado y que una disminución de los niveles de p38 hace que las células tumorales puedan generar metástasis pulmonares a partir de metástasis hepáticas previamente establecidas. Esta disminución de p38 hace que aumente la expresión de la citoquina PTHLH, lo cual contribuye a facilitar la extravasación al pulmón mediante la inducción de muerte celular de las células endoteliales de la microvasculatura pulmonar. También hemos encontrado evidencia de que los pacientes con el polimorfismo rs4939827 (el cual se asocia a mayor incidencia de CCR) tienen mayor riesgo de desarrollar tumores más invasivos (con mayor estadio pT).

Este polimorfismo está asimismo asociado diferencialmente con el estado de metilación de *RUNX3*, lo cual apoyaría que el efecto de rs4939827 (o de polimorfismos causales surrogados por éste) puede estar mediado por la vía molecular de TGFβ. Estos hallazgos pueden ayudar a explicar por qué el alelo de menor frecuencia de rs4939827 se asocia con menor riesgo de desarrollar CCR en individuos sanos, y con peor supervivencia en los pacientes diagnosticados de CCR.

A mis seres queridos.

Acknowledgements

Agradezco sinceramente a Jelena, Marc, Esther, Anna, María, Mili, David, Evarist, Herbert y Hongmei su ayuda. A Roger, Toni y Andy, su tutela.

He podido realizar este trabajo gracias a un *Ajut Josep Font* otorgado por el Hospital Clinic y a una Beca para estudios de postgrado otorgada por La Caixa.

Contents

List of Figures

LIST OF FIGURES

List of Tables

AIFM1: Apoptosis-inducing factor mitochondrion-associated 1.

APC: Adenomatous polyposis coli.

CI: Confidence interval.

CCM: Colon cancer metastatic gene set.

CCR: Cáncer de colon y recto.

CIMP: CpG island methylator phenotype.

CRC: Colorectal cancer.

DMA: Deoxyribonucleic acid.

EGFR: Epidermal growth factor receptor.

EMT: Epithelial to mesenquimal transition.

ERK: Extracellular signal-regulated kinases.

FAP: Familial adenomatous polyposis.

GWAS: Genome-wide association study.

HIF: Hypoxia-inducible factor.

HNPCC: Hereditary non-polyposis colorectal cancer.

HPEC: Human pulmonary endothelial cells.

HPFS: Health professionals follow-up study.

HR: Hazard ratio.

JNK: c-Jun N-terminal kinases.

KEGG: Kyoto Encyclopedia of Genes and Genomes.

MAPK: Mitogen-activated protein kinases.

MET: Mesenchymal to epithelial transition.

MMR: Mismatch repair.

MSC: Metastatic stem cell.

MSI: Microsatellite instability.

MUTYH: mutY homolog gene.

NHS: Nurses health study.

OR: Odds ratio.

OS: Overall survival.

PTHLH: Parathyroid hormone-like hormone.

PI3K-Act: phosphatidylinositol 3-kinases/Akt.

RUNX3: Runt domain transcription factor 3.

SMAD: A family of proteins that are involved in the translocation of signals from TGFβ receptors, bone morphogenetic protein receptors and other surface receptors to the cell nucleus.

SNP: Single nucleotide polymorfism.

TCF4: Transcription factor 4.

TGFβ: Transforming growth factor β.

TNC: Tenascin C .

VEGF: vascular endothelial growth factor.

1

Introduction

1.1 Epidemiology of colorectal cancer

1.1.1 Incidence and mortality

Worldwide, colorectal cancer (CRC) is the second most common cancer in women and the third most common in men, with 614,000 and 746,000 cases in 2012 respectively. Geographical variation in incidence across the world is notorious: Australia/New Zealand harbor the highest estimated incidences (44.8 and 32.2 cases per 100,000 in men and women respectively) and Western Africa has the lowest estimated incidences (4.5 and 3.8 per 100,000). Figure 1.1 represents the global incidence age-standardized rates for men and women respectively. CRC accounts approximately for 8.5% (694,000 deaths in 2012) of the cancer mortality worldwide (1).

In Spain, the incidence of CRC is similar as it is worldwide, with 19,261 cases in men (44 cases per 100,000) and 12,979 cases in women (24.2 cases per 100,000) in 2012 (1). CRC is the second cause of cancer mortality in men (first is lung cancer: 27.4% of cancer deaths) with 8,742 deaths (13.7 % of cancer deaths) in 2012. In women, CRC is also the second cause of cancer mortality (first is breast cancer: 15.5% of cancer deaths) with 5,958 deaths (15.2 % of cancer deaths) in 2012 (1). Figure 1.2 represents incidence and mortality age-standardized rates by sex of the 10 most frequent cancers.

1.1.2 Genetic susceptibility

Inherited susceptibility accounts for about 30% of all cases of CRC (2). The majority of the CRC are sporadic (as opposed to familial).

1. INTRODUCTION

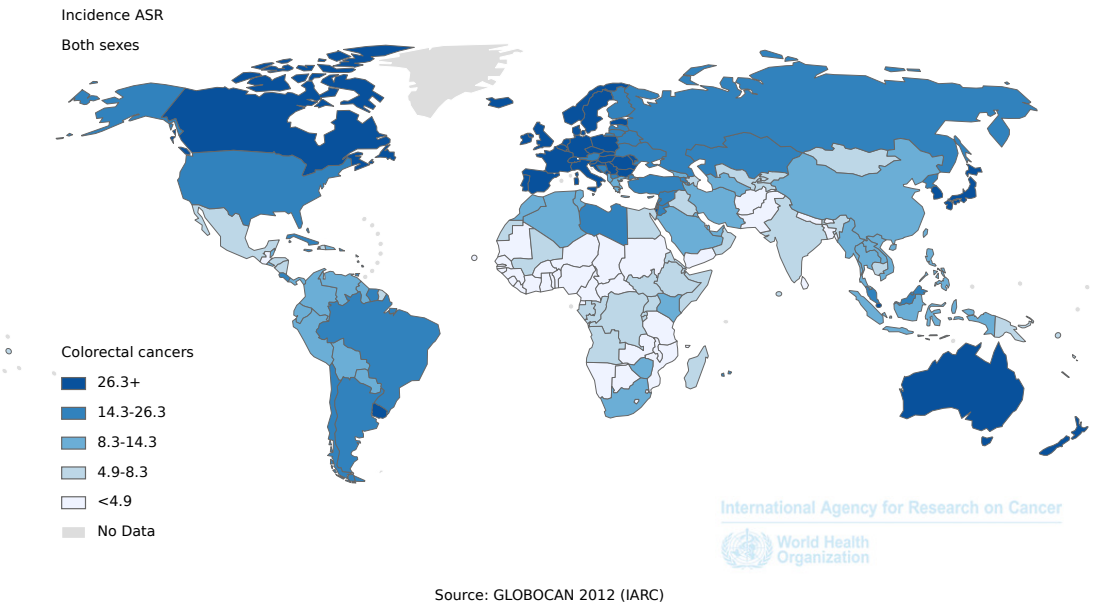

Figure 1.1: Global age-standardized colorectal cancer incidence rates - Source: GLOBOCAN

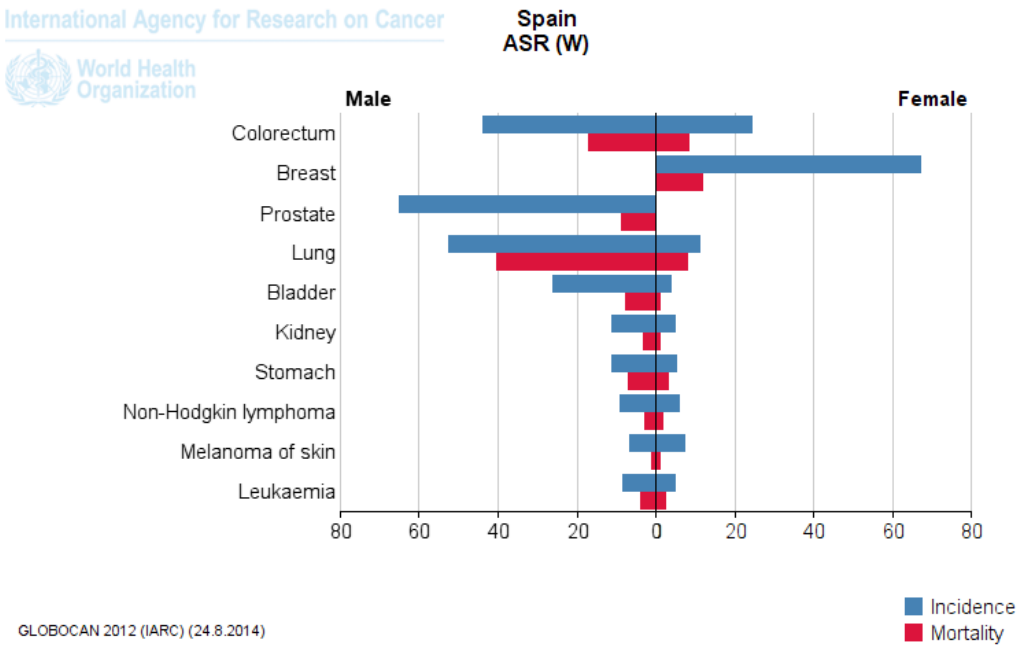

Figure 1.2: Incidence and mortality age-standardized rates by sex for the 10 most frequent cancers in Spain - Source: GLOBOCAN

1.1.2.1 Genetic susceptibility due to common variants

Genome-wide association studies (GWAS) have allowed the study of common single nucleotide polymorfisms (SNP –A SNP is a DNA variant that represents a variation in a single base– (3)) and CRC.

The main role of GWAS in CRC has been shedding light into the biology of the disease rather than providing practical risk stratification of the overall population (as opposed to familial syndromes, where their diagnosis conditions the screening and clinical management of the patients, often with preventive interventions). GWAS have identified over 30 CRC susceptibility SNPs corresponding to more than 20 loci (summarized in Table 1.1). Still, the majority of the phenotypic variance seems to be unaccounted for, coining the term *missing heritability* (4).

The challenges of studying the effect of common variants in CRC are that (i) the magnitude of the effect of the SNP in the disease risk is small and (ii) GWAS studies survey hundreds of thousands of base pairs. As a consequence the required sample size inflates (a small effect of the exposure increases the type II error and multiple comparisons increase the type I error) and these studies are thus feasible mainly inside large consortia that have the capacity to genotype thousands of individuals.

One of the earliest identified and most consistently validated variants is rs4939827 (18q21.1), which seems to be specific for CRC. Table 1.2 summarizes the studies supporting this association.

The SNP rs4939827 maps within intron 3 of the gene SMAD family member 7 (*SMAD7*), which is associated with the TGFβ (transforming growth factor-β) pathway. Specifically, *SMAD7* acts as an intracellular antagonist of TGFβ signaling by binding stably to the receptor complex and blocking activation of downstream signaling (24). The minor allele (G) in rs4939827 is associated with a lower risk of CRC, with the most recent GWAS observing an odds ratio (OR) of 0.88 [95% confidence interval (CI) 0.85-0.93, P-value = 1.1×10^{-7}] (23). Recently, in a pooled analysis of five prospective cohorts, we observed that the G allele is also associated with poorer survival [hazard ratio (HR) = 1.16, P-value = 0.02] (25).

SNP	Locus	Closest gene	References
rs6691170	1q41	*DUSP10*	Houlston et al. 2010 (5)
rs6687758	1q41	*DUSP10*	Houlston et al. 2010 (5)
rs11903757	2q32.3	*NABP1*	Peters et al. 2013 (6)
rs10936599	3q26.2	*MYNN*	Houlston et al. 2010 (5)
rs35509282	4q32.2	*FSTL5*	Stenzel et al. 2014 (7)
rs647161	5q31.1	*AK026965*	Jia et al. 2013 (8)
rs1321311	6p21	*CDKN1A*	Dunlop et al. 2012 (9)
rs7758229	6q25.3	*SLC22A3*	Cui et al. 2011 (10)
rs16892766	8q23.3	*EIF3H*	Tomlinson et al. 2008 (11)
rs10505477	8q24	*MYC*	Zanke et al. 2007 (12), Gruber et al. 2007 (13)
rs6983267	8q24	*MYC*	Zanke et al. 2007 (12), Haiman et al. 2007 (14), Tomlinson et al. 2007 (15), Hutter et al. 2010 (16)
rs7014346	8q24	*MYC*	Tenesa et al. 2008 (17)
rs719725	9p24	*TPD52L3*	Tomlinson et al. 2008 (11), Kocarnik et al. 2010 (18)
rs10795668	10p14	*LOC338591*	Tomlinson et al. 2008 (11)
rs3824999	11q13.4	*POLD3*	Dunlop et al. 2012 (9)
rs3802842	11q23	*C11orf93*	Tenesa et al. 2008 (17)
rs10774214	12p13.32	*CCND2*	Jia et al. 2013 (8)
rs7136702	12q13.12	*LARP4*	Houlston et al. 2010 (5)
rs11169552	12q13.12	*LARP4*	Houlston et al. 2010 (5)
rs4444235	14q22.2	*BMP4*	Houlston et al. 2008 (19), Tomlinson et al. 2011 (20)
rs1957636	14q22.2	*BMP4*	Tomlinson et al. 2011 (20)
rs16969681	15q13.3	*CRAC1,HMPS, GREM1*	Tomlinson et al. 2011 (20)
rs4779584	15q13.3	*CRAC1,HMPS, GREM1*	Jaeger et al. 2008 (21), Tomlinson et al. 2011 (20)
rs11632715	15q13.3	*CRAC1,HMPS, GREM1*	Tomlinson et al. 2011 (20)
rs9929218	16q22.1	*CDH1*	Houlston et al. 2008 (19)
rs4939827	**18q21**	***SMAD7***	Broderick et al. 2007 (22), Tenesa et al. 2008 (17)
rs10411210	19q13.1	*RHPN2*	Houlston et al. 2008 (19)
rs961253	20p12.3	*BMP2*	Houlston et al. 2008 (19), Tomlinson et al. 2011 (20)
rs4813802	20p12.3	*BMP2*	Tomlinson et al. 2011 (20), Peters et al. 2012 (23)
rs4925386	20q13.33	*LAMA5*	Houlston et al. 2010 (5)
rs5934683	Xp22.2	*SHROOM2*	Dunlop et al. 2012 (9)

Table 1.1: SNPs associated with CRC risk

Reference	Population	RAF	OR (95% CI)
Broderick et al.(22)	Discovery: 930 Eu ancestry cases, 960 Eu ancestry controls Replicaton: 7473 Eu ancestry cases, 5984 Eu ancestry controls	0.52	1.16 (1.09-1.27)
Tenesa et al.(17)	Discovery: 981 Eu ancestry cases, 1002 Eu ancestry controls Replication: 10287 Eu ancestry cases, 10401 Eu ancestry controls, 4400 Jap ancestry cases, 3179 Jap ancestry controls, 1789 other ancestry cases, 1771 other ancestry controls	0.52	1.20 (1.16-1.24)
Tomlinson et al.(11)	Discovery: 930 Eu ancestry cases, 960 Eu ancestry controls Replication: 17089 Eu ancestry cases, 16862 Eu ancestry controls, 783 Other ancestry cases, 664 Other ancestry controls	0.53	1.18 (1.10-1.25)
Peters et al. (23)	Discovery: 2906 Eu descent cases, 3416 Eu descent controls Replication: 8161 Eu descent cases, 9101 Eu descent controls	0.51	1.14 (1.08-1.18)
Peters et al. (6)	Discovery: 2696 Eu ancestry colorectal tumor cases, and 15113 Eu ancestry controls Replication: 958 Eu ancestry colorectal tumor cases, 2098 EA ancestry colorectal tumor cases, 909 Eu ancestry controls, 5749 EA ancestry controls	0.52	1.12 (1.09-1.16)

Table 1.2: GWAS studies identifying rs4939827 as a risk SNP for CRC. RAF: Risk Allele Frequency; OR: Odds Ratio; CI: Confidence Interval; Eu: European; Jap: Japanese; EA: East Asian

1.1.2.2 Hereditary syndromes

High-penetrance germ line mutations in known genes account for around 5-7% of the cases (26). The most relevant are:

1. **Lynch syndrome or hereditary non-polyposis colorectal cancer (HNPCC).** HNPCC is an autosomal dominant syndrome that accounts for approximately 3 to 5 percent of CRC. Families diagnosed with Lynch syndrome usually have a germline mutation in one allele of a mismatch repair (*MMR*) gene, usually *hMLH1*, *hMSH2*, *hMSH6*, or *PMS2*. Mutations in *EpCAM* can induce a *MSH2* mono allelic methylation. Phenotypically these are early (mean age at diagnosis is 48 years) right-sided CRC. Lynch syndrome also increases the risk of cancer in other locations (endometrium, ovary, stomach, small bowel) (27, 28).

2. **Familial adenomatous polyposis (FAP)**. FAP accounts for less than 1 percent of CRC. It is caused by germline mutations in the adenomatous polyposis coli (*APC*) gene. Sites of mutation in the APC gene can have different degree of phenotypic impact. Patients present with multiple polyps in the colon and develop CRC by age 45 in 90% of the cases (29).

3. ***MUTYH*-associated polyposis**. Patients with this disease mimic the FAP phenotype due to biallelic germline mutations in the base excision repair (the base excision repair system repairs mutations due to oxidative DNA damage) gene mutY homolog (*MUTYH*) (30).

1.2 Biology of colorectal cancer tumor progression

The transformation of the healthy colorectal mucosa into adenoma and CRC is a well documented process that involves the sequential alteration of several pathways: Wnt pathway through the loss of *APC* or through the accumulation of nuclear β-catenin, the acquisition of constitutive active mutations of *KRAS* or *BRAF*, mutations in the PI3K pathway, loss of the 18q chromosome and inactivation of *SMAD4* and *TP53* (31). Specifically:

1. **Adenomatous Polyposis Coli (*APC*) gene and Wnt signaling pathway**. *APC* is a tumor suppressor gene. Somatic mutations in both alleles are present in

a high percent of sporadic CRCs. As mentioned above, a single germline mutation in this gene is responsible for the FAP syndrome. *APC* loss is considered a very early event in CRC development (32). The Wnt pathway is an evolutionarily conserved signal transduction pathway that plays a central role in supporting intestinal epithelial renewal (33). The main tumor supressor funcion of APC is to destabilize free β-catenin. Therefore, the loss of *APC* causes nuclear β-catenin accumulation. Free β-catenin (either because of loss of *APC* or because mutations in β-catenin that stabilized it and cannot be degraded) leads to Wnt pathway activation (e.g. through activation of Tcf4) and an increase in size of the proliferating crypt compartment in the colon mucosa.

2. **Transfroming growth factor β (TGFβ)**. TGFβ signaling pathway plays a role in the control of cell proliferation, migration, differentiation and apoptosis and is commonly disregulated in CRC. Key elements of this pathway are the three TGFβ isoforms (TGFβ1-3, being the TGFβ1 the most commonly expressed isoform), the TGFβ receptors (TGFβR1 and TGFβR2) and the downstream transcription factors SMAD2, SMAD3 and SMAD4. The activation of the pathway ends up with a SMAD complexes (SMAD2, SMAD3 and SMAD4) translocating to the nucleus to regulate several TGFβ-responsive genes. Some of these TGFβ-responsive genes are important cell cycle checkpoint genes. In normal epithelium, TGFβ acts as a tumor suppressor. However, once cells are resistant to TGFβ-mediated proliferative inhibition (*i.e.* in established tumors), TGFβ appears to promote metastasis by enhancing angiogenesis and extracellular matrix disruption and inhibiting infiltrating tumor immune cells (34). SMAD7 acts as a downstream inhibitor of the action of TGFβ. TGFβ-related ligands can activate other pathways beyond SMADs, like MAPK pathway, JNK pathway and phosphatidylinositol 3-kinases/Akt (PI3K-Act) pathway (35).

3. **RAS**. Ras proteins are GTPases encoded by different variants of the *RAS* oncogene. These variants are H-ras, K-ras and N-ras. Ras proteins regulate different signaling pathways involved in the control of cell behavior like proliferation, differentiation, migration, survival and apoptosis (36). Best known effectors of Ras GTPases are Raf kinases and phosphatidylinositol 3-kinases. *RAS* mutations are found in up to 50 % of sporadic CRC. K-ras has been reported to be implicated

in the processes of colorectal cancer invasion and metastasis (37). Mutations of *RAS* are clinically relevant because their presence impedes response to monoclonal antibodies against the epidermal growth factor receptor (EGFR) (38) like cetuximab and panitumumab.

1.3 Mechanisms of metastasis

Each tumor type has a characteristic metastatic pattern and latency (*e.g.* prostate cancer has a tendency to metastasize to the bone whereas breast cancer spreads mainly to the bone, lung, brain and liver). In the case of CRC, distant metastasis appear primarily in the liver and second, by far, in the lung and bones. In some tumours like breast cancer important advances have been achieved in unveiling the metastatic process (39). Nevertheless, these cannot be directly extrapolated to CCR given its different metastatic behaviour.

The vascular drainage of the colon may play a role in this characteristic pattern of spread (40) as the mesenteric circulation drains to the liver, therefore those CRC cells detached from the primary tumor reach the liver capillary network as a first station for colonization. But beyond this passive role of circulation pattern, metastatic cells must gain additional functions to form macroscopic metastases. The development of metastasis reflect the evolutionary process involved in cancer, where the mediators of metastasis act as factors that slightly increase, cell by cell, the probability of successful completion of one or more steps of the metastatic process. The main steps are the following.

1.3.1 Angiogenesis

When circulating tumor cells arrive to a distant organ, one of the main stressors that they face is the lack of oxygen and nutrients. Thus their survival depends on a shift on the normal balance of angiogenesis. One of the main factors involved in angiogenesis is the vascular endothelial growth factor (VEGF). Some genes associated with higher metastatic capacity do so by increasing the angiogenic potential of the invading cells. As an example, *EREG*, *COX-2* and *MMP-1* cooperate in remodeling the vasculature by allowing neoangiogenesis in models of breast cancer (41). As another example, the

lack of oxygen stabilizes the hypoxia-inducible factor (HIF) which in turn activates mediators of angiogenesis (42). Several antiangiogenic drugs have been approved recently for the treatment of metastatic CRC.

1.3.2 Stroma activation

Tumor cells need to interact with the stroma to enter the circulation and have the possibility of reaching distant organs (43). They also need to interact with the stroma of the distant organ in orden to colonize it. Various stromal cell types can induce signals that cancer cells will use for survival, invasiveness, self-renewal, and migration. As an example, cancer cells interact with astrocytes in the brain parenquima to form brain metastasis (44, 45) and with osteoclasts in the bone marrow to form osteoclastic metastasis (46). This process is well characterized in breast cancer, where the PI3K-Akt pathway is involved in facilitating bone metastasis (via activation of CXCL12 and IGF1) (47) and the Noch and Wnt pathways are involved in lung metastasis (via periostin and protein tenascin c interaction) (48). The stroma of the tumor itself can also promote the attachment of circulating tumor cells favoring its clonal expansion (tumor self-seeding) (49).

In CRC, cells can become insensitive to the tumor suppressive effect of TGFβ due to the genetic inactivation of the TGFβ signaling pathway. This allows them to over express TGFβ. This cytokine can induce the secretion of interleukin 11 from stromal fibroblasts in the liver and facilitate the development of metastasis (50). Also, stromal fibroblasts can generate hepatocyte growth factor that enhances Wnt/β-catenin signaling to promote the stem cell potential of CRC cells (51).

1.3.3 Epithelial to Mesenquimal Transition (EMT)

EMT is a process where epithelial cells switch to a mesenchymal progenitor-cell phenotype, in which they de-polarize and become motile. Such transformation can be induced by reactivation of developmental programs in cancer cells by certain cytokines (52). Loss of E-cadherin is a requirement for EMT (53), and the pathways involved in EMT include the TGFβ signaling pathway, the Wnt pathway and multiple tyrosine kinase receptor pathways like fibroblast growth factor receptor, EGFR and platelet-derived growth factor receptor (53). EMT transformation allows the cells to gain functions that will favor metastasis, like stemness, motility and even resistance to therapy

(54), although the role of EMT in metastasis has to be further defined. Transcriptional regulators that promote EMT can both promote (55) and inhibit (56) metastatic colonization. Besides, metastasis usually show epithelial and not mesenchymal features. A likely explanation is that EMT is a transient estate that allows cancer cells to disseminate, but that has to be reverted by mesenchymal to epithelial transition (MET) at the metastatic site (57).

1.3.4 Intravasation, Circulation and Extravasation

Cancer cells can enter the circulation until the primary tumor is removed. Tumors can relesease cancer cells into the circulation in high numbers, as can be inferred from the presence of circulating tumor cells found in the blood of cancer patients (58). Experimental evidence using a mouse model of mammary tumors shows that macrophages can facilitate tumor cells intravasation, even in the absence of local angiogenesis (59). Once in the circulation, cells can be directed to specific organs depending on the site of origin by circulation patterns (*e.g.* liver in the case of colon cancer cells entering the mesenteric circulation). Surviving into circulation also requires the gaining of specific traits (60), which usually happen by genetic changes ocurring in the primary tumor (61). Finally, cancer cells have to be able to extravasate once they reach the distant organ. Several genes that mediate the extravasation of cancer cells to the brain (62), lungs (41, 63, 64, 65) and liver (64) have been described.

1.3.5 Colonization

Colonization is one of the main bottlenecks for metastasis formation. Colonization refers to the following steps: survival on arrival, formation of micro metastasis, adoption of latency, reactivation of growth, recirculation and even formation of tertiary lesions in the same or different organs. Still, cancer cells die easily at distant sites due to reasons not completely understood. Contributing factors can be the stress of passing through endothelial barriers, exposure to the immune system in the distant organ and lack of survival and proliferation signals in the host tissue.

1.3.5.1 Survival on arrival

Most cells that infiltrate a distant organ do not survive. Specific traits have to be gained by cancer cells in order to avoid exposure to lethal signals from the reactive stroma, upregulate cell survival and antiapoptotic pathways. Survival on arrival depends on a successful interaction with stromal elements like macrophages (66) and on gainig certain functions like the gain of Src activity of breast cancer cells to be able to survive on bone marrow (47).

1.3.5.2 Stemness

Cells that reach distant organs do not necessarily have the capacity to create metastasis; to do so they must be able to recapitulate tumor growth. The term "metastatic stem cell" (MSC) has been coined to refer to those cells that are able to reinitiate macroscopic tumor growth in a distant organ. This "stemness" can be present already in the primary tumor or can be gained through phenotypic plasticity once the MSC have left the tumor of origin. The fact that MSC can be already present in the primary tumor is supported by the following: (i) primary tumors that express a stem cell-like signature are associated with poor prognosis and early distant relapse (67) and (ii) cells isolated from primary tumors using stem cell markers can generate metastasis in animal models (68). In the case of CRC, it has been demonstrated that metastasis arise from cells with stem-like properties like long-term self-renewal capacity, quiescence and resistance to chemotherapy (69, 70). Epigenetic changes (*e.g.* methylation) can drive EMT, a stem-like featured that in this case can be gained once the cell has left the primary tumor.

1.3.5.3 Metastatic Niches

As pointed out above, metastatic cells need to find a favorable environment (*i.e.* stroma) to trhive. The term "metastatic niche" refers to the specific locations and environments (extracellular matrix proteins, stromal cell types and diffusible signals) that support the survival and self-renewal of metastatic cells. Three different sources of metastatic niches have been proposed (71):

- Native stem cell niches, which refer to locations where the stem cells reside under physiological conditions, like the intestinal epithelium, bone marrow, epidermis

and brain (72, 73). Recent evidence shows that prostate cancer cells benefit from an environment that enhances stem cells properties and metastasis in a native stem cell niche in the bone marrow (74).

- Niche functions provided by stromal cells outside of native stem cell niches. An example is the perivascular niche: cancer cells typically initiate growth around blood capillaries. This tendency to settle in perivascular niches is true for glioma, breast cancer, lung cancer and melanoma cells that infiltrate the brain (75, 76). Cells proliferate around blood vessels, forming a multilayered sheath that remodels the capillary network and becomes the core of an expanding lesion (71). In the case of brain metastasis, L1CAM -an adhesion molecule and marker of bad prognosis- plays a key role in allowing cancer cells to settle in this niche location (77). Beyond providing oxygen and nutrients, perivascular niches can stimulate growth by paracrine factors. In the case of CRC, this happens via the expression of Jagged-1 by the endothelial cells (78).

- Stem cell niche components that might be produced by the cancer cells themselves. Periostin and tenascin C (TNC) are examples of proteins produced by cancer cells that contribute to distant spread. Tumor cells can produce TGFβ that in turn recruits fibroblast that produce periostin which is required for the initiation of lung metastasis by breast cancer cells in mice (79). TNC can be expressed by breast cancer cells and regulates several factors that promote tumor growth (Musashi, Notch and Wnt) and lung metastasis (80).

1.3.6 Cellular latency

"Metastatic latency" is a clinical term to denote the time elapsed from the primary tumor diagnosis to the detection of overt metastases in imaging techniques. Different primary tumors have metastatic latencies of different legths: it is usually long in prostate cancer, sarcoma and melanoma, and short in lung and some breast cancers. At the celular level this latency depends both on the equilibrium of cell proliferation and cell death and on adoption of quiescent states by infiltrating cells (81). Entry in G_0 phase can be a defense under adverse conditions (82, 83). Other mediators of the transition between dormancy and proliferation are p38 and ERK (mitogen activated kinases) (84) as well as bone-morphogenetic proteins and their antagonists (85). This

aspect of metastasis mechanisms biology is not as developed as others, probably in part due to the difficulty to replicate long latencies in animal models.

1.4 Clinical Management

Clinical management of CRC is based in its classification into four stages (AJCC (86) stages I to IV) according to the information provided by clinical examination and imaging techniques. Initial diagnosis is usually done either by screening (i.e. screening colonoscopy or occult fecal blood test) or driven by symptoms of the primary tumor (*e.g.* anemia, gastrointestinal overt bleeding or gastrointestinal symptoms like changes in bowel habit or even large bowel obstruction). Staging and treatment is different for colon and rectal cancer.

1.4.1 Colon cancer

Clinical guidelines for the diagnosis and staging of colon cancer recommend the use of colonoscopy, abdominal and pelvic computed tomography scans and pathologic examination of the surgical specimen for localized tumors (87, 88, 89). Chest CT scan is not required (89, 90).

Stages I to III are considered as localized disease (absence of distant organ metastasis), with five-year overall survival ranging from 65% to 95% (91). The mainstay of treatment for stages I to III is surgical resection. Patients with a tumor that surpasses *muscularis propia* in the bowel wall but without regional lymph node involvement after an adequate evaluation (at least 12 lymph nodes) of the surgical specimen (*i.e.* stage II) can be offered treatment with adjuvant (*i.e.* postoperative) fluorouracil modulated with leucovorin. The benefits of this adjuvant therapy are modest. A trial that studied a population with 91% of stage II patients (92) found a 3.6% absolute increase in in overall survival (OS) at 5 years and no statistically significant benefit in OS among stage II patients. Three meta-analysis failed to prove a benefit of adjuvant fluoropyrimidine-based chemotherapy in stage II patients in terms of overall survival (93, 94, 95). As opposed to treatment of stage III patients (see below), the addition of oxaliplatin to the adjuvant chemotherapy regimen has proven of no benefit in stage II patients (91, 96).

The standard of care after resection of tumors with lymph nodes involvement and absence of distant metastasis (*i.e.* stage III) is oxaliplatin in combination with flu-

orouracil or capecitabine (91, 96). This regimen showed an statistically significant increase in OS of 4% at 5 years (91) when compared with an adjuvant therapy based solely in 5-FU.

In approximately 25% of the cases, CRC presents distant metastasis at diagnosis (stage IV) and about 30% of the patients with localised stages will suffer from distant metastasis during follow-up. Patients with metastasis have a median survival that ranges from 6 to 20 months (97). The main prognostic factors of stage IV CRC patients are the number, size and location of metastasis (which determine their resectability), LDH levels and performance status (98).

Treatment of advanced CCR is based on palliative chemotherapy containing 5-fluorouracil (or capecitabine) plus oxaliplatin or irinotecan. This can be complemented with monoclonal antibodies directed against EGFR (cetuximab (99), panitumumab (100)) for those patients with wild type *KRAS* and *NRAS* (100, 101). Other active drugs approved for the treatment of stage IV patients include regorafenib (102) (an orally active inhibitor of multiple angiogenic and non-angiogenic tyrosine kinases) and aflibercept (103) (a protein consisting of VEGF binding portions from the human VEGF receptors 1 and 2 that acts as a decoy receptor preventing pro-angiogenic efectors from binding to their receptors). The benefit of adding any of these targeted therapies rarely goes beyond an increment of 2 months in median OS. The role of bevacizumab, a monoclonal antibody against the vascular endothelial growth factor, is not well stablished since it has not proven to be effective in improving OS (97, 104).

The best way to combine and sequence all the approved drugs for metastatic CRC to optimize treatment is not yet established.

1.4.2 Rectal cancer

The main difference between the management of colon and rectal cancer relies on the local staging and local treatment, due to a higher propensity to local relapse in patients with rectal tumors because of its location. Besides the imaging techniques enumerated above for the staging of colon cancer, further local staging should be obtained with endoscopic ultrasonography or preferably, with magnetic resonance imaging.

The standard of care of localized rectal cancer is preoperative concomitant chemo and radiotherapy (105, 106) followed by surgery using total mesorectal excision (107). The value of postoperative chemotherapy is not well established, specially for those

patients that achieve a pathological complete response after preoperative chemo and radiation (108). Treatment of metastatic rectal cancer does not substantially differ from that of colon cancer (109).

2

Hypothesis

2.1 Hypothesis

- Germline variants can be associated with different patterns of invasion and or distant metastasis of CRC.
- Given that the CRC-risk variant rs4939827 is associated with survival in patients diagnosed with CRC, it may be differentially associated with CRC phenotypic and/or molecular subtypes.
- Tumor-derived genetic changes can drive the patterns of invasion and/or metastasis
- Cancer cells in stablished metastases can gain functions that allow them colonize a new distant organ (*i.e.* metastasis from metastasis).

3

Objectives

1. To evaluate the association of the germline variant rs4939827 with CRC risk according to specific clinical phenotypes and molecular characteristics.

2. To develop a murine model for colorectal metastasis and use it to enrich the metastatic phenotype of CRC lines. Use the highly metastatic cell line to identify novel mechanisms of invasion and/or metastasis

4

Publications

4.1 First publication

Phenotypic and tumor molecular characterization of colorectal cancer in relation to a susceptibility SMAD7 variant associated with survival

Xabier Garcia-Albeniz, Hongmei Nan, Linda Valeri, Teppei Morikawa, Aya Kuchiba, Amanda I. Phipps, Carolyn M. Hutter, Ulrike Peters, Polly A. Newcomb, Charles S. Fuchs, Edward L. Giovannucci, Shuji Ogino and Andrew T. Chan

Carcinogenesis *2013 Feb;34(2):292-8. doi:10.1093/carcin/bgs335*

4.1.1 Summary

The minor allele (G) of rs4939827 -an intronic variant of *SMAD7* (18q21)- is associated with a lower risk of developing CRC (OR of 0.88, 95% CI: 0.85 - 0.93)(23) and poorer survival after diagnosis (HR of 1.16, 95% CI: 1.06-1.27)(25). We evaluated the associations of this variant with tumor phenotype and several molecular characteristics. We used 1509 CRC cases and 2307 age-matched controls nested within the Nurses Health Study (NHS) and the Health Professionals Follow-up Study (HPFS).

The NHS is a cohort initiated in 1976 with over 120,000 registered nurses. The HPFS is a cohort initiated in 1986 with over 50,000 male health professionals. In both cohorts information is updated biennially via questionnaires, with a follow-up greater than 90%. Samples for DNA extraction (blood or buccal cell specimens) from both cohorts were obtained in more than 90,000 individuals. Information on CRC is extracted from medical records by study physicians after obtaining permission from

participants who reported CRC in the biennial questionnaires. We randomly selected between one and three controls (matched on ethnicity, year of birth and month/year of sampling) within the same cohort from participants who were free of CRC at the same time the CRC was diagnosed in the cases.

Among the 1509 cases with blood or buccal samples in this study, we were able to successfully obtain tissue suitable for molecular analyses in 658 cases. We genotyped rs4939827 (TaqMan®) successfully in 98% of the samples in NHS and 99.6% of the samples in HPFS. We used logistic regression to assess the association of rs4939827 with risk of CRC according to different phenotypic and molecular characteristics. The phenotipic features evaluated were: TNM stage, grade of differentiation, location of the primary tumor (colon *vs.* rectum) and age at diagnosis. The evaluated molecular characteristics were DNA methylation of *RUNX3* and *LINE-1* (long interspersed nucleotide element-1), CpG island methylator phenotype (CIMP), microsatellite instability, TP53 expression by immunohistochemistry and the mutational status of *BRAF*, *KRAS* and *PIK3CA*. We adjusted significance hypothesis testing by multiple comparisons.

We modeled each SNP using a log-additive approach, relating genotype dose (i.e. number of copies of the minor allele) to risk of CRC. We adjusted all analyses for age at sample collection, race, gender, aspirin use, non-steroidal anti-inflammatory drugs use, body mass index, physical activity, familial history of CRC, smoking, alcohol, meat consumption, energy-adjusted calcium and folate intake and type of sample (blood versus cheek). To assess heterogeneity in the association between rs4939827 and tumors according to clinical phenotype or molecular characteristics, we used a case-case design using logistic regression model comparing tumor subtypes.

We found that the minor allele (G) in rs4939827 was associated with a lower risk of developing tumor stage pT1 or pT2 CRC [multivariate odds ratio (OR), 0.73; 95% confidence interval (CI) 0.62-0.87] but not tumor stage pT3 or pT4 (multivariate OR, 1.07; 95% CI 0.93-1.23, P for heterogeneity = 1.2×10^{-4}). The association between rs4939827 and CRC also significantly differed by methylation of *RUNX3* (P for heterogeneity = 0.005). Among those with CRC, the minor allele (G) in rs4939827 was significantly associated with poorer overall survival (hazards ratio, 1.20; 95% CI, 1.02-1.42).

We performed mediation analyses (110, 111) to decompose the total effect of the exposure (rs4939827) on the outcome (T3-T4 tumors) into a "direct effect" plus an "indirect effect" The "direct effect" can be interpreted as the OR comparing the risk

of T3-T4 tumor stage with the genetic variant present *vs.* absent if the mediator (*e.g. RUNX3*) were what it would have been without the genetic variant. The "indirect effect" can be interpreted as the OR for T3-T4 tumor stage for those with the genetic variant present comparing the risk if the mediator were what it would have been with versus without the genetic variant (110).

The multivariate ORs that estimate the direct effect of rs4939827 were 1.96 (95% CI 1.183.25, P-value = 0.009) for one variant allele and 4.46 (95% CI 1.1916.6, P-value = 0.038) for two variant alleles. The multivariate ORs estimating the indirect effect of rs4939827 on risk of pT3 and pT4 tumors was 1.05 (95% CI 0.961.15, P = 0.32) for one variant allele and 1.50 (95% CI 0.445.10, P = 0.51) for two variant alleles. We did not found evidence of neither multiplicative nor additive interaction between rs4939827 and *RUNX3* methylation.

In conclusion, we found that the minor allele (G) of the germline intronic *SMAD7* variant rs4939827 is associated with a lower risk of CRC with earlier tumor stage and CRC without methylation of the tumor suppressor *RUNX3*. These findings suggest that individuals with this *SMAD7* variant that develop CRC are more probably to have tumors with greater invasiveness and methylation of *RUNX3*, which potentially contributes to their poorer observed survival.

Carcinogenesis vol.34 no.2 pp.292–298, 2013
doi:10.1093/carcin/bgs335
Advance Access publication October 26, 2012

Phenotypic and tumor molecular characterization of colorectal cancer in relation to a susceptibility *SMAD7* variant associated with survival

Xabier Garcia-Albeniz[1,2], Hongmei Nan[2,3], Linda Valeri[4], Teppei Morikawa[5,6], Aya Kuchiba[6,7], Amanda I.Phipps[8], Carolyn M.Hutter[8], Ulrike Peters[8], Polly A.Newcomb[8], Charles S.Fuchs[2,6], Edward L.Giovannucci[1,2,7], Shuji Ogino[1,5,6,9,†] and Andrew T.Chan[2,10,*,†]

[1]Department of Epidemiology, Harvard School of Public Health, 677 Huntington Avenue, Boston, MA 02115, USA, [2]Department of Medicine, Channing Division of Network Medicine, Brigham and Women's Hospital and Harvard Medical School, Boston, MA 02115, USA, [3]Department of Epidemiology and Public Health, Division of Cancer Epidemiology, University of Maryland School of Medicine, Baltimore, MD 21201, USA, [4]Department of Biostatistics, Harvard School of Public Health, Boston, MA 02115, USA, [5]Center for Molecular Oncologic Pathology, Dana-Farber Cancer Institute, Boston, MA 02215, USA, [6]Department of Medical Oncology, Dana-Farber Cancer Institute and Harvard Medical School, Boston, MA 02215, USA, [7]Department of Nutrition, Harvard School of Public Health, Boston, MA 02115, USA, [8]Cancer Prevention Program, Public Health Sciences Division, Fred Hutchinson Cancer Research Center, Seattle, WA 98109, USA, [9]Department of Pathology, Brigham and Women's Hospital and Harvard Medical School, Boston, MA 02115, USA and [10]Division of Gastroenterology, Massachusetts General Hospital and Harvard Medical School, Boston, MA 02114, USA

*To whom correspondence should be addressed. Tel: +1-617-726-3212; email: achan@partners.org

The minor allele (G) of rs4939827, a *SMAD7* (18q21) intronic variant, is associated with a lower risk of developing colorectal cancer (CRC) and poorer survival after diagnosis. Our objective was to evaluate the associations of this variant with different tumor phenotype and intratumoral molecular characteristics. We evaluated 1509 CRC cases and 2307 age-matched controls nested within the Nurses' Health Study and the Health Professionals Follow-up Study. We used the TaqMan assay to genotype rs4939827 and logistic regression to assess the association of rs4939827 with risk of CRC according to different phenotypic and molecular characteristics. We found that the minor allele (G) in rs4939827 (*SMAD7,* 18q21) was associated with a lower risk of developing tumor stage pT1 or pT2 CRC [multivariate odds ratio (OR), 0.73; 95% confidence interval (CI) 0.62–0.87] but not tumor stage pT3 or pT4 (multivariate OR, 1.07; 95% CI 0.93–1.23, *P* for heterogeneity = 1.2×10^{-4}). The association between rs4939827 and CRC also significantly differed by methylation of *RUNX3* (*P* for heterogeneity = 0.005). Among those with CRC, the minor allele (G) in rs4939827 was significantly associated with poorer overall survival (hazards ratio, 1.20; 95% CI, 1.02–1.42). We can conclude that the minor allele (G) of the germline intronic *SMAD7* variant rs4939827 is associated with a lower risk of CRC with earlier tumor stage and CRC without methylation of the tumor suppressor *RUNX3*. These findings suggest that individuals with this *SMAD7* variant that develop CRC are more probably to have tumors with greater invasiveness and methylation of *RUNX3*, which potentially contributes to their poorer observed survival.

Abbreviations: BH, Benjamini and Hochberg; BMI, body mass index; CI,confidence interval; CIMP, CpG island methylator phenotype; CRC, colorectal cancer; GWAS, genome-wide association study; HPFS,Health Professionals Follow-up Study; HR,hazards ratio; LINE-1, long interspersed nucleotide element-1; MPE,molecular pathological epidemiology; MSI, microsatellite instability; MSS, microsatellite stable; NHS, Nurses' Health Study; NSAIDs, non-steroidal anti-inflammatory drugs; OR, odds ratio; RERI, relative excess risk due to interaction.

[†]These authors contributed equally to this work.

Introduction

Genome-wide association studies (GWAS) have identified 20 colorectal cancer (CRC) susceptibility variants, corresponding to 16 loci (1–8). One of the earliest identified and most consistently validated variants, rs4939827 (18q21.1), resides in an intronic region of the gene *SMAD* family member 7 (*SMAD7*), which is associated with the TGFB1 (transforming growth factor-β) pathway. The minor allele (G) in rs4939827 is associated with a lower risk of CRC, with the most recent GWAS observing an odds ratio (OR) of 0.88 [95% confidence interval (CI) 0.85–0.93, *P*-value = 1.1×10^{-7}] (9). Recently, in a pooled analysis of five prospective cohorts, we observed that the G allele is also associated with poorer survival [hazards ratio (HR) = 1.16, *P*-value = 0.02] (10). Based on these results, we hypothesized that rs4939827 may be differentially associated with CRC subtypes associated with worsened outcomes or are related to the TGFB1 pathway, including methylation of *RUNX3*. Thus, we examined the association of rs4939827 with CRC risk according to specific clinical or molecular phenotypes within the Nurses' Health Study (NHS) and the Health Professionals Follow-up Study (HPFS), two of the prospective cohorts included in our prior analysis (10).

Materials and methods

Study population

The NHS was initiated in 1976, when 121 700 female USA registered nurses between the ages of 30 and 55 years returned a mailed health questionnaire. The HPFS was established in 1986 with a parallel cohort of 51 529 USA male dentists, pharmacists, optometrists, osteopath physicians, podiatrists and veterinarians between the ages of 40 and 75 years. In both cohorts, we have subsequently updated information biennially with greater than 90% follow-up. In 1989–90, we collected blood samples from 32 826 participants in the NHS cohort. In 1993–95, we collected blood samples from 18 159 participants in HPFS. The samples were collected in heparinized tubes and sent to us by overnight courier in chilled containers. In 2001–04, 29 684 women in NHS and 13 956 men in HPFS mailed in a 'swish-and-spit' sample of buccal cells. Participants who provided buccal cells had not previously provided a blood specimen. On receipt, blood and buccal cells were centrifuged, aliquoted and stored at −70°C.

In both cohorts, we requested permission to obtain medical records and pathology reports from participants who reported CRC on our biennial questionnaires. We identified fatal cases from the National Death Index and from next-of-kin (11). Study physicians blinded to exposure data reviewed all medical records to confirm cases of CRC. As described previously, we randomly selected between one and three controls within the same cohort from participants who were free of CRC at the same time the CRC was diagnosed in the cases (12). We matched controls with blood specimens (1013 in NHS and 673 in HPFS) to cases with blood specimens (483 in NHS and 372 in HPFS); similarly, controls with buccal specimens (423 in NHS and 198 in HPFS) were separately matched to cases with buccal specimens (439 in NHS and 215 in HPFS). Controls were matched to each case on ethnicity, year of birth and month/year of blood or buccal sampling (12). In total, 1509 (922 in the NHS and 587 in the HPFS) cases and 2307 (1436 in the NHS and 871 in the HPFS) controls were included in our analysis. The institutional review boards at Brigham and Women's Hospital and the Harvard School of Public Health approved this study.

Genotyping

The SNP rs4939827 was genotyped by the 5′ nuclease assay (TaqMan®), using the ABI PRISM 7900HT Sequence Detection System (Applied Biosystems, Foster City, CA). TaqMan® primers and probes were designed using the Primer Express® Oligo Design software v2.0 (ABI PRISM). Laboratory personnel were blinded to case-control status, and 10% blinded quality control samples (duplicated samples) were inserted to validate genotyping procedures; concordance for the blinded quality control samples was 100%. Primers, probes and conditions for genotyping are available upon request. We successfully genotyped rs4939827 in 98% of samples in NHS and 99.6% of samples in HPFS. We confirmed that rs4939827 was in Hardy-Weinberg Equilibrium among the controls ($\chi 2$ *P*-values = 0.93 for NHS and 0.85 for HPFS).

Pathological assessment of molecular characteristics

Beginning in 1997 in the HPFS and 2001 in the NHS, we began retrieving, from the pathology departments of treating hospitals, available pathological specimens from participants whom we confirmed had received a diagnosis of CRC up to 2006 (13). Among the 1509 cases with blood or buccal samples in this study, we were able to successfully obtain tissue suitable for molecular analyses in 658 cases. Real-time PCR (MethyLight) was used for quantitative DNA methylation to determine CpG island methylator phenotype (CIMP) status using DNA extracted from paraffin-embedded tissue. We quantified DNA methylation in eight CIMP-specific promoters (including *RUNX3*) as detailed elsewhere (14). CIMP-high was defined as >6 of 8 methylated markers using the eight-marker CIMP panel, and CIMP-low/0 was defined as 0 of 8 to 5 of 8 methylated markers, according to the previously established criteria (15). Microsatellite instability (MSI) analysis was performed using 10 microsatellite markers (D2S123, D5S346, D17S250, BAT25, BAT26, BAT40, D18S55, D18S56, D18S67 and D18S487). MSI-high was defined as the presence of instability in >30% of the markers, and MSI-low/microsatellite stable (MSS) as instability in 0–29% of markers (15). Long interspersed nucleotide element-1 (LINE-1) methylation level was assessed by pyrosequencing using the PyroMark kit and the PSQ HS 96 System (Qiagen, Valencia, CA). The average of the relative amounts of C in the four CpG sites evaluated was used as overall LINE-1 methylation level in a given sample (16). We performed PCR and pyrosequencing targeted for *KRAS* (codons 12 and 13), *BRAF* (codon 600) and *PIK3CA* (exons 9 and 20 (15,17,18)). TP53 expression was assessed by immunohistochemistry as detailed elsewhere (19).

Statistical analysis

We used logistic regression to estimate OR and corresponding 95% CIs for the association of variant rs4939827 with CRC among subgroups defined by tumor phenotype (T3-4 and T1-2; N1-2 and N0; M1 and M0; poorly differentiation and moderately well differentiation; rectum and colon location and age of diagnosis <60 and >60 years) and by molecular characteristics [*RUNX3* promoter methylation and absence of methylation; *KRAS* mutant and wild type (WT); *BRAF* mutant and wild type; *PIK3CA* mutant and wild type; LINE-1 methylation-low and methylation-high; MSI-H and MSI-L/MSS]. We obtained similar results using unconditional or conditional logistic regression adjusting for matching factors (data not shown). Thus, we present unconditional regression models adjusting for matching factors and other known or suspected risk factors. The Cochran's chi-square-based Q statistic test was used to assess the extent of heterogeneity across the two studies. Because there was little evidence for heterogeneity for the association of the SNP rs4939827 with CRC risk between women and men (P for heterogeneity = 0.32), we pooled data from the two studies.

We modeled each SNP using a log-additive approach, relating genotype dose (i.e. number of copies of the minor allele) to risk of CRC. We adjusted all analyses for age at sample collection, race, gender, regular aspirin use (yes or no), regular non-steroidal anti-inflammatory drugs (NSAIDs) use (yes or no), body mass index (BMI; in tertiles), physical activity (in tertiles), history of CRC in a parent or sibling (yes or no), smoking status (never, former or current smoker), alcohol consumption (0–4.9, 5–9.9, 10–14.9 or ≥ 15.0 g per day), consumption of beef, pork or lamb as a main dish (0–3 times per month, once a week, 2–4 times per week or ≥5 times per week), energy-adjusted calcium and folate intake (in tertiles) and type of sample (blood versus cheek). To assess heterogeneity in the association between rs4939827 and tumors according to clinical phenotype or molecular characteristics, we used a case–case design using logistic regression model comparing tumor subtypes (20).

We performed mediation analyses as described in (21,22). In brief, this approach decomposes the total effect of the exposure (rs4939827) on the outcome (T3-T4 tumors) into a 'direct effect' plus an 'indirect effect.' The 'direct effect' consists of the effect of rs4939827 on T-stage at a fixed level of the mediator variable [i.e. the direct effect can be interpreted as the OR comparing the risk of T3-T4 tumor stage with the genetic variant present versus absent if the mediator (e.g. *RUNX3*) were what it would have been without the genetic variant]. The 'indirect effect' is the effect on the outcome (T-stage) of changes of the exposure (rs4939827) that operate through the methylation status of *RUNX3*. (The indirect effect can be interpreted as the OR for T3-T4 tumor stage for those with the genetic variant present comparing the risk if the mediator were what it would have been with versus without the genetic variant.) This approach allows for the adjustment of covariates and for the presence of interaction between the variables of interest (21). We computed additive interaction in the form of relative excess risk due to interaction (RERI) using the delta method (23) and multiplicative interaction by entering a product term in the model and assessing its significance by the Wald method.

For analyses of rs4929827 in relation to survival, we confined the cohort to the 646 incident cases of CRC diagnosed after collection of blood or buccal cells. We calculated the time from CRC diagnosis to death from CRC, death from any cause or the end of follow-up (1 June 2010), whichever came first. For CRC-specific survival, deaths from other causes were censored at the time of death. We used Cox proportional hazards regression to calculate HRs and 95% CI for the association between the SNP and survival, adjusting for age, race, sex (cohort), tumor stage, grade of differentiation, regular aspirin use, smoking status at diagnosis, alcohol consumption, consumption of beef, pork or lamb as a main dish and energy-adjusted calcium and folate intake as described above. The proportional hazards assumption was verified by plotting the cumulative martingale residuals and assessing for significance. We corrected for multiple comparisons with several tumor subtypes using the Benjamini and Hochberg (BH) false discovery rate adjustment (24). We corrected for the 14 assessed interactions; the values of the corrected P-values, when significant, are presented as footnotes in the tables. SAS V9.2 (SAS Institute, Cary, NC) was used for the analysis.

Table I. Baseline characteristics of cases and controls[a]

	NHS (women)		HPFS (men)		Total	
	Cases	Controls	Cases	Controls	Cases	Controls
	(n = 922)	(n = 1436)	(n = 587)	(n = 871)	(n = 1509)	(n = 2307)
Age at diagnosis [years, mean (SD)]	66.8 (9.2)		69.2 (9.2)		67.7 (9.3)	
Age at sample draw (years, mean)	59.5 (6.6)	59.6 (6.5)	64.8 (8.5)	64.9 (8.4)	62.5 (8.2)	62.1 (7.9)
Non-white (%)	13 (1.4)	6 (0.4)	49 (8.4)	59 (6.8)	62 (4.1)	65 (2.5)
Regular aspirin use (%)[b]	324 (35.1)	656 (45.7)	269 (45.8)	450 (51.7)	593 (39.3)	1106 (47.9)
Regular NSAID drug use (%)[c]	303 (32.9)	570 (39.7)	136 (23.2)	190 (21.8)	439 (29.1)	760 (32.9)
BMI [kg/m^2, mean (SD)][d]	26.1 (5.1)	26.0 (5.0)	26.2 (3.3)	25.6 (3.3)	26.1 (4.5)	25.8 (4.5)
Physical activity [METs - h/week, mean (SD)][e]	15.7 (14.3)	16.0 (14.0)	29.4 (24.2)	31.1 (25.2)	21.1 (20.0)	21.8 (20.5)
CRC in a parent or sibling (%)	212 (23.0)	239 (16.6)	114 (19.4)	132 (15.2)	326 (21.6)	371 (16.1)
Former or current smoker (%)	537 (59.0)	791 (55.0)	319 (60.0)	441 (55.0)	856 (59.0)	1232 (55.0)
Alcohol consumption [g/day, mean (SD)]	6.8 (10.2)	6.3 (9.4)	13.4 (15.7)	11.8 (13.2)	9.4 (13.1)	8.4 (11.3)
Beef, pork or lamb as a main dish [servings/week, mean (SD)]	2.8 (0.8)	2.8 (0.8)	2.7 (0.9)	2.6 (0.9)	2.7 (0.8)	2.7 (0.8)
Total calcium intake (mg/day, mean)[f]	952.4 (364.1)	1007.5 (386.9)	916.1 (399.4)	950.6 (382.5)	938.1 (378.7)	985.8 (386.2)
Total folate intake (µg/day, mean)[f]	426.8 (179.1)	447.8 (194.9)	526.0 (226.2)	566.2 (231.6)	465.9 (204.7)	492.9 (217.3)

[a]At blood draw or cheek cell sampling.
[b]Regular aspirin user was defined as the consumption of at least two 325 mg tablets per week in the NHS and at least two times per week in the HPFS. Non-regular user was defined otherwise.
[c]Regular NSAID user was defined as the consumption of NSAIDs at least two times per week. Non-regular user was defined otherwise.
[d]The BMI is the weight in kilograms divided by the square of the height in meters.
[e]Metabolic Equivalent of Task (MET) denotes metabolic equivalent. Met (h) = sum of the average time/week in each activity × MET value of each activity. One MET, the energy spent sitting quietly, is equal to 3.5 ml of oxygen uptake per kilograms of body weight per minute for a 70 kg adult.
[f]Nutrient values (calcium and folate) represent the mean of energy-adjusted intakes.

Results

Among our total study population of 1509 CRC cases and 2307 controls, the minor allele (G) frequency for rs4939827 was 48.6%, consistent with the HapMap CEU population. The baseline characteristics of the cases and controls are presented in Table I. Compared with controls, CRC cases in both women and men were less probably to have regularly used aspirin or NSAIDs, have a family history of CRC, were more probably to smoke, consumed higher amounts of alcohol and had lower intakes of calcium and folate. Among men, cases had a higher BMI and were less physically active. Among women, cases were less probably to have used postmenopausal hormones. Although the minor allele (G) of rs4939827 was not significantly associated with CRC in our total population, the trend was in the direction previously reported (multivariate OR, 0.93; 95% CI 0.84–1.04, $P = 0.22$).

We confirmed our prior findings relating rs4939827 with survival among cases of CRC (10). Among the 646 cases of CRC diagnosed after blood or buccal cell collection, we observed that the minor allele of rs4939827 was significantly associated with poorer overall survival (multivariate HR, 1.20; 95% CI 1.02–1.42, $P = 0.031$) and a trend toward poorer CRC-specific survival (HR = 1.20, 95% CI 0.98–1.47, $P = 0.08$).

To determine if the survival difference we observed according to the G allele was related to a differential association with tumor phenotypes, we examined the influence of rs4939827 on CRC susceptibility according to traditional clinicopathological features in our total study population. The association of the G allele of rs4929827 with CRC risk appeared to differ according to pT stage or the depth of invasion of the tumor (P for heterogeneity = 1.0×10^{-4}). The G allele of rs4929827 was inversely associated with a risk of tumors staged as pT1 or pT2 (multivariate OR, 0.73; 95% CI 0.62–0.87, P-value = 2.8×10^{-4}). In contrast, there was no association between rs4939827 and tumors staged as pT3 or pT4 (multivariate OR, 1.07; 95% CI 0.93–1.23, P-value = 0.38). Hence, the prevalence of tumors

Table II. Associations of rs4939827 with tumor phenotypes[a]

	Controls	Cases	OR (95% CI)	Cases	OR (95% CI)	Case-only analysis
		pT1/pT2		pT3/pT4		pT3/pT4 versus pT1/pT2
TT	600	155	1	200	1	1
TG	1120	241	0.84 (0.65–1.10)	363	1.19 (0.93–1.53)	1.54 (1.10–2.15)
GG	538	95	0.51 (0.36–0.72)	182	1.14 (0.85–1.53)	2.31 (1.50–3.56)
P trend			2.8×10^{-4}		0.38	1.0×10^{-4}[b]
G allele[c]			0.73 (0.62–0.87)		1.07 (0.92–1.23)	1.52 (1.23–1.88)
		N0		N1-2		N1-2 versus N0
TT	600	236	1	114	1	1
TG	1120	407	1.10 (0.87–1.38)	191	0.88 (0.65–1.20)	0.79 (0.55–1.14)
GG	538	190	0.84 (0.63–1.11)	81	0.71 (0.49–1.04)	0.83 (0.53–1.31)
P trend			0.27		0.08	0.36
G allele			0.93 (0.81–1.06)		0.85 (0.70–1.02)	0.90 (0.72–1.13)
		M0		M1		M1 versus M0
TT	600	358	1	40	1	1
TG	1120	622	1.04 (0.85–1.27)	68	0.90 (0.56–1.44)	0.88 (0.54–1.44)
GG	538	287	0.84 (0.66–1.07)	26	0.70 (0.39–1.26)	0.78 (0.41–1.46)
P trend			0.20		0.24	0.43
G allele			0.93 (0.82–1.04)		0.84 (0.63–1.12)	0.88 (0.64–1.20)
		Moderately or well-differentiated tumors		Poorly differentiated tumors		Poorly versus moderately well differentiated tumors
TT	600	299	1	56	1	1
TG	1120	494	1.00 (0.81–1.24)	104	1.01 (0.66–1.54)	1.08 (0.68–1.69)
GG	538	235	0.85 (0.66–1.10)	50	0.95 (0.57–1.57)	1.28 (0.74–2.21)
P trend			0.23		0.84	0.39
G allele			0.93 (0.82–1.05)		0.98 (0.76–1.25)	1.13 (0.86–1.48)
		Colon cancer		Rectal cancer		Rectum versus colon
TT	600	118	1	36	1	1
TG	1120	233	1.14 (0.86–1.52)	66	1.03 (0.65–1.64)	0.90 (0.55–1.49)
GG	538	90	0.84 (0.59–1.18)	28	0.83 (0.48–1.45)	0.88 (0.48–1.62)
P trend			0.36		0.54	0.66
G allele			0.92 (0.78–1.09)		0.92 (0.70–1.20)	0.93 (0.69–1.27)
		Age of diagnosis >60 years		Age of diagnosis <60 years		<60 versus >60 years
TT	600	337	1	80	1	1
TG	1120	598	1.04 (0.85–1.28)	134	0.96 (0.65–1.40)	0.83 (0.52–1.33)
GG	538	263	0.83 (0.65–1.07)	67	0.95 (0.61–1.48)	1.19 (0.68–2.08)
P trend			0.18		0.81	0.63
G allele			0.92 (0.82–1.04)		0.97 (0.78–1.21)	1.07 (0.81–1.42)

[a]ORs and P-values are adjusted for age at sample collection, race, gender, regular aspirin use, regular NSAIDs use, BMI, physical activity, history of CRC in a parent or sibling, smoking status, alcohol consumption, consumption of beef, pork or lamb as a main dish, energy-adjusted calcium and folate intake and type of sample (more details in the text).
[b]BH-adjusted P-value = 0.0014.
[c]Log-additive model, representing the OR for each additional G allele as compared with TT.

with pT3-4 stage was 65.7% for cases of CRC with two variant alleles, 60.1% for cases of CRC with one variant allele, compared with 56.3% for cases of CRC with no variant alleles of rs4939827 (Mantel–Haenszel *P*-value = 0.018). The rs4939827 SNP was not significantly differentially associated with any of other evaluated clinical and pathological phenotypes, including nodal status, presence of distant metastases, tumor grade, anatomic location and age at diagnosis (Table II).

We also examined rs4939827 genotype according to molecular subtypes among 658 cases for whom we had available tumor tissue data. Because rs4939827 is located in an intronic region of *SMAD7*, which modulates TGFB1 signaling, we evaluated rs4939827 according to promoter methylation of the *RUNX3* gene, which is related to the TGFB1 pathway. The G allele of rs4939827 was associated with a lower CRC risk in tumors without methylation of *RUNX3* (multivariate OR, 0.84; 95% CI 0.71–0.99, *P* = 0.035). In contrast, there was a suggestive, although not statistically significant, increased risk of tumors with methylation of *RUNX3* associated with the minor allele of rs4939827 (multivariate OR, 1.27; 95% CI 0.94–1.74, *P* = 0.12) (Table III). The difference between rs4939827 and risk of tumors with methylation of *RUNX3* compared with tumors without methylation of *RUNX3* was statistically significant after adjustment for multiple comparisons (*P* for heterogeneity = 0.0053, BH-corrected *P*-value = 0.037). The risk of CRC associated with rs4939827 also appeared to be modified by *BRAF* mutational status. However, the *P* for heterogeneity was 0.021, non-significant after adjustment for multiple comparisons (BH-corrected *P*-value = 0.10). The association between the rs4939827 SNP and CRC did not significantly differ according to any of the other markers examined, including CIMP status, LINE-1 methylation, *KRAS* mutation, *PIK3CA* mutation, MSI status and TP53 mutation.

RUNX3 methylation was associated with a higher risk of pT3 and pT4 tumors (multivariate OR, 2.12; 95% CI 1.18–3.80, *P* = 0.012) even after adjusting for rs4939827. The multivariate ORs estimating the indirect effect of rs4939827 on risk of pT3 and pT4 tumors was 1.05 (95% CI 0.96–1.15, *P* = 0.32) for one variant allele and 1.50 (95% CI 0.44–5.10, *P* = 0.51) for two variant alleles (Table IV). Given the width of the CIs, we cannot exclude a possible indirect effect of rs4939827 through *RUNX3* methylation on pT stage. The multivariate ORs that estimate the direct effect of rs4939827 were 1.96 (95% CI 1.18–3.25, *P*-value = 0.009) for one variant allele and 4.46 (95% CI 1.19–16.6, *P*-value = 0.038) for two variant alleles. There was no evidence of interaction between the *SMAD7* variant rs4939827 and *RUNX3* methylation in either the additive scale (RERI = 0.48; 95% CI −1.42 to 2.37, *P*-value = 0.62) or multiplicative scale (OR, 0.93; 95% CI 0.39–2.19, *P*-value = 0.87).

Discussion

In this large study of 1509 cases of CRC and 2307 controls nested in two prospective cohorts, the CRC-susceptibility locus *SMAD7* intronic rs4939827 was associated with a lower risk of CRCs with pT1 and pT2 stage but not pT3 and pT4 stage. Hence, among individuals diagnosed with CRC, those with at least one G allele had 1.5-fold higher odds of having a pT3 or pT4 tumor compared with a pT1 or pT2 tumor. This finding may explain in part observed associations of the G allele of rs4939827 with lower overall risk of incident CRC (9), but worsened survival after diagnosis (10,25).

This study represents a strategy of investigations, which has been recently termed 'molecular pathological epidemiology' (MPE) (20,26). MPE is conceptually based on inherent heterogeneity of a disease, which is typically regarded as a single entity in traditional epidemiology studies, including GWAS (20,26). MPE can decipher how risk factors are associated with specific alterations in molecular pathways in cancer. Moreover, the MPE design can be used to help shed insight into the function of susceptibility variants identified by GWAS based upon their association with specific molecular subtypes of CRC (20).

The seemingly contrary associations of this SNP in *SMAD7* with decreased risk of incident disease but poorer outcomes in patients with established disease may be due to *SMAD7*'s known involvement in modulating the TGFB1 pathway. In normal epithelium, TGFB1 functions as a tumor suppressor through induction of cell arrest and inhibition of cell proliferation. However, once cells are resistant to TGFB1-mediated proliferative inhibition (i.e. in established tumors), TGFB1 appears to promote metastasis by enhancing angiogenesis and extracellular matrix disruption and inhibiting infiltrating tumor immune cells. A role for rs4939827 in the TGFB1 pathway is further supported by our findings of significant association of rs4939827 with *RUNX3* methylation status in the tumors. *RUNX3* is a Runt domain transcription factor 3 involved in TGFB1 signaling by interaction with SMAD transcription factors and is considered a suppressor of solid tumors. The *RUNX3* promoter is commonly aberrantly methylated in a CpG island in CRC (27–29), leading to gene inactivation.

Differential methylation of *RUNX3* according to rs498327 could plausibly explain the worsened survival among individuals with CRC who have a variant G allele (30). In addition to TGFB1, *RUNX3* is involved in WNT regulation by forming a ternary complex with TCF4 and CTNNB1 (β-catenin) (31). Both TGFB1 and WNT signaling are involved in the induction of epithelial-mesenchymal transition, a process that mediates invasion and metastasis in CRC. However, our mediation analysis does not suggest that the association between rs4939827 on risk of CRC according to pT stage is primarily related to *RUNX3*. Nonetheless, the mediation analysis should be interpreted in the context of some limitations (22), including the assumption of a lack of other, strong unmeasured confounders.

Previous studies of CRC-susceptibility variants and tumor phenotype have observed only a few significant differential associations between rs4939827 and CRC according to other clinical phenotype or molecular features. A case-only analysis of 1531 cases did not find any association between this variant and pT3-4 compared with pT1–2-staged tumors (*P* = 0.94) (32). In a study of 1096 patients from the Epicolon I cohort (33), the G allele of rs4939827 was significantly associated with well-differentiated tumors under a log-additive model (HR, 0.67; *P*-value = 0.027). However, this association was not replicated in a validation cohort, EPICOLON II (34). Neither of these two studies found any association between rs4939827 and other tumor features, including grade of differentiation, stage or tumor site. On the other hand, two studies have observed that the G allele of rs4939827 increased the risk of harboring a rectal tumor as compared with colon tumors (35,36).

We also examined several other molecular markers other than *RUNX3* and did not observe strong differences in the association with rs4939827. Our findings are consistent with Slattery *et al*., who did not observe significant heterogeneity in associations of rs4939827 with CIMP status, MSI, *KRAS* or p53 mutational status (36). Nonetheless, in our study, it is notable that *BRAF*-status did appear to be differentially associated with rs4939827, despite the lack of a significant *P* for heterogeneity after correction for multiple comparisons. An interplay between TGFB1 and *BRAF* mutations is biologically plausible (37), and *BRAF* mutations are strongly associated with CRC prognosis. Thus, given the low frequency of *BRAF* mutations in CRC, it is possible that statistically significant heterogeneity may be evident with a larger sample size.

Our study has several strengths. First, we used prospectively collected, biennially updated, detailed data on CRC risk factors over long-term follow-up. This permitted us to account for the main potential confounders of our associations. Second, our case-control study was nested within two large well-characterized cohorts within which matched controls were selected from the same cohort from which the case developed, minimizing the likelihood of population stratification or selection bias. Third, our findings were consistent between two independent cohorts. Moreover, we have previously demonstrated a consistent association between rs498327 and CRC and overall survival that has been validated by results in other populations (10). Last, among a large number of participants, we had germline DNA as well as available tumor tissue to examine the expression of molecular

Table III. Association of rs4939827 with tumor molecular characteristics[a]

	Controls	Cases	OR (95% CI)	Cases	OR (95% CI)	Case-only analysis
		RUNX3 promoter unmethylated		*RUNX3* promoter methylated		Methylation versus unmethylation
TT	600	142	1	25	1	1
TG	1120	254	1.07 (0.82–1.40)	63	1.40 (0.79–2.50)	1.43 (0.74–2.78)
GG	538	95	0.66 (0.47–0.94)	35	1.65 (0.87–3.12)	2.97 (1.39–6.35)
P trend			0.04		0.12	0.0053[b]
G allele[c]			0.84 (0.71–0.99)		1.27 (0.94–1.74)	1.74 (1.18–2.56)
		WT *BRAF*		Mutant *BRAF*		Mutant versus WT *BRAF*
TT	600	162	1	19	1	1
TG	1120	286	1.05 (0.81–1.35)	41	1.09 (0.53–2.24)	1.86 (0.77–4.48)
GG	538	126	0.80 (0.58–1.09)	24	1.64 (0.75–3.58)	3.17 (1.19–8.47)
P trend			0.19		0.21	0.02
G allele			0.90 (0.78–1.05)		1.29 (0.86–1.93)	1.77 (1.09–2.88)
		LINE-1 methylation-high		LINE-1 methylation-low		Methylation-high versus low
TT	600	108	1	67	1	1
TG	1120	210	1.23 (0.91–1.66)	115	0.92 (0.63–1.33)	0.80 (0.51–1.27)
GG	538	101	1.13 (0.80–1.60)	43	0.57 (0.35–0.93)	0.55 (0.31–1.00)
P trend			0.48		0.03	0.05
G allele			1.06 (0.90–1.26)		0.78 (0.62–0.98)	0.75 (0.56–1.00)
		CIMP-low/negative		CIMP-high		CIMP-high versus low/ negative
TT	600	146	1	21	1	1
TG	1120	267	1.07 (0.82–1.40)	50	1.53 (0.78–3.00)	1.65 (0.76–3.59)
GG	538	108	0.76 (0.55–1.06)	24	1.41 (0.65–3.05)	2.27 (0.93–5.56)
P trend			0.15		0.40	0.07
G allele			0.89 (0.76–1.04)		1.17 (0.81–1.68)	1.50 (0.97–2.34)
		MSI-L/MSS		MSI-H		MSI-H versus MSI-L/MSS
TT	600	159	1	21	1	1
TG	1120	268	1.00 (0.77–1.29)	54	1.63 (0.85–3.14)	1.93 (0.95–3.90)
GG	538	120	0.79 (0.58–1.08)	26	1.47 (0.70–3.09)	1.99 (0.87–4.55)
P trend			0.16		0.33	0.10
G allele			0.90 (0.77–1.04)		1.19 (0.84–1.68)	1.40 (0.94–2.07)
		WT *KRAS*		Mutant *KRAS*		Mutant versus WT *KRAS*
TT	600	113	1	69	1	1
TG	1120	215	1.24 (0.91–1.67)	113	0.86 (0.60–1.22)	0.69 (0.44–1.09)
GG	538	93	0.94 (0.65–1.36)	55	0.77 (0.51–1.18)	0.87 (0.50–1.51)
P trend			0.85		0.23	0.51
G allele			0.98 (0.82–1.17)		0.88 (0.71–1.09)	0.91 (0.69–1.20)
		WT *PIK3CA*		Mutant *PIK3CA*		Mutant versus WT *PIK3CA*
TT	600	139	1	31	1	1
TG	1120	251	1.07 (0.81–1.40)	57	0.94 (0.56–1.58)	0.85 (0.48–1.52)
GG	538	120	0.90 (0.65–1.25)	18	0.62 (0.31–1.23)	0.64 (0.30–1.37)
P trend			0.58		0.19	0.26
G allele			0.96 (0.82–1.12)		0.81 (0.58–1.11)	0.81 (0.56–1.17)
		TP53 negative		TP53 positive		TP53 positive versus negative
TT	600	76	1	67	1	1
TG	1120	151	1.14 (0.81–1.61)	120	1.15 (0.78–1.69)	0.83 (0.50–1.39)
GG	538	66	0.86 (0.56–1.31)	51	0.84 (0.52–1.36)	0.81 (0.43–1.55)
P trend			0.54		0.56	0.50
G allele			0.94 (0.77–1.15)		0.93 (0.74–1.17)	0.90 (0.65–1.24)

[a]ORs and *P*-values are adjusted for age at sample collection, race, gender, regular aspirin use, regular NSAIDs use, BMI, physical activity, history of CRC in a parent or sibling, smoking status, alcohol consumption, consumption of beef, pork or lamb as a main dish, energy-adjusted calcium and folate intake and type of sample (more details in the text).
[b]BH-adjusted *P*-value = 0.0371.
[c]Log-additive model, representing the OR for each additional G allele as compared with TT.

markers, including *RUNX3*, which is directly relevant to the TGFB1 pathway. This permitted us to examine rs4939827 in relation to tumor subtypes with greater mechanistic specificity.

We acknowledge the limitations to our study. First, we did not have tumor specimens available for analysis for all of our cases. However, the risk factors in cases with available tumor tissue did not appreciably differ

Table IV. Mediation and interaction analysis of *RUNX*3 methylation in the association of rs4939817 with pT stage

Association with pT3/4 stage	OR (95% CI)		*P*-value	
	2.12 (1.18–3.80)		0.0120	
Mediation analysis	TG versus TT		GG versus TT	
	OR (95% CI)	*P*-value	OR (95% CI)	*P*-value
Direct effect	1.96 (1.18–3.25)	0.0088	4.46 (1.19–16.6)	0.038
Indirect effect	1.05 (0.96–1.15)	0.32	1.50 (0.44–5.10)	0.51
Marginal total effect	2.06 (1.22–3.46)	0.0068	6.70 (0.89–50.35)	0.064
Proportion mediated, %	9.3		39.2	
Interaction analysis				
Additive	RERI[a] (95% CI)		*P*-value	
	0.48 (−1.42 to 2.37)		0.62	
Multiplicative	OR (95% CI)		*P*-value	
	0.93 (0.39–2.19)		0.87	

[a]RERI (also known as 'interaction contrast ratio').

from those in cases without tumor tissue (38). Second, although we did correct for multiple comparisons in our primary analyses, we cannot rule out the possibility that the associations we observed with rs4939827 and tumor subtypes represent false-positive findings. However, the biological plausibility of our findings and the consistent association of this allele with CRC survival increase the likelihood that our observed associations are true. Third, we did include some cases of CRC in which participants provided DNA samples after diagnosis. However, for analyses of survival, we restricted our cohort to incident cases diagnosed after DNA was collected to minimize any effect of survival bias.

In summary, individuals with the rs4939827 CRC-susceptibility locus diagnosed with CRC tend to develop tumors with greater invasiveness (pT stage). Moreover, we also observed a differential association of rs4939827 with *RUNX3* methylation status, supporting an effect of rs4939827 or causal variants tagged by this SNP on carcinogenesis mediated through the TGFB1 pathway. These findings support present understanding of the dual function of TGFB1/SMAD7 pathways in inhibiting early tumorigenesis yet facilitating metastasis. Taken together, these results could explain, at least in part, the lower risk of CRC associated with the G allele of rs4939827 yet poorer survival (10).

Funding

National Institutes of Health (NIH) / National Cancer Institute (NCI) (grant CA137178, CA059045, CA151993, CA055075, CA087969, CA127003, CA094880, CA154337); 'La Caixa' fellowship to X.G.A.; A.T.C. is a Damon Runyon Cancer Foundation Clinical Investigator.

Acknowledgements

We wish to acknowledge Patrice Soule and Hardeep Ranu for genotyping at the Dana-Farber Harvard Cancer Center High Throughput Polymorphism Core, under the supervision of Immaculata Devivo, as well as Carolyn Guo for programming assistance. We also thank the participants of the Health Professionals Follow-up Study and Nurses' Health Study and the following state cancer registries: AL, AZ, AR, CA, CO, CT, DE, FL, GA, ID, IL, IN, IA, KY, LA, ME, MD, MA, MI, NE, NH, NJ, NY, NC, ND, OH, OK, OR, PA, RI, SC, TN, TX, VA, WA and WY.

Contribution

All the authors have contributed significantly to the submitted work and have read and approved the final version of this manuscript.

Conflict of Interest Statement: None declared.

References

1. Tenesa,A. *et al.* (2010) Ten common genetic variants associated with colorectal cancer risk are not associated with survival after diagnosis. *Clin. Cancer Res.*, **16**, 3754–3759.
2. Houlston,R.S. *et al.* (2010) Meta-analysis of three genome-wide association studies identifies susceptibility loci for colorectal cancer at 1q41, 3q26.2, 12q13.13 and 20q13.33. *Nat. Genet.*, **42**, 973–977.
3. Houlston,R.S. *et al.* (2008) Meta-analysis of genome-wide association data identifies four new susceptibility loci for colorectal cancer. *Nat. Genet.*, **40**, 1426–1435.
4. Tomlinson,I.P. *et al.* (2008) A genome-wide association study identifies colorectal cancer susceptibility loci on chromosomes 10p14 and 8q23.3. *Nat. Genet.*, **40**, 623–630.
5. Tomlinson,I.P. *et al.* (2011) Multiple common susceptibility variants near BMP pathway loci GREM1, BMP4, and BMP2 explain part of the missing heritability of colorectal cancer. *PLoS Genet.*, **7**, e1002105.
6. Kocarnik,J.D. *et al.* (2010) Characterization of 9p24 risk locus and colorectal adenoma and cancer: gene-environment interaction and meta-analysis. *Cancer Epidemiol. Biomarkers Prev.*, **19**, 3131–3139.
7. Hutter,C.M. *et al.* (2010) Characterization of the association between 8q24 and colon cancer: gene-environment exploration and meta-analysis. *BMC Cancer*, **10**, 670.
8. Dunlop,M.G. *et al.* (2012) Common variation near CDKN1A, POLD3 and SHROOM2 influences colorectal cancer risk. *Nat. Genet.*, **44**, 770–776.
9. Peters,U. *et al.* (2012) Meta-analysis of new genome-wide association studies of colorectal cancer risk. *Hum. Genet.*, **131**, 217–234.
10. Phipps,A.I. *et al.* (2012) Association between colorectal cancer susceptibility loci and survival time after diagnosis with colorectal cancer. *Gastroenterology*, **143**, 51–4.e4.
11. Stampfer,M.J. *et al.* (1984) Test of the National Death Index. *Am. J. Epidemiol.*, **119**, 837–839.
12. Pai,J.K. *et al.* (2004) Inflammatory markers and the risk of coronary heart disease in men and women. *N. Engl. J. Med.*, **351**, 2599–2610.
13. Morikawa,T. *et al.* (2011) Association of CTNNB1 (beta-catenin) alterations, body mass index, and physical activity with survival in patients with colorectal cancer. *JAMA*, **305**, 1685–1694.
14. Ogino,S. *et al.* (2007) Evaluation of markers for CpG island methylator phenotype (CIMP) in colorectal cancer by a large population-based sample. *J. Mol. Diagn.*, **9**, 305–314.
15. Ogino,S. *et al.* (2009) CpG island methylator phenotype, microsatellite instability, BRAF mutation and clinical outcome in colon cancer. *Gut*, **58**, 90–96.
16. Ogino,S. *et al.* (2008) A cohort study of tumoral LINE-1 hypomethylation and prognosis in colon cancer. *J. Natl. Cancer Inst.*, **100**, 1734–1738.
17. Ogino,S. *et al.* (2005) Sensitive sequencing method for KRAS mutation detection by Pyrosequencing. *J. Mol. Diagn.*, **7**, 413–421.
18. Ogino,S. *et al.* (2009) PIK3CA mutation is associated with poor prognosis among patients with curatively resected colon cancer. *J. Clin. Oncol.*, **27**, 1477–1484.
19. Morikawa,T. *et al.* (2012) Tumor TP53 expression status, body mass index and prognosis in colorectal cancer. *Int. J. Cancer*, **131**, 1169–1178.
20. Ogino,S. *et al.* (2011) Molecular pathological epidemiology of colorectal neoplasia: an emerging transdisciplinary and interdisciplinary field. *Gut*, **60**, 397–411.
21. Vanderweele,T.J. *et al.* (2010) Odds ratios for mediation analysis for a dichotomous outcome. *Am. J. Epidemiol.*, **172**, 1339–1348.

22. Valeri,L. *et al.* Mediation analysis allowing for exposure-mediator interactions and causal interpretation: theoretical assumptions and implementation with SAS and SPSS macros. *Psychol. Methods*, in press.
23. Knol,M.J. *et al.* (2007) Estimating interaction on an additive scale between continuous determinants in a logistic regression model. *Int. J. Epidemiol.*, **36**, 1111–1118.
24 Benjamini,Y. *et al.* (1995) Controlling the false discovery rate: a practical and powerful approach to multiple testing. *J. R. Stat. Soc. Series B. Stat. Methodol.*, **57**, 289–300.
25. Passarelli,M.N. *et al.* (2011) Common colorectal cancer risk variants in SMAD7 are associated with survival among prediagnostic nonsteroidal anti-inflammatory drug users: a population-based study of postmenopausal women. *Genes. Chromosomes Cancer*, **50**, 875–886.
26. Ogino,S. *et al.* (2010) Lifestyle factors and microsatellite instability in colorectal cancer: the evolving field of molecular pathological epidemiology. *J. Natl. Cancer Inst.*, **102**, 365–367.
27. Ahlquist,T. *et al.* (2008) Gene methylation profiles of normal mucosa, and benign and malignant colorectal tumors identify early onset markers. *Mol. Cancer*, **7**, 94.
28. Soong,R. *et al.* (2009) The expression of RUNX3 in colorectal cancer is associated with disease stage and patient outcome. *Br. J. Cancer*, **100**, 676–679.
29. Subramaniam,M.M. *et al.* (2009) RUNX3 inactivation in colorectal polyps arising through different pathways of colonic carcinogenesis. *Am. J. Gastroenterol.*, **104**, 426–436.
30. Slattery,M.L. *et al.* (2011) Genetic variation in the transforming growth factor-β signaling pathway and survival after diagnosis with colon and rectal cancer. *Cancer*, **117**, 4175–4183.
31. Ito,K. *et al.* (2008) RUNX3 attenuates beta-catenin/T cell factors in intestinal tumorigenesis. *Cancer Cell*, **14**, 226–237.
32. Ghazi,S. *et al.* (2010) Colorectal cancer susceptibility loci in a population-based study: associations with morphological parameters. *Am. J. Pathol.*, **177**, 2688–2693.
33. Piñol,V. *et al.* (2005) Accuracy of revised Bethesda guidelines, microsatellite instability, and immunohistochemistry for the identification of patients with hereditary nonpolyposis colorectal cancer. *JAMA*, **293**, 1986–1994.
34. Abulí,A. *et al.* (2010) Susceptibility genetic variants associated with colorectal cancer risk correlate with cancer phenotype. *Gastroenterology*, **139**, 788–96, 796.e1.
35. Lubbe,S.J. *et al.* (2012) Relationship between 16 susceptibility loci and colorectal cancer phenotype in 3146 patients. *Carcinogenesis*, **33**, 108–112.
36. Slattery,M.L. *et al.* (2010) Increased risk of colon cancer associated with a genetic polymorphism of SMAD7. *Cancer Res.*, **70**, 1479–1485.
37. Fleming,Y.M. *et al.* (2009) TGF-beta-mediated activation of RhoA signalling is required for efficient (V12)HaRas and (V600E)BRAF transformation. *Oncogene*, **28**, 983–993.
38. Chan,A.T. *et al.* (2007) Aspirin and the risk of colorectal cancer in relation to the expression of COX-2. *N. Engl. J. Med.*, **356**, 2131–2142.

Received August 23, 2012; revised October 11, 2012; accepted October 18, 2012

4.2 Second publication

Colon cancer cells colonize the lung from established liver metastases through p38 MAPK signalling and PTHLH

Jelena Urosevic, Xabier Garcia-Albeniz *(co-first author)*, Evarist Planet, Sebastian Real, Maria Virtudes Cespedes, Marc Guiu, Esther Fernandez, Anna Bellmunt, Sylwia Gawrzak, Milica Pavlovic, Ramon Mangues, Ignacio Dolado, Francisco M. Barriga, Cristina Nadal, Nancy Kemeny, Eduard Batlle, Angel R. Nebreda and Roger R. Gomis.

Nature Cell Biology *2014 Jul;16(7):685-94. doi: 10.1038/ncb2977.*

4.2.1 Summary

The metastatic pattern of advanced CRC is somehow homogeneous. Liver is the most frequently affected organ, followed by the lung, peritoneum and bone. We studied the mechanisms driving the metastatic spread in CRC, focusing in the MAPK pathway. We developed *in vivo* a highly metastatic cell line using a *KRAS*-mutated cell line (SW620) using an ortothopic xenograft mouse model. First we introduced in these cells an expression vector for luciferase, which allowed us to monitor the kinetics of emergence of liver metastatic lesions by quantitative bioluminescence imaging. The SW620 luciferase-expressing cells were inoculated into portal circulation of immunodeficient mice via intrasplenic injection followed by splenectomy, in order to isolate cell populations that target the liver. Second, the SW620-derived liver metastasis were expanded in culture and the resulting population (Liver Metastatic derivative, LiM1) were subjected to a second round of in vivo selection, producing the LiM2 cell population that showed a significant increase in liver and lung metastatic activity. As opposed to the metastasis originating from the parental cell line that showed wide areas of necrosis, the LiM2 cells showed a higher stromal response.

Comparative transcriptomic analysis identified 194 genes differentially expressed between the parental and the highly metastatic cell line. This colon cancer metastatic (CCM) gene set was contrasted against a cohort of 267 patients with stage I-III CRC, and those genes that were upregulated were associated with shorter time to relapse. We investigated the signaling pathways regulating the expression of our set of genes with increased metastatic capacity. Using KEGG annotated signaling pathways, we found pathways of nitrogen metabolism, cell adhesion molecules and mitogen-activated

protein kinases (MAPKs). These three pathways are relevant in the metastatic process by mediating nucleotide synthesis, invasion/migration and modulation of cellular responses respectively. We focused on the MAPKs given the *KRAS*-mutated status of our cell line (and because patients harboring certain mutations in KRAS/BRAF have fewer therapeutic options that patients without them), finding that the activating phosphorylation of ERK1/ERK2 was increased, the p38 MAPKs was reduced and the phosphorylation of JNKs did not change. Downregulation of ERK2 (but not of ERK1) in the highly metastatic cell line reverted its metastatic capacity to the liver, but not to the lung in our mice model. We thus hypothesized that the ability to metastasize the lung by the highly metastatic derivative had to be driven by other mechanism.

The analysis of clinical samples evidenced that tumor biopsies with low phospho-38 MAPK were associated with metastasis to the lung but not to other organs. Treating mice harboring liver metastasis from the parental cell line with a p38 MAPK specific inhibitor produced an increase in the percentage of mice with lung metastasis. We validated this increased capacity to generate lung metastasis with the inhibition of phospho-38 MAPK using a different cell line (HCT116) and a different experimental setting (mice intracecum injection). Conversely, activation of the p38 MAPK pathway by expression of MKK6^{EE} (MKK6 is a MAP kinase-kinase that phosphorylates and activates p38 MAP kinase) diminished the lung metastatic capacity of the HCT116 cell line. Of note, inhibition of phospho-38 MAPK did not affect proliferation or apoptosis.

The expression of parathyroid hormone-like hormone (PTHLH) was upregulated (3.3 fold) in our highly metastatic derivative and was inversely correlated with the expression of *MKK6* in CRC primary tumors. Downregulation of PHTLH in the highly metastatic derivative decreased its capacity to colonize the lung without decreasing its capacity to colonize the liver after intra porta inoculation. Interestingly, tail vein (draining directly to the lungs) injections of the highly metastatic derivative did not yield any lung metastasis and silencing PHTLH in LiM2 cells did not affect its growth when injected directly into the lung. This suggested that the role of PTHLH in regulating lung metastasis did not depended on growth promotion but more probably on extravasation. This was supported by an experiment where we injected in the tail vein LiM2 cells overexpressing or not PTHLH and quantified extravasation 48 hours later. Mice injected with LiM2 cells overexpressing PTHLH presented a five-fold increase in the number of cells extravasated in the lungs.

We finally evidenced that PTHLH induced apoptosis of human pulmonary endothelial cells (HPEC) by increasing Ca^{+} levels that in turn induces mobilization of the apoptosis-inducing factor mitochondrion-associated 1 (AIFM1), from the mitochondria to the cytosol, a caspase-independent cell death mechanism. This disrupts the lung vasculature increasing the permeability of the lung to metastatic cells.

nature cell biology

Colon cancer cells colonize the lung from established liver metastases through p38 MAPK signalling and PTHLH

Jelena Urosevic[1,8], Xabier Garcia-Albéniz[1,2,8], Evarist Planet[1], Sebastián Real[1], María Virtudes Céspedes[3,4], Marc Guiu[1], Esther Fernandez[1], Anna Bellmunt[1], Sylwia Gawrzak[1], Milica Pavlovic[1], Ramon Mangues[3,4], Ignacio Dolado[1,7], Francisco M. Barriga[1], Cristina Nadal[2], Nancy Kemeny[5], Eduard Batlle[1,6], Angel R. Nebreda[1,6] and Roger R. Gomis[1,6,9]

The mechanisms that allow colon cancer cells to form liver and lung metastases, and whether *KRAS* mutation influences where and when metastasis occurs, are unknown. We provide clinical and molecular evidence showing that different MAPK signalling pathways are implicated in this process. Whereas ERK2 activation provides colon cancer cells with the ability to seed and colonize the liver, reduced p38 MAPK signalling endows cancer cells with the ability to form lung metastasis from previously established liver lesions. Downregulation of p38 MAPK signalling results in increased expression of the cytokine PTHLH, which contributes to colon cancer cell extravasation to the lung by inducing caspase-independent death in endothelial cells of the lung microvasculature. The concerted acquisition of metastatic traits in the colon cancer cells together with the sequential colonization of liver and lung highlights the importance of metastatic lesions as a platform for further dissemination.

Colorectal cancer (CRC) metastasis follows an ordered and hierarchical pattern. CRC cells initially spread to the lymph nodes and peritoneal area. When metastases to the liver occur, a substantial number of patients develop also lung and less frequently bone or brain metastases[1]. Patients with metastasis are treated with systemic chemotherapy, mostly in a palliative manner. Nevertheless, in selected patients with isolated liver metastasis, increased 5 year survival can be achieved by multimodal treatment that includes combination of surgery with modern chemotherapy[2]. However, only about 25% of patients can benefit from this type of treatment and the presence of metastases in other organs is, in most cases, a contraindication for resection[3]. After liver, lung is the most frequently involved organ[4,5], which highlights the need to understand mechanisms of CRC lung metastasis to further improve disease control. The metastatic pattern in CRC could be partially explained by the fact that the gut-draining mesenteric vein together with the splenic vein forms the portal system that drains directly into the liver. Beyond this simplistic anatomical interpretation, mechanisms that regulate intravasation, survival in portal circulation, infiltration and colonization of the liver are also likely to contribute to the propensity of CRC metastasis for the liver[6]. In addition, there is no explanation for why liver metastasis is accompanied by lung colonization only in some patients. Interestingly, CRC patients who underwent primary tumour resection show a different pattern of relapse depending on the *KRAS* mutational status[7]. In particular, *KRAS*-mutated CRC has a higher incidence of lung metastasis. This phenomenon suggests a *KRAS*-linked mechanism that favours targeting of colon tumour cells to the lungs[8].

RESULTS

An experimental model of colon cancer metastasis

To investigate the hierarchical mechanisms of liver and subsequent lung metastasis in *KRAS*-mutated CRC, we established an orthotopic xenograft mouse model to select for human CRC cells with enhanced ability to colonize the liver and the lungs[9,10]. We focused on the human colon adenocarcinoma cell line SW620, which harbours the $KRAS^{G12V}$ mutation. First, we introduced in these cells an expression vector for

[1]Institute for Research in Biomedicine (IRB Barcelona), 08028 Barcelona, Spain. [2]Institut de Malalties Hemato-Oncològiques, Hospital Clínic de Barcelona-IDIBAPS and CIBER-EHD), 08036 Barcelona, Spain. [3]Grup d'Oncogenesi i Antitumorals, Hospital de Sant Pau, 08026 Barcelona, Spain. [4]Grup d'Oncogenesi i Antitumorals, Institute of Biomedical Research (IIB Sant Pau), Network Research Center on Bioengineering, Biomaterials and Nanomedicine (CIBER-BBN), 08026 Barcelona, Spain. [5]Memorial Sloan-Kettering Cancer Center, 10065 New York, USA. [6]Institució Catalana de Recerca i Estudis Avançats (ICREA), 08010 Barcelona, Spain. [7]Molecular Partners AG, 8952 Schlieren, Switzerland. [8]These authors contributed equally to this work. [9]Correspondence should be addressed to R.R.G. (e-mail: roger.gomis@irbbarcelona.org)

Received 17 July 2013; accepted 28 April 2014; published online 1 June 2014; DOI: 10.1038/ncb2977

luciferase, which allowed us to monitor the kinetics of emergence of liver metastatic lesions by quantitative bioluminescence imaging. The SW620 luciferase-expressing cells (parental) were inoculated into the portal circulation of immunodeficient mice through intrasplenic injection followed by splenectomy, to isolate cell populations that target the liver (Fig. 1a). The initial SW620-derived liver metastasis cells were expanded in culture and the resulting population (Liver Metastatic derivative, LiM1) was subjected to a second round of *in vivo* selection, producing the LiM2 cell population that showed a significant increase in liver metastatic activity (Fig. 1a–d). Within 10 weeks post inoculation of LiM2 cells, 15 out of 18 mice developed liver metastasis as opposed to 6 out of 18 injected with parental SW620 cells, suggesting that LiM2 cells acquired the ability to survive and adjust to the liver environment (Fig. 1b–d). Besides the increased ability to form liver metastasis, LiM2 cells also showed increased lung metastatic activity compared with parental SW620 cells (Fig. 1c,e), whereas peritoneal metastasis and ascites production were observed at lower but comparable rates in the two populations (Fig. 1c). Histological examination revealed that, in most cases, liver metastatic lesions derived from LiM2 cells developed stromal response, as opposed to the typical necrotic lesions derived from parental SW620 cells (Fig. 1d). Interestingly, LiM2 cells showed an increased invasive capacity *in vitro* compared with parental cells, suggesting the potential gain of metastatic features (Supplementary Fig. 1a). Furthermore, LiM2 cells also showed enhanced liver and lung metastatic capabilities in orthotopic mouse xenografts, whereas primary tumours grew similarly to the parental cell population, indicating that proliferation was not enhanced in LiM2 cells by the *in vivo* selection protocol (Supplementary Fig. 1b–d).

Deregulated MAPK signalling in colon cancer cells is associated with metastatic capacity

To investigate the molecular basis for aggressive concerted liver and lung metastatic behaviour of *KRAS*-mutated CRC cells, we performed transcriptomic analysis of the LiM2 and parental SW620 cell populations. Comparative genome-wide expression analysis yielded a list of 194 genes that were overexpressed or underexpressed at least 2.5-fold in the highly liver metastatic derivative LiM2 (Fig. 2a and Supplementary Table 1). This group of genes showed a concordant trend of regulation in metastatic derivatives and was named the colon cancer metastatic (CCM) gene set. We divided the CCM set of genes in two groups depending on whether their expression was upregulated or downregulated, and performed a cross-validation in a combined expression data set of 267 stage I–III clinically annotated human primary CRC tumours from three independent institutions (combined GSE17537 and GSE14333) (refs 11–13). The outcome of interest was time to recurrence after primary tumour retrieval. Using gene set enrichment analysis[14] (GSEA), we found a strong association between the upregulated CCM gene set and an increased risk of recurrence (hazard ratio, HR) on treatment (false discovery rate $<1\times10^{-6}$) (Fig. 2b). In contrast, the downregulated CCM gene set was not found to be significantly associated with reduced risk of recurrence (Supplementary Fig. 2a). Similar conclusions were obtained using GSE17537 and GSE14333 expression data sets independently. Survival analysis establishing subgroups by the median expression of the upregulated CCM gene set also revealed that this gene set was associated with reduced time to recurrence (Fig. 2b). Patients in the combined GSE17537 plus GSE14333 cohort with higher expression of the CCM gene set had an increment of 120% in the rate of recurrence along time (HR = 2.20, 95% CI 1.22–3.98, $P = 0.007$). Stage- and study-adjusted multivariate analysis yielded a HR of similar magnitude (HR = 1.88, 95% CI 1.04–3.36, $P = 0.037$) supporting the independent predictive capacity of the upregulated CCM gene set.

The integration of different oncogenic hits into particular signalling pathways and cellular functions is key to understand how the expression of groups of genes is collectively changed in metastatic cell populations. Thus, we investigated the signalling pathways predicted to regulate the expression of genes associated with increased metastatic capacity of LiM2 cells. By using BGSEA (ref. 14), we found several pathway-specific gene expression signatures (KEGG gene sets) that were differentially represented in the gene expression profiles of parental and LiM2 cells (Fig. 2c and Supplementary Table 2). These included the pathways of nitrogen metabolism, which supports nucleotide synthesis, cell adhesion molecules, which are fundamental for invasion and migration, and mitogen-activated protein kinases (MAPKs), which are important modulators of cellular responses[15] (Supplementary Table 2). We focused our attention on MAPK signalling alterations given the *KRAS*-mutated status of our initial CRC cell population. We analysed the activation status of the three main MAPK pathways in LiM2 cells and found that the activating phosphorylation of ERK1/ERK2 was increased, whereas that of p38 MAPKs was reduced (Fig. 2d and Supplementary Fig. 2b) and the phosphorylation of JNKs did not change (Fig. 2d). Significantly, when the relative levels of phosphorylated (active) ERK2 and ERK1 were compared, we found that phospho-ERK2 levels were specifically increased over phospho-ERK1 in CRC tumour biopsies from patients that developed metastasis within 2 years post-surgery compared with healthy mucosa from the same patients (distance from the tumour >10 cm) or to CRC tumours of patients free of metastasis (Fig. 2e). In 6 out of 7 primary tumours from CRC patients that developed metastasis, the phospho-ERK2/phospho-ERK1 ratio was above 1, whereas only 3 out of 13 non-metastatic CRC primary tumours had higher phospho-ERK2 than phospho-ERK1 levels (Fig. 2e, $P = 0.036$). Furthermore, in a set of 20 healthy mucosa samples obtained from the same patients as the CRC primary tumours, phospho-ERK2 levels were roughly equal to those of phospho-ERK1 in 80% of the samples similarly to non-metastatic CRC primary tumours (Fig. 2e). Next, we investigated the implication of the p38 MAPK pathway, which was downregulated in LiM2 cells, and found that the reduced levels of phosphorylated (active) p38 MAPK correlated with the downregulation of MKK6 (*MAP2K6*), a key activator of p38 MAPKs (ref. 16; Fig. 2f). Notably, in CRC primary tumours (pooled GSE17537 and GSE14333; $n = 267$ including stages I, II and III), *MKK6* messenger RNA expression levels were inversely associated with a high probability of relapse in the patients (Fig. 2g). These results support that high phospho-ERK2 and low phospho-p38 MAPK activities are associated with risk of metastasis in CRC patients.

ERK2 mediates colon cancer metastasis to the liver

Given that lung and liver metastatic events are co-selected in CRC patients (Supplementary Table 3), particularly bearing *KRAS*-mutated tumours, we wondered whether concerted changes in signalling

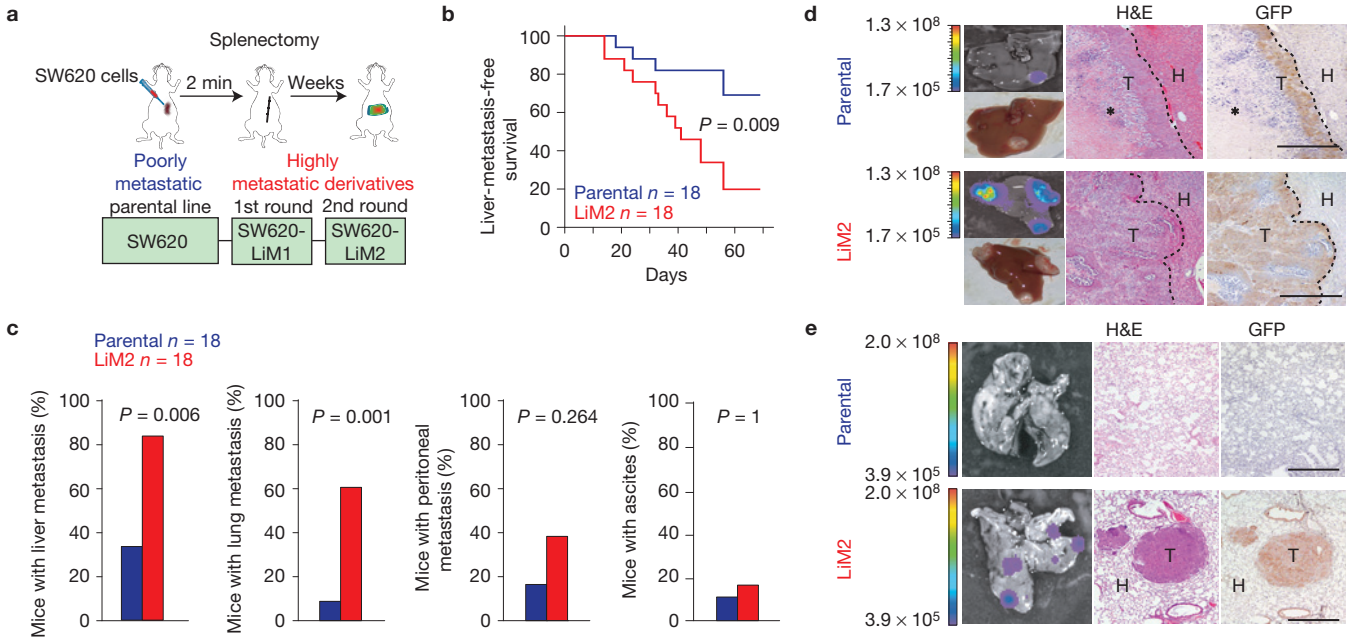

Figure 1 Isolation and characterization of liver metastatic derivatives from SW620 *KRAS*-mutated colorectal cancer (CRC) cells. (**a**) Schematic representation of *in vivo* selection and isolation of liver metastatic derivatives. (**b**) Liver-metastasis-free survival of mice injected intrasplenically with SW620 poorly metastatic (parental) or highly metastatic (LiM2) cells. $n = 18$ mice (pooled from two independent experiments) used per cell line. Log-rank test was used to determine statistical significance. (**c**) Percentage of liver metastasis, lung metastasis, peritoneal metastasis and ascites in mice on intrasplenic injections of SW620 parental and LiM2 cells determined post-mortem. Results were obtained using 18 mice (n) per cell line, and two-sided Fisher's exact test was used to calculate statistical significance. (**d**) Representative bioluminescent images and photographs of livers, and haematoxylin and eosin (H&E) and GFP staining of the liver sections. Scale bars, 500 μm. H, healthy tissue; T, tumour; *, necrotic area. (**e**) Representative bioluminescent images of lungs, and H&E and GFP staining of the lung sections from mice injected intrasplenically with SW620 parental and LiM2 cells. Scale bars, 500 μm.

pathways might be responsible for lung and liver colonization. Thus, we next evaluated the contribution of each MAPK signalling pathway to *KRAS*-mutated CRC liver and lung metastasis. As ERK2 activation was increased in primary tumours of patients that developed metastases, we downregulated the expression of ERK2 or ERK1 in LiM2 cells by means of two independent short hairpin RNAs (shRNAs; Fig. 3a and Supplementary Fig. 3a) Importantly, ERK2-knockdown significantly decreased the capacity of LiM2 cells to colonize the liver on intrasplenic injection into nude mice (Fig. 3a,b) whereas ERK1-knockdown had no effect (Supplementary Fig. 3b). Of note, neither ERK2 nor ERK1 depletion caused significant differences in orthotopic tumour growth, proliferation or apoptosis (Supplementary Fig. 3c–e). Interestingly, ERK2, but not ERK1, has been proposed to regulate, through changes in expression of the transcription factors FRA1 and ZEB1, a set of epithelial to mesenchymal transition responses in breast cancer cells[17], which has been associated with metastatic behaviour[6]. We confirmed that high *FRA1* expression levels were associated with relapse in the combined colon cancer primary tumour gene expression cohort described above (Supplementary Fig. 3f). These results support that ERK2 signalling drives liver metastasis in *KRAS*-mutated CRC cells.

p38 MAPK signalling mediates colon cancer metastasis to the lung

Unexpectedly, ERK2 downregulation did not affect the capacity of *KRAS*-mutated CRC cells to colonize the lungs (Fig. 3b). Thus, we reasoned that lung colonization was controlled by an independent mechanism. The p38 MAPK pathway has been implicated in several pro and anti-tumorigenic functions[15] and we found that human fresh CRC tumour biopsies with low phospho-p38 MAPK levels were associated with metastasis to lung but not to other tissues (Supplementary Fig. 4a). To test the potential contribution of this pathway to CRC metastasis to the lung, we used the p38 MAPK specific inhibitor PH-797804 (ref. 18). Parental cells were implanted directly into the liver of nude mice (one implant per mouse) and, when liver tumour photon flux signal reached a certain value ($>10^8$ photons s^{-1}), mice were randomly allocated to daily systemic treatment with either vehicle or PH-797804 (Fig. 3c). Fifteen days post treatment, an increase in lung metastatic events was observed in PH-797804-treated mice, whereas liver tumour growth was similar in both groups of mice (Fig. 3c). Histological analysis confirmed p38 MAPK inhibition in PH-797804-treated mice (Fig. 3c). As an alternative experimental setting to test the implication of the p38 MAPK pathway in liver and lung metastasis from the primary colon tumour, we used HCT116 cells. These *KRAS*-mutated CRC cells have the ability to form liver and lung metastasis when implanted orthotopically in nude mice as opposed to SW620 parental cells, which mainly produced lymph node metastasis[19] (Supplementary Fig. 1). We generated two derivatives of HCT116 cells expressing either shRNA to downregulate p38α (Fig. 3d), the most abundant p38 MAPK family member, or $MKK6^{EE}$ to constitutively activate the p38 MAPK pathway[16]. The two cell populations together with parental HCT116 cells were implanted

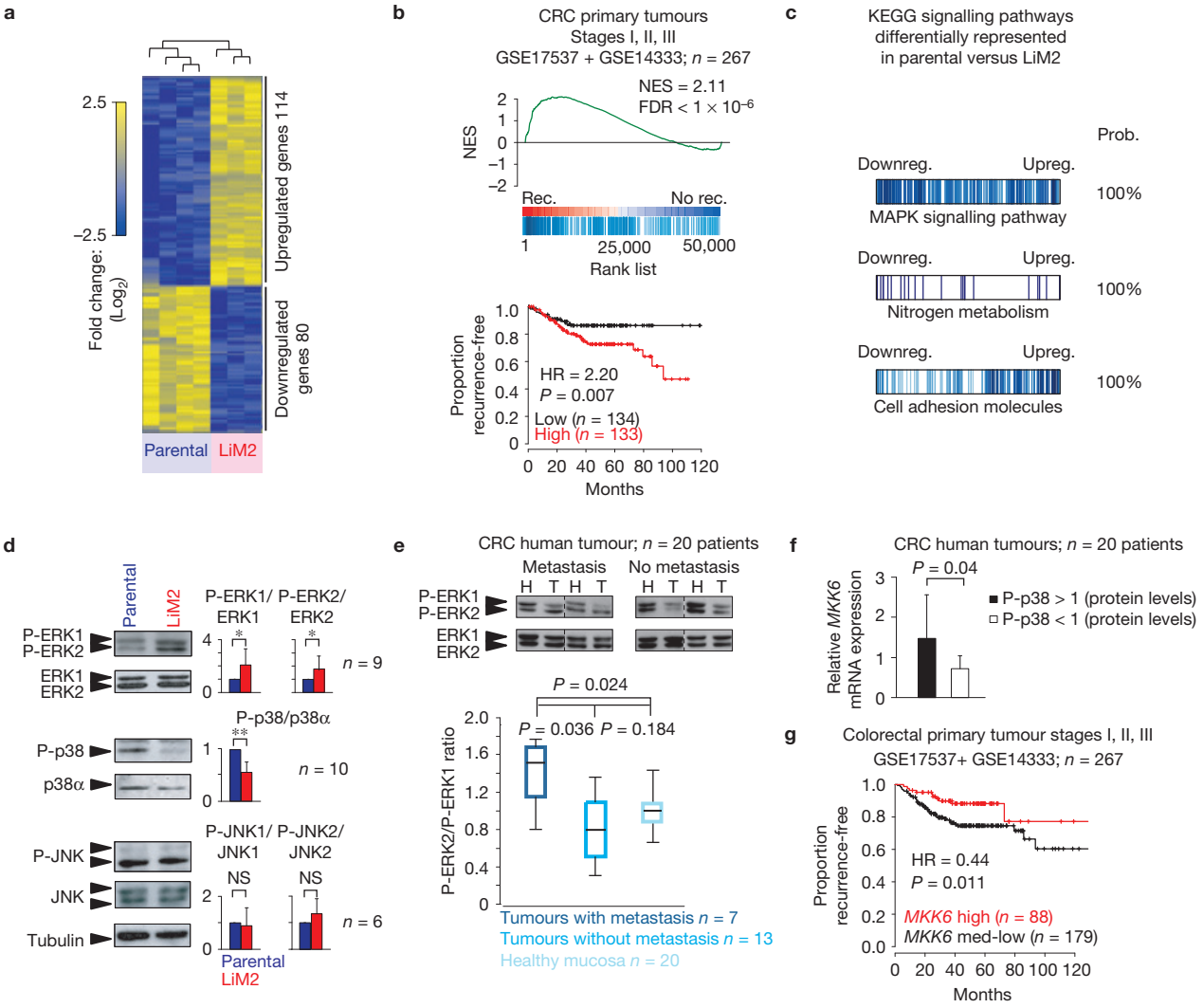

Figure 2 Liver metastatic derivatives from SW620 *KRAS*-mutated CRC cells present changes in MAPK signalling pathways. (**a**) Heat map representing differential gene expression pattern between parental and LiM2 cells, using 2.5-fold change as a cutoff. 114 genes were found upregulated (yellow) and 80 downregulated (blue) in LiM2 compared to parental cells. (**b**) Gene set enrichment analysis (GSEA; top) and Kaplan–Meier plot (bottom) representing association of HR of recurrence with the upregulated CCM gene set in the human colon cancer data set (pooled GSE17537 and GSE14333; $n=267$). NES, normalized enrichment score; FDR, false discovery rate; HR, hazard ratio. (**c**) KEGG analysis representing signalling pathways differentially represented in parental and LiM2 cells. (**d**) Left: Western blot of phosphorylated ERK1/2, p38 and JNK MAPKs (P-ERK1/2, P-p38, P-JNK) in SW620 parental and LiM2 cells. Total protein levels of ERK1/2, p38 and JNK were analysed. Tubulin was used as a loading control. Right: Quantification of phosphorylated ERK1/2, p38 and JNK MAPKs normalized to total amount of the same proteins. $n=9$ (ERK1/2), $n=10$ (p38) and $n=6$ (JNK) biological replicates pooled from at least three independent experiments. Plots represent average plus s.d. $^{*}P<0.05$; $^{**}P<0.001$; NS, not significant. (**e**) Top: Levels of phosphorylated ERK1/2 (P-ERK1/2) and total ERK1/2 proteins were analysed in samples of 20 primary CRC tumour samples (T) and their respective healthy mucosa (H) by western blotting and representative blots are shown. The dashed lines separate representative patient samples spliced from different gels. Bottom: Ratio of P-ERK2/P-ERK1 normalized to total amount of protein in samples of CRC tumours determined by western blotting; $n=7$ tumours with metastasis, $n=13$ tumours without metastasis, $n=20$ healthy mucosa. Statistics: two-tailed Mann–Whitney test; the box: 25th–75th percentile where the black line within the box represents the median; whiskers: 10th–90th percentile. (**f**) Association of *MKK6* mRNA levels with the ratio of phosphorylated p38 (P-p38) protein levels in CRC tumours from $n=20$ patients. Plots represent average plus s.d. (**g**) Kaplan–Meier curves representing the proportion of recurrence-free patients stratified according to *MKK6* mRNA levels in CRC patient samples (pooled GSE17537 and GSE14333; $n=267$). Statistical analysis was done using Cox proportional hazard's model in **b** and **g**, and two-tailed Student's *t*-test in **d** and **f**. Uncropped images of blots are shown in Supplementary Fig. 8.

orthotopically into the caecum, intestinal wall, of nude mice and 4 months later the mice were euthanized and primary tumours and metastatic lesions to the liver and lungs were quantified. No differences in proliferation and apoptosis rates in the primary tumours were detected among the groups (Supplementary Fig. 4b). Histological analysis of the number and area of liver metastasis showed no significant differences between control and p38α-knockdown cell populations, whereas the percentage of mice with liver metastasis was decreased in the latter group (Supplementary Fig. 4c,d). Interestingly, HCT116 cells with reduced levels of p38α showed a significantly higher capacity to colonize the lungs (Fig. 3d). Conversely, activation of the p38 MAPK pathway by expression of $MKK6^{EE}$ markedly

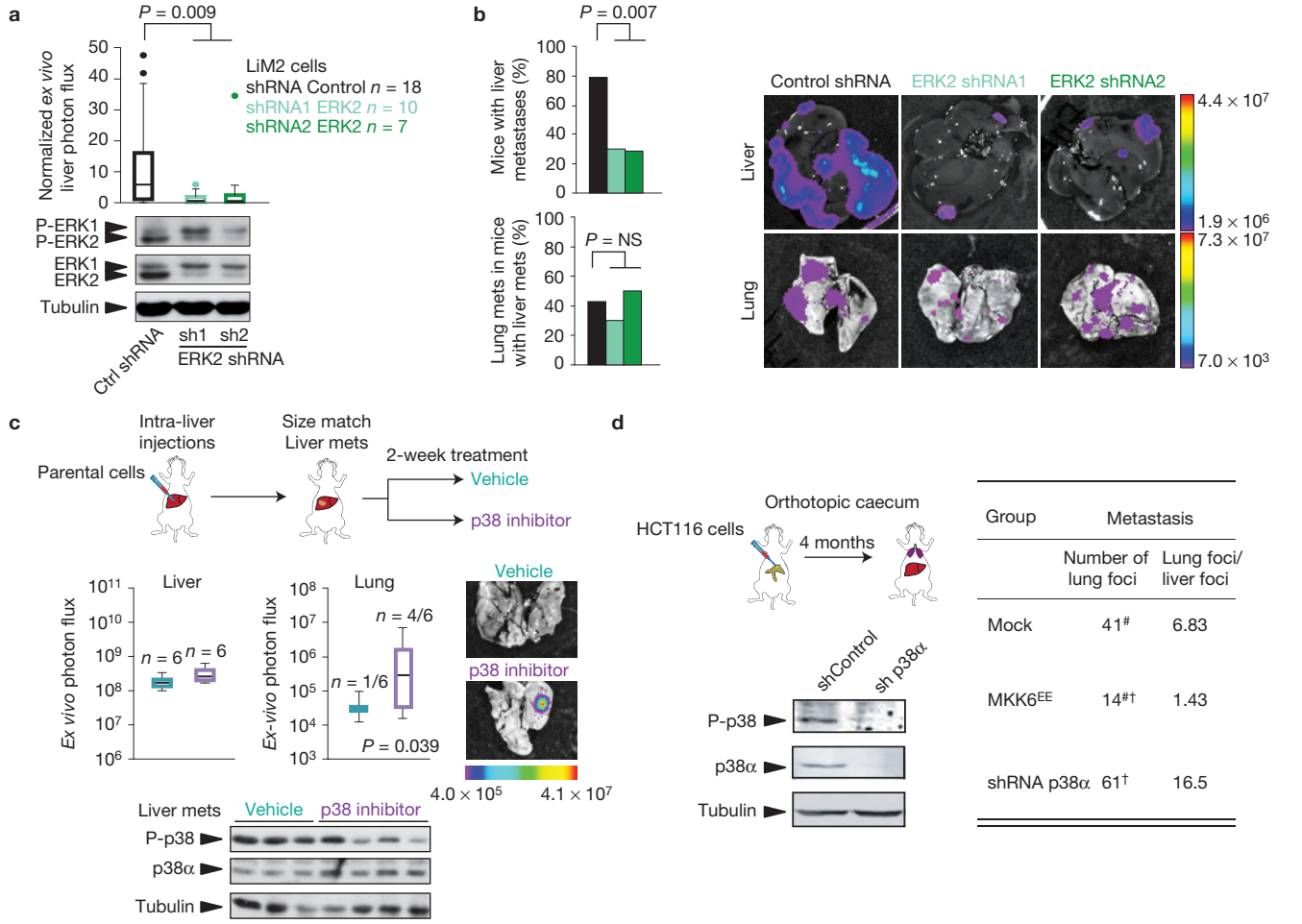

Group	Metastasis	
	Number of lung foci	Lung foci/ liver foci
Mock	41#	6.83
MKK6EE	14#†	1.43
shRNA p38α	61†	16.5

Figure 3 MAPK pathways mediate liver and lung metastasis in CRC. (**a**) Top: Normalized *ex vivo* liver photon flux of mice injected intrasplenically with LiM2 cells expressing control shRNA or two different ERK2 shRNAs. Bottom: ERK2 downregulation was confirmed by western blot analysis; $n=18$ (Control shRNA), $n=10$ (ERK2 shRNA1) and $n=7$ (ERK2 shRNA2) mice used in each group pooled from two independent experiments. Statistical significance was calculated using two-tailed Mann–Whitney test; the whiskers extend from min. to max. of 1.5 interquartile range (Tukey box plot). (**b**) Percentage of mice intrasplenically injected with LiM2 cells expressing the indicated shRNAs that developed liver metastasis (top) or lung metastasis (bottom). Representative bioluminescent images of livers and lungs are shown; *n*, number of mice used in each group is stated in **a**; statistical significance was calculated using two-sided Fisher's exact test. NS, not significant. (**c**) Top: SW620 parental cells were injected intra-liver and when lesions reached a size of $>10^8$ photons s^{-1}, mice were randomly separated into groups for two-week treatment with vehicle ($n=6$) or the p38 MAPK inhibitor PH-797804 ($n=6$). *Ex-vivo* liver and lung photon flux of the 2 groups of mice together with representative bioluminescent images of lungs are shown. One-sided chi-squared test was used to calculate statistical significance. The whiskers extend from the 10th to 90th percentile. Bottom: Western blot analysis of P-p38 MAPK and p38α protein levels in metastatic lesions on two-week treatment with vehicle or PH-797804. Tubulin was used as a loading control. (**d**) Left: Western blot analysis of P-p38 MAPK and p38α levels in HCT116 cells infected with lentivirus expressing the indicated shRNAs. HCT116 cells expressing p38α shRNAs or constitutively active $MKK6^{EE}$ were injected orthotopically into mice caecum, and the number of lung foci and the ratio between the number of lung and liver foci was determined. $n=5$ (Mock), $n=5$ ($MKK6^{EE}$) and $n=4$ (p38α shRNA) mice that developed lung metastasis in each group. $^{\#}P=0.043$, $^{\dagger}P=0.031$ indicate statistical significance between the groups. Statistical significance was calculated using one-tailed Mann–Whitney test. In **a** and **c** the box extends from the 25th to 75th percentile and the black line within the box represents the median. Uncropped images of blots are shown in Supplementary Fig. 8. Representative western blot images in **a** and **d** from three independent experiments.

reduced the ability of HCT116 cells to colonize the lungs, without changing the liver colonization capacity (Fig. 3d and Supplementary Fig. 4c,d) Collectively, these results suggest that the p38 MAPK pathway negatively regulates the ability of *KRAS*-mutated CRC cells to metastasize to the lung without affecting liver colonization.

p38 MAPK signalling controls *PTHLH* expression in metastatic colon cancer cells

Next we investigated the mechanism by which p38 MAPK signalling may drive lung metastasis from a previously established liver metastasis. First, we excluded any differences in apoptosis rates of metastatic emerging colonies due to variations in p38 MAPK activity in HCT116 or SW620 cell derivatives (Supplementary Fig. 4e,f). Next, we focused on genes under the control of this pathway that could potentially interact with the liver or lung stroma to trigger lung colonization. Among the genes that correlated with *MKK6* expression levels in CRC primary tumours ($p < 0.05$) and whose expression changed at least 1.7-fold in metastatic LiM2 over parental SW620 cells, the parathyroid hormone-like hormone (*PTHLH*) captured our attention as a gene that was upregulated

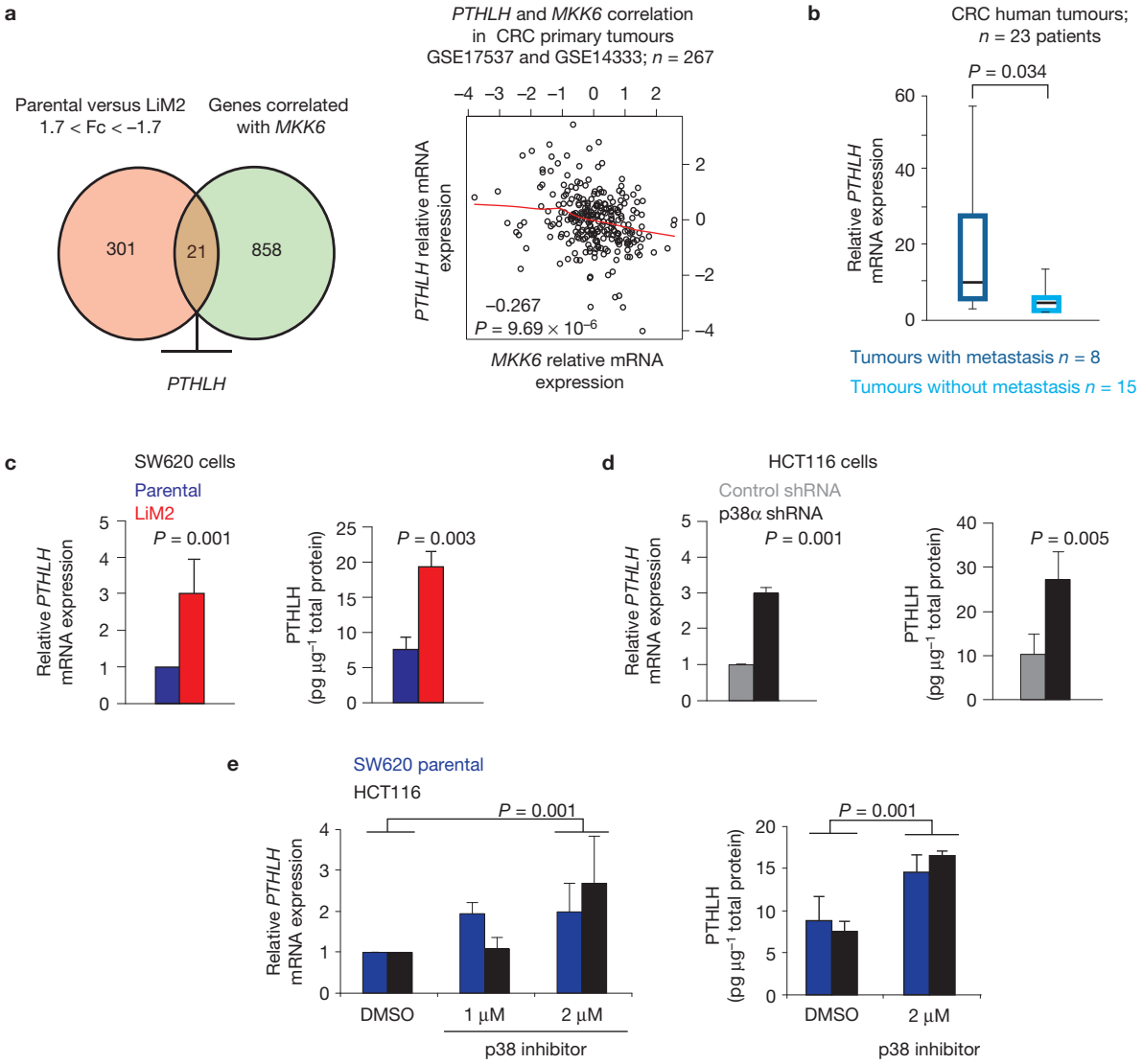

Figure 4 p38 MAPK pathway controls the expression of PTHLH cytokine. (**a**) Left: Venn diagram showing the overlap between genes that are differentially expressed in parental and LiM2 cells (cutoff 1.7), orange group, and genes that correlate significantly with *MKK6* expression in CRC primary tumour set GSE14333 (stages II and III), green group. Right: *PTHLH* and *MKK6* Spearman correlation in CRC primary tumours (GSE17537 and GSE14333; $n = 267$). (**b**) qRT–PCR analysis of *PTHLH* mRNA levels in CRC primary tumours that developed or did not develop metastases; $n = 8$ tumours with metastasis and $n = 15$ tumours without metastasis. The box extends from the 25th to 75th percentile and the black line within the box represents the median; the whiskers extend from the 10th to 90th percentile. (**c**) mRNA and protein levels analysis of PTHLH in SW620 parental and LiM2 cells. $n = 3$ values per group from independent experiments. Plots represent average plus s.d. (**d**) mRNA and protein levels of PTHLH in extracts of HCT116 cells infected with lentivirus expressing the indicated shRNAs. $n = 3$ values per group for mRNA studies and $n = 4$ values per group for protein studies. Each value is obtained in independent experiments. Plots represent average plus s.d. (**e**) mRNA and protein levels of PTHLH in SW620 parental and HCT116 cells treated with the indicated doses of the p38 MAPK inhibitor PH-797804. $n = 4$ (SW620 parental) and $n = 3$ (HCT116) for mRNA studies. $n = 3$ values per group for protein studies. Each value is obtained in an independent experiment. Plots represent average plus s.d. Statistical analysis was done using two-tailed Student's *t*-test in **b**–**e**.

(3.3-fold) and capable of conducting cancer cell–stroma interactions (Fig. 4a and Supplementary Table 4). The association of high *PTHLH* expression levels with metastatic relapse was confirmed in the combined primary tumour gene expression cohort described above (Supplementary Fig. 5a). We further validated the association of high risk of metastasis with increased levels of *PTHLH* in an independent set of 23 CRC tumour samples, including normal mucosa from the same patients (Fig. 4b). Previous reports have implicated *PTHLH* in endochondral bone development and epithelial–mesenchymal interactions[20,21] although, so far, it has never been associated with lung metastasis. Importantly, *PTHLH* was upregulated not only in highly metastatic LiM2 cells but also in p38α-knockdown HCT116 cells and in p38 MAPK inhibitor treated SW620 parental and HCT116 cells (Fig. 4c–e and Supplementary Fig. 5b,c).

PTHLH as mediator of lung metastasis extravasation

To test the implication of PTHLH in lung metastasis of *KRAS*-mutated CRC cells, we downregulated PTHLH protein in highly metastatic

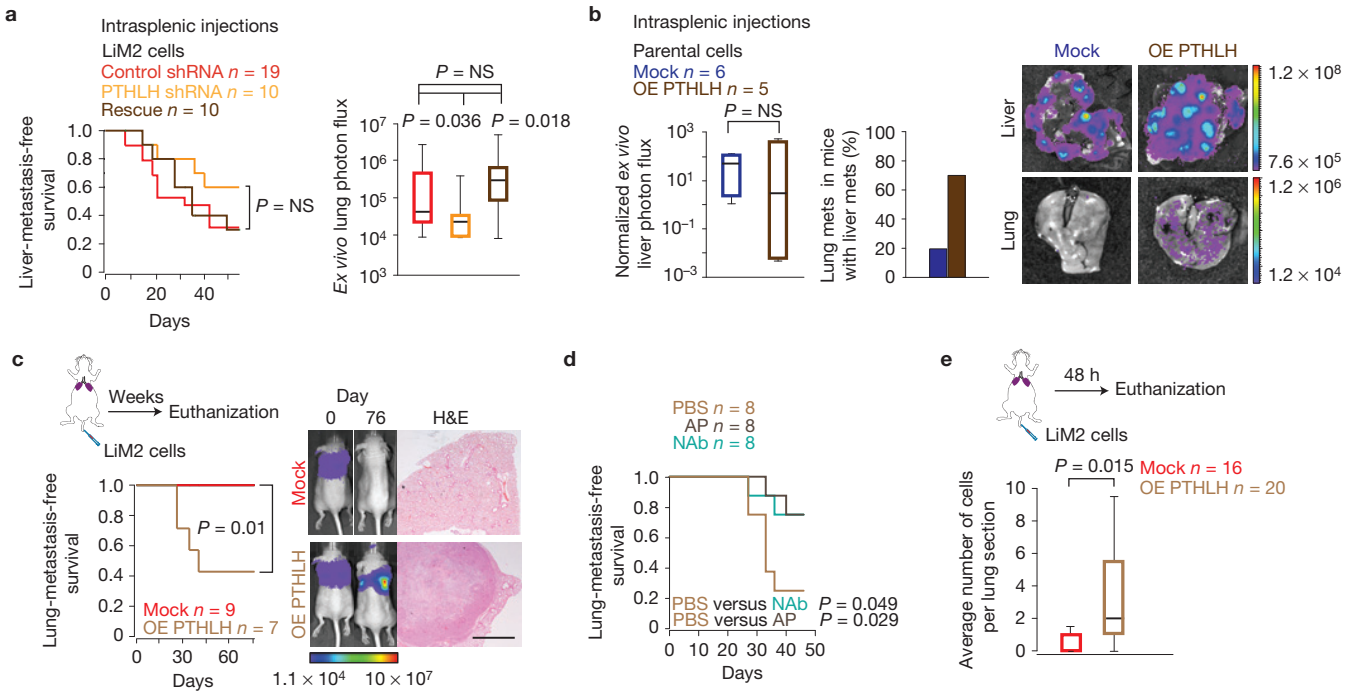

Figure 5 PTHLH controls CRC metastasis to the lung. (**a**) Left: Liver-metastasis-free survival curve of mice injected intrasplenically with LiM2 cells infected with lentivirus expressing control shRNA or PTHLH shRNA and with cells in which PTHLH shRNA was combined with exogenous expression of PTHLH (rescue). Right: *Ex vivo* lung photon flux in mice injected intrasplenically with the above mentioned cell lines; $n=19$ (control shRNA), $n=10$ (PTHLH shRNA) and $n=10$ (rescue) number of mice used in each group pooled from two independent experiments; for *ex vivo* lung photon flux statistics was calculated using one tailed Mann–Whitney test. NS, not significant. (**b**) Left: Normalized liver *ex vivo* photon flux on intrasplenic injections of SW620 parental cells either mock infected or infected with a retrovirus that expresses PTHLH. Percentage of lung metastasis in mice that developed liver metastasis on intrasplenic injection of the indicated cells; $n=6$ (mock) and $n=5$ (overexpressing (OE) PTHLH) number of mice used in each group. Right: Representative bioluminescent images of liver and lung metastatic lesions. (**c**) Left: Lung-metastasis-free survival on tail vein injections of control LiM2 cells (mock) or PTHLH-expressing LiM2 cells (OE PTHLH). $n=9$ (mock) and $n=7$ (OE PTHLH) mice used in each group. Right: Representative bioluminescent images of mice at days 0 and 76 on injection and representative H&E staining of lung sections are shown. Scale bar, 500 μM. (**d**) Lung-metastasis-free survival on tail vein injections of PTHLH-expressing LiM2 cells treated with PBS, PTHLH-neutralizing antibody (+NAb) or antagonist PTHLH peptide (+AP). $n=8$ (PBS), $n=8$ (AP) and $n=8$ (NAb) number of mice used in each group. (**e**) Average number of cells found per lung section 48 h after tail vein injection of LiM2 cells either mock infected or overexpressing *PTHLH*. Four 30 μm distant sections per animal were counted. $n=16$ (mock) and $n=20$ (OE PTHLH) total number of sections counted per group. In **a**,**b** and **e** the box extends from the 25th to 75th percentile and the black line within the box represents the median; whiskers: 10th to 90th percentile. Statistics: **a** left, **c** and **d** log-rank test; **b** and **e** two-tailed Mann–Whitney test.

LiM2 cells (Supplementary Fig. 5d). We found that PTHLH-deficient LiM2 cells were not significantly affected in liver metastatic activity (Fig. 5a) but had decreased ability to form lung metastasis in mice (Fig. 5a). On the other hand, PTHLH downregulation did not affect the growth of LiM2 cells directly implanted in the lung parenchyma of nude mice, indicating a possible role for PTHLH in the process of lung metastatic extravasation (Supplementary Fig. 6a,b). Importantly, PTHLH overexpression sufficed to provide SW620 parental cells with the ability to efficiently colonize lungs from the liver irrespectively of p38 MAPK activity levels (Fig. 5b). We reasoned that a constant and continuous release of PTHLH from an established liver metastasis could be necessary for priming the lung before colonization. Consistent with the idea that distant preparation of the niche might precede colonization, LiM2 cells were not able to colonize the lung when delivered to the mice through the tail vein (Supplementary Fig. 6c). Interestingly, LiM2 cells overexpressing large quantities of PTHLH were capable of lung colonization when injected into mice through the tail vein bypassing the requirement for the existence of a pre-established liver metastatic lesion (Fig. 5c). This was dependent on PTHLH because interfering with this cytokine, by systemic administration of either a neutralizing antibody or an antagonist peptide, impaired the lung colonization process (Fig. 5d). As this experimental model is largely dependent on the extravasation capabilities of metastatic cells and no significant differences were observed in invasion, survival and migration functions, we tested the contribution of PTHLH to cancer cell extravasation at the lung. LiM2 cells overexpressing or not PTHLH, were injected through the tail vein and mice were euthanized 48 h later. Subsequently, lungs were extracted and the amount of cells extravasated into the lung parenchyma was determined. This experiment showed a fivefold increase in the number of cells detected per lung section in mice injected with PTHLH-overexpressing LiM2 cells (Fig. 5e). Similar results were obtained using an *in vitro* surrogate assay based on the migration of LiM2 cells through a monolayer of endothelial cells (Supplementary Fig. 7a).

To understand how the PTHLH released from tumour cells supports extravasation, tight monolayers of human pulmonary endothelial cells (HPMEC), which express the PTHLH receptor

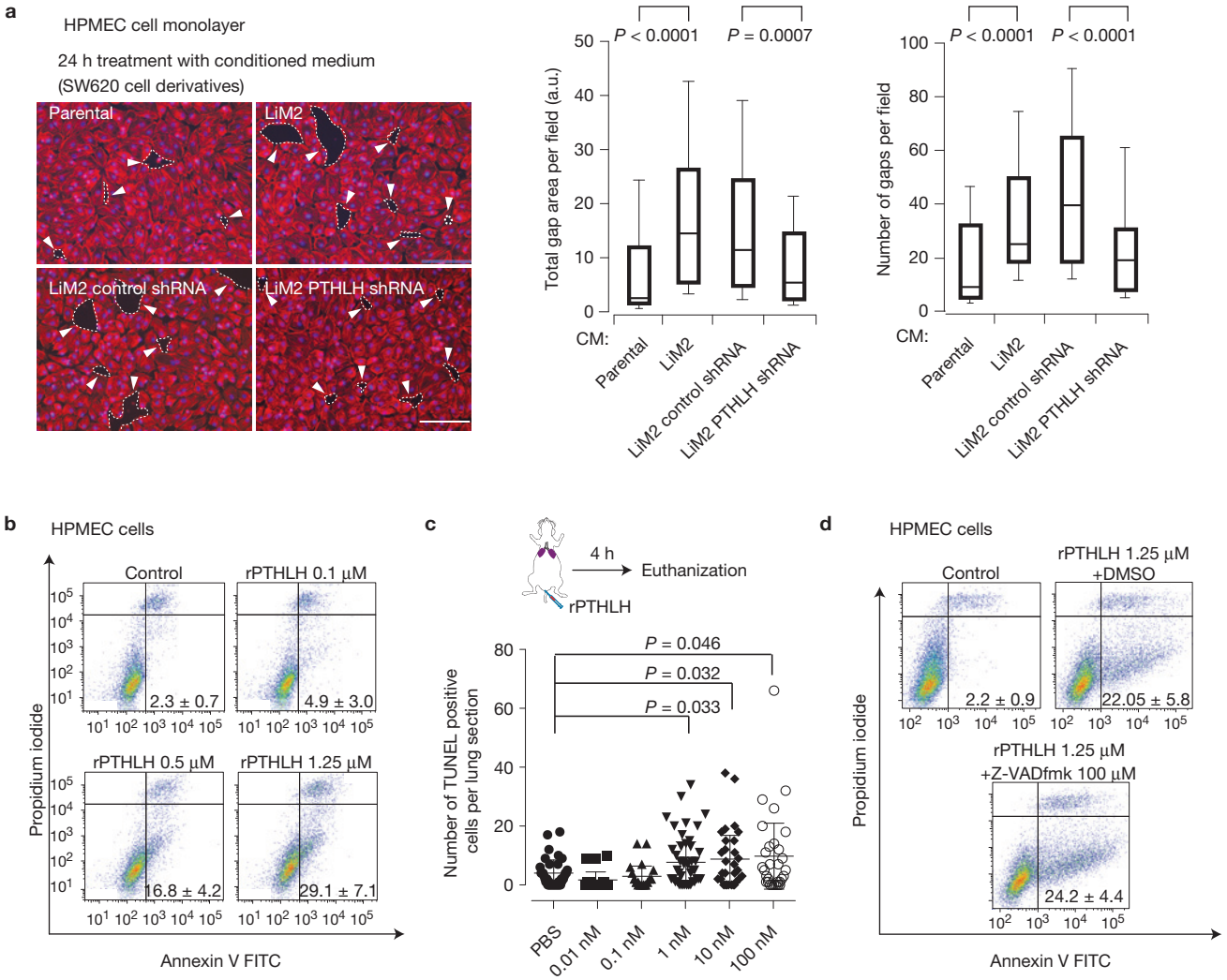

Figure 6 PTHLH induces caspase-independent death of human lung vasculature endothelial cells. (**a**) Left: HPMEC cells were grown until reaching tight confluence and then were treated with SW620 parental, LiM2, LiM2 control shRNA and LiM2 PTHLH shRNA cells conditioned medium for 24 h. Next, phalloidin (red) and DAPI (blue) stainings were performed. Gaps that are formed in the monolayer on conditioned media treatment are indicated with arrowheads and delineated with dashed lines. Scale bar, 200 µm. Right: Total gap area and number of gaps per field were determined. Results represent three independent experiments where each sample was seeded in duplicate and at least ten fields per coverslip were analysed (gap area: n=64, 85, 86 and 77 fields per group were analysed, respectively; and gap number: n=63, 85, 66 and 78 fields per group were analysed, respectively). Statistical significance was calculated using two-tailed Student's t-test; the box extends from the 25th to 75th percentile and the black line within the box represents the median; the whiskers extend from the 10th to 90th percentile. (**b**) Annexin V flow cytometry analysis of HPMEC cells treated for 4 h with the indicated concentrations of PTHLH. (**c**) Average number of TUNEL-positive endothelial cells in lungs 4 h post tail vein injection of recombinant PTHLH (1–34). At least four 30 µm distant sections per animal were counted. PBS (n=47 sections; 10 mice), 1 nM rPTHLH (n=48 sections; 10 mice), 0.01 nM (n=20 sections; 5 mice), 0.1 nM (n=20 sections; 5 mice), 10 nM (n=30 sections; 5 mice), and 100 nM (n=30 sections; 5 mice). Statistical significance was determined using two-tailed Mann–Whitney test. All values are presented in the graphs together with average ±s.d. (**d**) Annexin V flow cytometry analysis of HPMEC cells treated for 4 h with the indicated doses of PTHLH. Before PTHLH addition, some cells were pretreated for 2 h with the Z-VADfmk caspase inhibitor. In **b** and **d** numbers indicate the average percentages of Annexin-V-positive (apoptotic) cells obtained from three independent experiments where each sample was done in duplicate (n = average of 6 replicates ±s.d.).

(PTH1R) (Supplementary Fig. 7b), were treated for 24 h with conditioned media from parental and LiM2 cells or PTHLH-deficient LiM2 cells. We found that only the media from cells expressing high levels of PTHLH (LiM2 cells media, 0.02 ± 0.003 nM PTHLH) caused a disruption of the HPMEC monolayer, suggesting that PTHLH induced cell death (Fig. 6a). We corroborated PTHLH contribution to this effect by pre-treatment of the conditioned media with a PTHLH antagonist peptide, which prevented the PTHLH-induced disruption of the HPMEC monolayer (Supplementary Fig. 7c). Next, we confirmed by Annexin V staining *in vitro* and TUNEL staining *in vivo* that recombinant PTHLH (1–34) was able to induce HPMEC apoptosis in a dose-dependent manner (Fig. 6b,c and Supplementary Fig. 7d). Interestingly, HPMEC apoptosis induced by PTHLH was neither affected by the caspase inhibitor Z-VADfmk (Fig. 6d) nor resulted in PARP or caspase-3 and caspase-7 cleavage (Supplementary Fig. 7e), suggesting that the process was caspase-

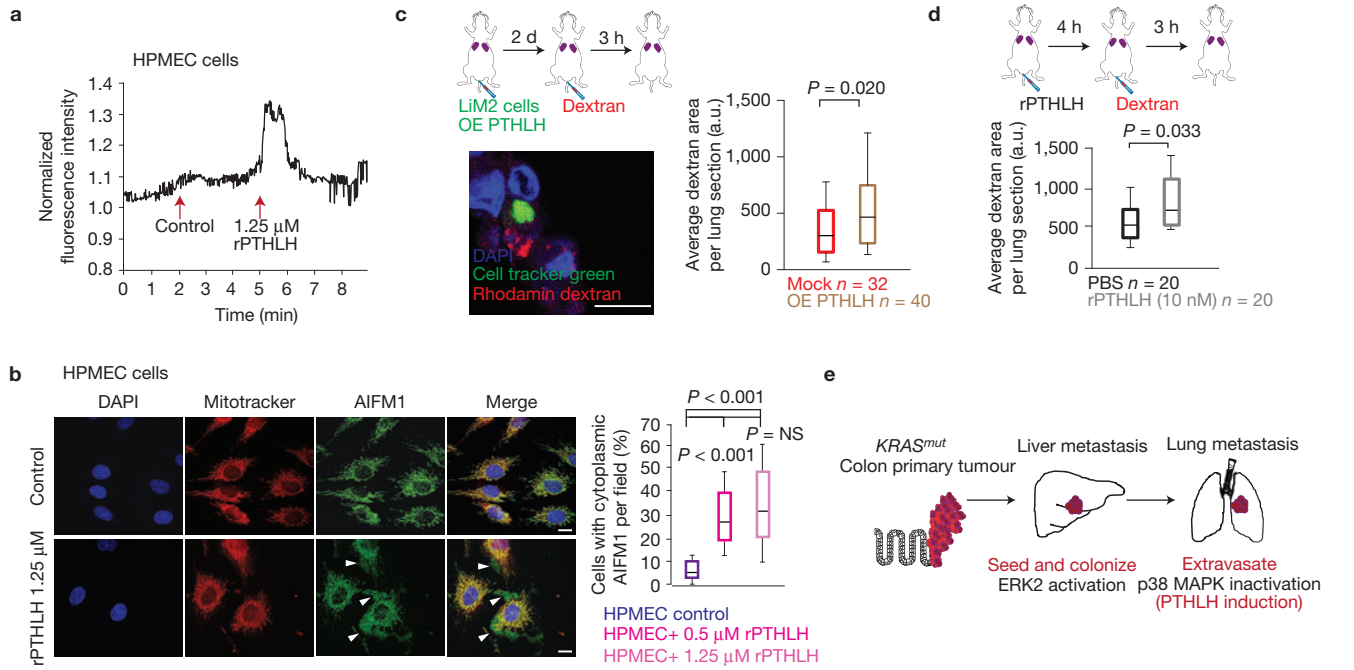

Figure 7 PTHLH induces Ca^{2+}-dependent death of human lung vasculature endothelial cells. (**a**) Relative fluorescence of Fluo4-AM calcium indicator was determined in the course of 9 min. Cells were treated with control medium at 2 min and with medium containing 1.25 µM PTHLH at 5 min . All values were normalized to the lowest value obtained in the first two minutes (basal level). Results represent the average of three independent experiments. (**b**) Left: Representative images from three independent experiments of AIFM1 localization in HPMEC cells treated for 4 h with PTHLH. Arrowheads indicate cytosolic AIFM1. Scale bar, 114 µm. Right: Percentage of cells with cytoplasmic AIFM1 from three independent experiments. Each condition was done in duplicate and a total of 10 fields per condition were scored ($n = 30$ fields per group). Statistical significance was determined using two-tailed Mann–Whitney test. (**c**) Mice were injected in the tail vein with LiM2 cells mock infected or infected with retrovirus expressing PTHLH. Two days later, rhodamine dextran was injected. Representative image of staining is presented. Scale bar, 12.5 µm. Vascular permeability was measured by determining the average area of rhodamine dextran per lung section using ImageJ software. Eight sections per mouse were analysed. $n = 32$ (mock) and $n = 40$ (OE PTHLH) total number of sections analysed per group. (**d**) Mice were injected in the tail vein with LiM2 cells treated with or without recombinant PTHLH. Four hours later, rhodamine dextran was injected and vascular permeability was measured by determining the average area of rhodamine dextran per lung section using ImageJ software. Four sections were analysed per mouse and 5 mice per group were used ($n = 20$ sections per group). Statistical analysis in **c** and **d** was done using two-tailed Student's *t*-test. (**e**) Schematic representation of p38 MAPK and PTHLH implication in lung metastasis by CRC cells. The box in **b**,**c** and **d** extends from the 25th to 75th percentile and the black line within the box represents the median; whiskers extend from the 10th to 90th percentile.

independent. Consistent with this possibility, levels of proapoptotic (Bak and Bid) and anti-apoptotic (Bcl-xl and Mcl-1) proteins were not changed on PTHLH treatment (Supplementary Fig. 7f).

PTHLH induces Ca^{2+}-dependent death of endothelial cells of the lung

Previous studies indicated that increased intracellular Ca^{2+} levels can lead to cell death independently of both caspases and Bcl-2 family members[22,23]. In addition, PTH1R belongs to a group of G-protein-coupled receptors, which on ligand binding can increase Ca^{2+} levels in the cytosol[24]. Indeed, we found that PTHLH treatment increased Ca^{2+} levels in HPMEC cells (Fig. 7a and Supplementary Video 1). Next, we focused on the apoptosis-inducing factor mitochondrion-associated 1 (AIFM1, also known as AIF), a mitochondrial protein that is thought to play a central role in caspase-independent cell death[25,26] and that is released from the mitochondria when cytosolic Ca^{2+} levels increase[22,23]. Interestingly, we observed AIFM1 translocation from the mitochondria to the cytosol on PTHLH treatment (Fig. 7b and Supplementary Fig. 7g). In summary, PTHLH can trigger Ca^{2+} release and AIFM1 mobilization leading to caspase-independent endothelial cell death, which, in turn, destabilizes the vasculature increasing permeability at the lung metastatic site (Fig. 7c,d). Collectively, these results support that p38 MAPK signalling downregulation couples lung and liver metastasis in *KRAS*-mutant CRC cells through the control of PTHLH expression. The release of PTHLH either from established liver lesions or from metastatic cells trapped at the lung vasculature is likely to increase lung endothelial permeability and facilitate metastatic cells extravasation (Fig. 7e).

DISCUSSION

Our analysis of clinical samples indicates that high levels of ERK2 activity probably drive liver metastasis, whereas low p38 MAPK activity further accounts for the capacity to colonize the lung (Fig. 7e). Moreover, our findings emphasize the ability of the cytokine PTHLH to trigger caspase-independent cell death at the lung vasculature as a previously unrecognized contributor to the hierarchical process of metastasis by facilitating the seeding of the lungs by *KRAS*-mutated CRC cells growing in liver metastatic lesions. Previous studies have implicated PTHLH in breast and squamous cell carcinoma tumour progression to bone metastasis through its activity in the bone remodelling process[27–29]. Our work illustrates the systemic contribution of

PTHLH released from tumour cells in supporting distant metastatic processes by triggering vascular permeability, and provides an explanation for the enhanced expression of PTHLH reported in CRC tissue compared with normal colorectal mucosa or polyps[30]. Moreover, our results suggest that genetic changes that allow the primary metastasis to the liver must be followed by additional genetic alterations that allow secondary metastases from the liver to the lung, which emphasizes the concept of metastases from metastases. We provide evidence for a distinct mechanism that relies on different signalling pathways whose hierarchical modulation enhances the ability of departing tumour cells to consecutively seed the liver and the lungs (Fig. 7e). The observation that liver and lung colonization is linked to tumour-specific or circulating cell-specific factors may create opportunities for the development of targeted therapies to prevent disease dissemination from the colon to the liver, and subsequently to the lungs. □

METHODS

Methods and any associated references are available in the online version of the paper.

Note: Supplementary Information is available in the online version of the paper

ACKNOWLEDGEMENTS

We would like to thank J. Maurel for providing the data on patients with colon and rectal cancers depicted in Supplementary Table 3. We also thank H. Auer, J. Colombelli and M. Gay from the Functional genomics, Microscopy and Mass spectrometry core facilities of IRB Barcelona, respectively. J.U. was supported by Fundación BBVA, a Juan de la Cierva grant from Spanish Ministerio de Ciencia e Innovación (MICINN) and a grant from Fundación Olga Torres. X.G-A. was supported by Hospital Clinic-IDIBAPS (Ajut a la Recerca Josep Font) and an ASISA-Harvard Fellowship for Excellence in Clinical Research. S.R. was supported by a S. Borrel contract from Instituto de Salud Carlos III. S.G. and M.P. were supported by La Caixa Fellowships and A.B. by FPI from MICINN. R.R.G., E.B. and A.R.N. are supported by the Institució Catalana de Recerca i Estudis Avançats (ICREA). Research support was provided by MICINN (BFU2010-17850), the European Commission FP7 (ERC 294665) and the Fundación BBVA to A.R.N, by the Generalitat de Catalunya (2009 SGR 1437), MINECO P12/01861 and CIBER-BBN NanoCoMets to R.M., and by the Fundación BBVA, AECC, Generalitat de Catalunya (2009 SGR 1429) and MICINN (SAF2010-21171) to R.R.G.

AUTHOR CONTRIBUTIONS

J.U. designed and performed experiments, analysed data and participated in text writing. X.G-A designed and established the model system, performed microarrays and participated in text writing and statistical analyses of microarrays and patient data. E.P. performed statistical analyses of patient data. S.R., I.D. and F.M.B. performed experiments and analysed data on p38 MAPK. M.V.C. and R.M carried out intracaecum injections and analysed the data. A.B. and S.G. contributed to western blots and immunohistochemical analysis. M.G. and M.P. carried out intrasplenic, tail vein and intracaecum injections. E.F. carried out immunohistochemical analysis. C.N. provided and analysed patient data. N.K, E.B. and A.R.N. participated in data analyses and manuscript writing. R.R.G conceived the project, analysed data, supervised the overall project and wrote the manuscript.

COMPETING FINANCIAL INTERESTS

The authors declare no competing financial interests.

Published online at www.nature.com/doifinder/10.1038/ncb2977
Reprints and permissions information is available online at www.nature.com/reprints

1. Edge, S. B., Byrd, D. R., Compton, C. C. & Fritz, A. G. *AJCC Cancer Staging Manual* (Springer, 2009).
2. Gallagher, D. J. & Kemeny, N. Metastatic colorectal cancer: from improved survival to potential cure. *Oncology* **78,** 237–248 (2010).
3. Wanebo, H. J. *et al.* Meeting the biologic challenge of colorectal metastases. *Clin. Exp. Metastasis* **29,** 821–839 (2012).
4. Sadahiro, S. *et al.* Recurrence patterns after curative resection of colorectal cancer in patients followed for a minimum of ten years. *Hepatogastroenterology* **50,** 1362–1366 (2003).
5. Kievit, J. Follow-up of patients with colorectal cancer: numbers needed to test and treat. *Eur. J. Cancer* **38,** 986–999 (2002).
6. Nguyen, D. X., Bos, P. D. & Massagué, J. Metastasis: from dissemination to organ-specific colonization. *Nat. Rev. Cancer* **9,** 274–284 (2009).
7. Tie, J. *et al.* KRAS mutation is associated with lung metastasis in patients with curatively resected colorectal cancer. *Clin. Cancer Res.* **17,** 1122–1130 (2011).
8. Schlüter, K. *et al.* Organ-specific metastatic tumor cell adhesion and extravasation of colon carcinoma cells with different metastatic potential. *Am. J. Pathol.* **169,** 1064–1073 (2006).
9. Ding, L. *et al.* Genome remodelling in a basal-like breast cancer metastasis and xenograft. *Nature* **464,** 999–1005 (2010).
10. Fidler, I. J. The pathogenesis of cancer metastasis: the 'seed and soil' hypothesis revisited. *Nat. Rev. Cancer* **3,** 453–458 (2003).
11. Kaiser, S. *et al.* Transcriptional recapitulation and subversion of embryonic colon development by mouse colon tumor models and human colon cancer. *Genome Biol.* **8,** R131 (2007).
12. Smith, J. J. *et al.* Experimentally derived metastasis gene expression profile predicts recurrence and death in patients with colon cancer. *Gastroenterology* **138,** 958–968 (2010).
13. Merlos-Suárez, A. *et al.* The intestinal stem cell signature identifies colorectal cancer stem cells and predicts disease relapse. *Cell Stem Cell* **8,** 511–524 (2011).
14. Subramanian, A. *et al.* Gene set enrichment analysis: a knowledge-based approach for interpreting genome-wide expression profiles. *Proc. Natl Acad. Sci. USA* **102,** 15545–15550 (2005).
15. Wagner, E. F. & Nebreda, A. R. Signal integration by JNK and p38 MAPK pathways in cancer development. *Nat. Rev. Cancer* **9,** 537–549 (2009).
16. Cuadrado, A. & Nebreda, A. R. Mechanisms and functions of p38 MAPK signalling. *Biochem. J.* **429,** 403–417 (2010).
17. Shin, S., Dimitri, C. A., Yoon, S-O., Dowdle, W. & Blenis, J. ERK2 but not ERK1 induces epithelial-to-mesenchymal transformation via DEF motif-dependent signaling events. *Mol. Cell* **38,** 114–127 (2010).
18. Xing, L. *et al.* Discovery and characterization of atropisomer PH-797804, a p38 MAP kinase inhibitor, as a clinical drug candidate. *Chem. Med. Chem.* **7,** 273–280 (2012).
19. Céspedes, M. V. *et al.* Orthotopic microinjection of human colon cancer cells in nude mice induces tumor foci in all clinically relevant metastatic sites. *Am. J. Pathol.* **170,** 1077–1085 (2007).
20. Adams, S. L., Cohen, A. J. & Lassová, L. Integration of signaling pathways regulating chondrocyte differentiation during endochondral bone formation. *J. Cell. Physiol.* **213,** 635–641 (2007).
21. Hens, J. R. *et al.* BMP4 and PTHrP interact to stimulate ductal outgrowth during embryonic mammary development and to inhibit hair follicle induction. *Development* **134,** 1221–1230 (2007).
22. Norberg, E. *et al.* An increase in intracellular Ca^{2+} is required for the activation of mitochondrial calpain to release AIF during cell death. *Cell Death Differ.* **15,** 1857–1864 (2008).
23. Sanges, D., Comitato, A., Tammaro, R. & Marigo, V. Apoptosis in retinal degeneration involves cross-talk between apoptosis-inducing factor (AIF) and caspase-12 and is blocked by calpain inhibitors. *Proc. Natl Acad. Sci. USA* **103,** 17366–17371 (2006).
24. Vilardaga, J-P., Romero, G., Friedman, P. A. & Gardella, T. J. Molecular basis of parathyroid hormone receptor signaling and trafficking: a family B GPCR paradigm. *Cell. Mol. Life Sci.* **68,** 1–13 (2011).
25. Susin, S. A. *et al.* Two distinct pathways leading to nuclear apoptosis. *J. Exp. Med.* **192,** 571–580 (2000).
26. Joza, N. *et al.* Essential role of the mitochondrial apoptosis-inducing factor in programmed cell death. *Nature* **410,** 549–554 (2001).
27. Gallwitz, W. E., Guise, T. A. & Mundy, G. R. Guanosine nucleotides inhibit different syndromes of PTHrP excess caused by human cancers *in vivo*. *J. Clin. Invest.* **110,** 1559–1572 (2002).
28. Takayama, Y., Mori, T., Nomura, T., Shibahara, T. & Sakamoto, M. Parathyroid-related protein plays a critical role in bone invasion by oral squamous cell carcinoma. *Int. J. Oncol.* **36,** 1387–1394 (2010).
29. Guise, T. A. Molecular mechanisms of osteolytic bone metastases. *Cancer* **88,** 2892–2898 (2000).
30. Malakouti, S., Asadi, F. K., Kukreja, S. C., Abcarian, H. A. & Cintron, J. R. Parathyroid hormone-related protein expression in the human colon: immunohistochemical evaluation. *Am. Surg.* **62,** 540–544 (1996).

METHODS

Cell culture. The SW620 colorectal cell line was obtained from ATCC. Cells were transduced with retrovirus expressing the triple-fusion reporter gene encoding herpes simplex virus thymidine kinase 1, GFP and firefly luciferase[31]. GFP-expressing cells were sorted and maintained in 5% CO_2 at 37 °C in DMEM medium (Gibco) supplemented with 5% fetal bovine serum (FBS) (Biological Industries), 0.29 mg ml^{-1} glutamine (Biological Industries), 100 U ml^{-1} penicillin (Biological Industries) and 0.1 mg ml^{-1} streptomycin (Biological Industries).

The HCT116 cell line was maintained in DMEM culture medium (Gibco) supplemented with 10% fetal bovine serum (FBS; Biological Industries), 0.29 mg ml^{-1} glutamine (Biological Industries), 100 U ml^{-1} penicillin (Biological Industries) and 0.1 mg ml^{-1} streptomycin (Biological Industries). Clonetics HPMEC cell line was from Promo Cell and was maintained in Endothelial Cell Growth Medium MV2 (Promo Cell). PTHLH (1–34) recombinant protein (H-6630), (Asn 10, Leu 11, D-Trp 12-PTHLH (7–34) amide antagonist peptide (no. H-3274), rabbit anti-PTHLH (1–34) IgG (no. T-4512) and Z-VADfmk (no. n1560) were purchased from Bachem.

Hyperactivation of the p38 MAPK pathway in HCT116 cells was achieved by stable transfection of MKK6^{EE} cloned into pCDNA3.1(+) using Fugene 6 (Roche), followed by treatment with 100–200 μg ml^{-1} hygromycin (Invitrogen) for 2 weeks or until death of the non-transfected control. Mock cells were transfected with empty pCDNA3.1(+) and subjected to the same procedure.

Lentiviral production. 293T cells were used for lentiviral production. Lentiviral vectors expressing shRNAs against human *PTHLH, MAPK1 (ERK2)*, *MAPK3 (ERK1)* and *MAPK14* (p38α) from Mission shRNA Library were purchased from Sigma-Aldrich. Transfection of 293T cells with lentiviral vectors was done using standard procedures and viral supernatant was used for infection of SW620 cells. Selection was done using puromycin (2 μg ml^{-1}) for 48 h. As a negative control in all of the infections, lentivirus with non-target shRNA was used (catalogue no. SHC016-1EA).

PTHLH shRNA1 clone ID TRCN0000083846; sequence: 5′-CCGGCCAAGATT TA CGGCGACGATTCTCGAGAATCGTCGCCGTAAATCTTGGTTTTTG-3′.

PTHLH shRNA2 clone ID TRCN0000083847; sequence:5′-CCGGCCCGTCC GA TTTGGGTCTGATCTCGAGATCAGACCCAAATCGGACGGGTTTTTG-3′.

ERK1 shRNA1 clone ID TRCN0000006150; sequence: 5′-CCGGCCAAGATTT ACGGCGACGATTCTCGAGAATCGTCGCCGTAAATCTTGGTTTTTG-3′.

ERK1 shRNA2 clone ID TRCN0000006152; sequence: 5′-CCGGCTATACCAA GTCCATCGACATCTCGAGATGTCGATGGACTTGGTATAGTTTTT-3′.

ERK2 shRNA1 clone ID TRCN0000010050; sequence: 5′-CCGGTATCCATTCA GCTAACGTTCTCTCGAGAGAACGTTAGCTGAATGGATATTTTT-3′.

ERK2 shRNA2 clone ID TRCN0000010040, sequence: 5′-CCGGCAAAGTTC GAGTAG CTATCAACTCGAGTTGATAGCTACTCGAACTTTGTTTTT-3′.

p38α shRNA clone ID TRCN0000010051, sequence: 5′-CCGGGTTACGTGTG GCAGTGAAGAACTCGAGTTCTTCACTGCCACACGTAACTTTTT-3′.

Animal studies. The institutional Animal Care and Use Committee of IRB Barcelona approved all animal work. BALB/c nude female mice (Harlan) of 6–8 weeks of age were used for all studies.

For intrasplenic injections, animals were anaesthetized with a mixture of ketamine (80 mg kg^{-1}) and xilacine (8 mg kg^{-1}) and 3×10^6 cells resuspended in 100 μl of cold PBS were injected as previously reported[32]. On injection, cells were allowed for 2 min to pass from the spleen and enter the liver through the portal circulation and next splenectomy was performed. Tumour development was followed twice a week by bioluminescence imaging using the IVIS-200 imaging system from Xenogen. Quantification of bioluminescent images was done with LivingImage 2.60.1 software. For liver metastasis both ventral images of the abdomen and dorsal images of the upper right side of the mice back were quantified. All values were normalized to those obtained at day 0. For metastasis-free survival curves, metastatic events were scored when the measured value of either abdominal or dorsal bioluminescence bypassed the value of day 0. On necropsy, the development of metastasis was confirmed by performing *ex vivo* liver and lung bioluminescent images as well as in histological sections. For tail vein injections 1×10^6 cells were resuspended in 200 μl of cold PBS and injected into the tail vein. Lung tumour development was followed once a week by bioluminescence imaging taking a photo of the upper dorsal region that corresponds to the lung position. Quantification of bioluminescent images was performed with LivingImage 2.60.1 software. All obtained values were normalized to those obtained at day 0. For lung-metastasis-free survival curves, metastatic events were scored when the measured value of bioluminescence bypassed that of day 0. In Fig. 5d, before tail vein inoculation of LiM2-overexpressing PTHLH cells, those were treated with PBS, PTHLH antagonist peptide (AP) ((Asn 10, Leu 11, D-Trp 12)-PTHLH (7-34; Bachem); (5 μg ml^{-1}) and PTHLH-neutralizing antibody (Nab; rabbit anti PTHLH (1–34) IgG; Bachem; 5 μg ml^{-1}). Next, cells were injected through the tail vein and mice were continuously treated with PBS or PTHLH AP (6 μg per dose, intraperitoneum injection) twice a day or PTHLH NAb (6 μg per dose, intraperitoneum injection) once a day. Lung metastasis was scored as described above.

Orthotopic injections were done as previously described[33]. Lung injections were done using 5×10^5 cells that were resuspended in 25 μl of cold PBS mixed with 25 μl of growth factor reduced Matrigel (BD Biosciences, no. 354230). Animals were anaesthetized with a mixture of ketamine (80 mg kg^{-1}) and xilacine (8 mg kg^{-1}). A small incision was made in the skin on the left side of the back of the mouse, level with the lungs, and cells were injected into the lung using a 25G needle. For intraliver injections animals were anaesthetized with a mixture of ketamine (80 mg kg^{-1}) and xilacine (8 mg kg^{-1}). A small incision in the skin and peritoneum was made in the liver area and liver lobules were gently removed. Injections were done using insulin syringes (29Gx1/2 needle) and each mouse was injected with 5×10^5 cells that were resuspended in 25 μl of cold PBS mixed with 25 μl of growth factor reduced Matrigel matrix (BD Biosciences). Liver tumour development was followed once a week by bioluminescence imaging, taking a photo of the ventral region. Quantification of bioluminescent images was performed with LivingImage 2.60.1 software. Once the tumour signal reached an established threshold (>108 photons s^{-1}), mice were randomly allocated to daily oral treatment with 10 mg kg^{-1} of p38 inhibitor PH-797804 (Selleckchem, no. S2726) or vehicle (0.5% methylcellulose and 0.025% Tween 20 in PBS) for two weeks. For extravasation assays CellTracker Green (Life Technologies, no. C7025)-marked cells (5×10^5) were resuspended in 200 μl of cold PBS and injected into the tail vein. Forty eight hours later mice were perfused by heart with 5 ml of PBS and euthanized. The lungs were removed, the trachea was perfused and these were fixed in formalin. Paraffin-embedded lungs were sectioned and analysed.

For the *in vivo* lung permeability assay, 5×10^5 cells marked with 5 μM CellTracker Green (Life Technologies) were resuspended in 200 μl of cold PBS and injected into the tail vein. Two days after mice were injected intravenously with rhodamine dextran (M_r 70K, Life Technologies, no. D1841) at 2 mg per 20 g of body weight and 3 h later mice were perfused by heart with 5 ml of PBS and euthanized. The lungs were extracted, the trachea was perfused and these were fixed in formalin. Paraffin-embedded lungs were sectioned and analysed.

In addition, lung permeability was tested on injection of PBS or 10 nM (0.08 μg in 100 μl of PBS) recombinant PTHLH (1–34) through the tail vein. Of note, the molar concentration of rPTHLH was adjusted to 2 ml of the total mouse blood volume. Four hours later, mice were injected intravenously with rhodamine dextran (M_r 70K, Life Technologies) at 2 mg per 20 g of body weight and 3 h later mice were perfused by heart with 5 ml of PBS and euthanized. The lungs were extracted, the trachea was perfused and these were fixed in formalin. Paraffin-embedded lungs were sectioned and analysed.

For scoring of apoptotic cells in lungs, liver and ovary, PBS and indicated concentrations of rPTHLH were injected through the tail vein of mice. Four hours later mice were euthanized, and tissues were extracted and fixed in formalin.

Isolation of liver metastatic derivatives. Tumour formation on intrasplenic injections was followed by bioluminescence imaging (see above). Mice were euthanized when they presented the first signs of cachexia. Liver metastatic lesions were localized by *ex vivo* bioluminescence imaging and resected under sterile conditions. The lesions were minced and placed in culture medium containing a mixture of DMEM and Ham F-12 (GIBCO) (1:1) supplemented with 0.125% collagenase III and 0.1% hyaluronidase. Samples were incubated at room temperature for 4–5 h, with gentle rocking. After collagenase treatment, cells were briefly centrifuged, resuspended in culture medium and allowed to grow. GFP+ cells were sorted for further propagation in culture or for inoculation in mice.

Gene expression profiling. RNA was extracted from cells using the RNeasy mini kit (Qiagen). Labelling and hybridization of the samples to the HG1.0ST gene expression chip (Affymetrix) were performed by the Functional Genomics Core Facility of IRB Barcelona using standard methodology. Data analysis was performed using R (Bioconductor). Quantile normalization and RMA summarization were used to obtain probe set level expression estimates as implemented in the 'oligo' package of Bioconductor[34]. Both box plot and MA plots were checked before and after normalization. To prevent nonspecific or mis-targeted probe sets biasing the gene level expression estimates, for each gene we selected the 50% of the probe sets with the highest inter-quartile range across all samples and obtained a gene level expression estimate through median polishing, in a fashion analogous to RMA. Class comparison of differential expression between parental and LiM2 cells was performed with a linear-model-based moderated t-test as implemented in the lima package. The t-test statistics were used to obtain a posterior probability for differential expression following the semi-parametric empirical Bayes procedure[35]. The posterior expected false discovery rate was set at 0.05. A heat map was used to plot the expression of genes on a colour scale. A Euclidean distance metric was used to compute the distance matrix of the gene expression levels and hierarchical

DOI: 10.1038/ncb2977

clustering using a complete agglomeration method was used. Ranks of the data were used for setting the colour scheme.

GSEA analysis. GSEA analysis was done as implemented in the phenoTest package of Bioconductor.

BGSEA analysis. Gene set enrichment was assessed through Bayesian enrichment[36]. We generated 1,000 posterior samples for the differential expression indicator, according to the posterior probabilities of differential expression obtained from pairwise comparisons. For each gene set we computed the probability of enrichment as the proportion of posterior samples for which the percentage of differentially expressed genes in the set was larger than the percentage of differentially expressed genes in the rest of the genome.

MKK6 gene expression correlation. Gene expression data of stage II and III patients of the GSE14333 human CRC cohort were used. A Spearman correlation test was performed for each gene against *MKK6* (*MAP2K6*). We corrected for multiple testing using the Benjamini and Hochberg method[37].

Migration assay. Cells were marked with 5 μM CellTracker Green (Life Technologies) following the manufacturer's instructions and kept overnight in medium with 0.1% FBS. The next day 5×10^4 cells were seeded on human-fibronectin-coated Biocoat Cell Culture Inserts (BD Biosciences, no. 354543) in medium with 0.1% FBS, and the wells were loaded with complete medium. Eight hours after the seeding, cells were washed and fixed with 4% paraformaldehyde. Cells on the apical side of each insert were scraped off and the migration to the basolateral side was visualized with a Nikon Eclipse TE2000-U fluorescence microscope.

Trans-endothelial migration assay. HPMEC cells (1×10^5) were seeded on human-fibronectin-coated Biocoat Cell Culture Inserts (BD Biosciences) and allowed to grow for four days until closing the monolayer. Tumour cells were marked with 5 μM CellTracker Green (Life Technologies) following the manufacturer's instructions and then were conditioned overnight in ECGM-MV2 (Promo Cell) medium with 0.1% FBS and without supplements. The next day 5×10^4 tumour cells were seeded into Trans-well inserts with an endothelial monolayer in ECGM-MV2 medium with 0.1% FBS and the wells were loaded with complete medium. Eight hours after the seeding, cells were washed and fixed with 4% paraformaldehyde. Cells on the apical side of each insert were scraped off and the migration to the basolateral side was visualized with a Nikon Eclipse TE2000-U fluorescence microscope.

Invasion assay. Cells were marked with 5 μM CellTracker Green (Life Technologies) following the manufacturer's instructions and were kept overnight in medium with 0.1% FBS. The next day, 5×10^4 cells were seeded on BD BioCoat Matrigel Invasion Chambers in medium with 0.1% FBS, and the wells were loaded with complete medium. Eight hours after the seeding, cells were washed and fixed with 4% paraformaldehyde. Cells on the apical side of each insert were scraped off and the migration to the basolateral side was visualized with a Nikon Eclipse TE2000-U fluorescence microscope.

Flow cytometry analysis. 2×10^5 HPMEC cells were seeded in ECGM-MV2 (Promo Cell) complete medium. The following day cells were washed with PBS and treated for 4 h with PTHLH in ECGM-MV2 medium with 0.1%FBS and without supplements. In experiments where Z-VAD-fmk (Bachem) inhibitor was used cells were pretreated for 2 h with this pan-caspase inhibitor before PTHLH was added. Cells were stained with Annexin V Apoptosis Detection Kit (Santa Cruz, sc-4252AK) following the manufacturer's instruction. Data were obtained using a BD FACSAria cell sorter and analysed using FlowJo software.

Western blot analysis. Protein extracts obtained from whole-cell lysates (35 μg) were fractionated in SDS–PAGE gels, transferred onto Immobilion-P (Millipore) membranes, and subjected to immunoblot analysis according to standard procedures. The following antibodies were used: rabbit polyclonal antibodies to phospho-p38 (Cell Signaling, no. 9211; dilution 1:500), goat polyclonal antibodies against p38α (Santa Cruz, no. sc-525-G; dilution 1:500), a home-made rabbit antiserum against MKK6 (ref. 38), rabbit monoclonal against phospho-ERK1/2 (Cell Signaling, no. 4377S; dilution 1:500), rabbit polyclonal against ERK1/2 (Cell Signaling no. 9102; dilution 1:500), mouse monoclonal against anti-phospho JNK (BD Transduction Laboratories, no. 612541; dilution 1:500), rabbit polyclonal against JNK (Santa Cruz, no. sc-571; dilution 1:500), rabbit polyclonal against PARP (Cell Signaling no. 9542; dilution 1:500), rabbit polyclonal against caspase-3 (Cell Signaling no. 9662; dilution 1:500), rabbit polyclonal against caspase-7 (Cell Signaling no. 9492; dilution 1:500), rabbit polyclonal against AIF (AIFM1; Cell Signaling no. 4642; dilution 1:500), rabbit polyclonal against Bid (Cell Signaling no. 2002; dilution 1:1,000), rabbit polyclonal against Bak (Cell Signaling no. 3814; dilution 1:1,000), rabbit monoclonal against Bcl-xl (Cell Signaling no. 2764, clone 54H6; dilution 1:500), rabbit monoclonal against Mcl-1 (Cell Signaling no. 5453, clone D35A5; dilution 1:500) and mouse monoclonal antibody against Tom20 (Santa Cruz, sc-17764, clone F-10; dilution 1:500) and against tubulin (Sigma no. T5168, clone B-5-1-2; dilution 1:5,000).

Primary antibodies were detected with appropriate HRP-conjugated secondary antibodies against mouse (Cell Signaling no. 7076, dilution 1:5,000), rabbit (GE Healthcare UK Limited, no. LNA934V dilution 1:5,000) or goat IgGs (Santa Cruz no. sc-2020, dilution 1:5,000). Separation of cytoplasmic and mitochondrial fractions was done using Mito Isolation Kit for Mammalian Cells (Thermo Scientific) following the manufacturer's instructions.

Quantitative RT–PCR analysis. Real-time qPCR was performed using TaqMan Gene Expression Assay *PTHLH* probe Hs 00174969_m1; *MKK6/MAP2K6* probe Hs00992389_m1 and ABI Prism Fast 7900HT Instrument. The levels of expression were normalized to human B2M (Applied Biosystems) and data were analysed using the comparative ΔCT method.

Histopathology and immunohistochemistry. Tissues were dissected, fixed in 10%-buffered formalin (Sigma) and embedded in paraffin. Sections (2–3 μm thick) were stained with haematoxylin and eosin (H&E). For immunohistochemistry rat polyclonal rabbit polyclonal antibodies against GFP (Abcam, ab13970; dilution 1:2,000) and P-p38 (Cell Signaling, no. 9211; dilution 1:1,000) were used.

Immunofluorescence. HPMEC cells were grown to confluence on glass coverslips. The cells were fixed for 10 min in 10% neutral buffered formalin solution (Sigma) at room temperature and incubated for 5 min in 0.1% Triton X-100 in PBS. Next, the samples were blocked with 1% BSA for 30 min and then stained for 20 min with rhodamine phalloidin (Life Technologies, no. R415) and DAPI (Sigma).

For AIF staining 5×10^4 of HPMEC cells were seeded on glass coverslips. The next day, cells were treated for 4 h with 1.25 mM PTHLH in 0.1%FBS ECGM-MV2 (Promo Cell) medium without supplements and stained with 80 nM MitoTracker Red CMXRos (Lonza no. PA3017) for 15 min. Next, cells were fixed in complete growth medium containing 3.7% formaldehyde for 15 min at 37 °C and permeabilized for 10 min in PBS containing 0.2% Triton X-100. Blocking was done in PBS containing 3% BSA for 1 h at room temperature. Samples were incubated with AIF (AIFM1) antibody (Cell Signaling no. 4642; dilution 1:100) overnight at 4 °C and 1 h at room temperature with secondary antibody that recognizes rabbit IgGs (Alexa Fluor 488, Molecular Probes Invitrogen) and mounted with ProLong Gold antifade reagent with DAPI.

For PTHLH immunofluorescence LiM2 and PTHLH-overexpressing LiM2 cells were seeded on glass coverslips. Next, cells were fixed with 4% PFA for 15 min at room temperature and permeabilized for 10 min in PBS containing 0.2% Triton X-100. Blocking was performed in PBS containing 3% BSA for 1 h at room temperature. Samples were incubated with PTHLH antibody (Abcam Ab115488; dilution 1:100) overnight at 4 °C and 1 h at room temperature with secondary antibody that recognizes mouse IgGs and mounted with ProLong Gold antifade reagent with DAPI.

PTHLH ELISA assay. For the ELISA assay, 36.4 μg of total protein lysate was used. ELISA was purchased from Uscn Life Science (USA) and performed following the manufacturer's instructions.

TUNEL assay. For the TUNEL assay formalin-fixed paraffin-embedded sections were used. *In Situ* Cell Death Detection Kit was purchased from Roche and assay was used following the manufacturer's instructions.

Live-cell imaging for intracellular Ca^{2+} level detection. HPMEC cells (3×10^5) were seeded on 14 mm glass coverslips. The next day, cells were washed and treated for 15 min with 1 μM Fluo-4 AM (Life Technologies, no. F14201) in ECGM-MV2 medium without supplements. Next, the cells were mounted in a special chamber for live-cell imaging using a Scan∧R Olympus microscope and images were taken every second. Obtained videos were analysed using Fiji software.

Human samples. Informed consent was obtained prospectively before surgery from each patient and a total of 23 primary tumours and healthy mucosa were obtained. Patient identifiers were removed from the samples to protect patient confidentiality as per institutional guidelines. All human samples were manipulated with the approval and following the guidelines of the Ethic Committee of Hospital Clinic de Barcelona and IRB-Barcelona. Information on tumour relapse and follow-up was extracted from the medical records; patients were followed with CT scan every three months. Owing to the lack of material 3 samples could be subjected only to mRNA isolation whereas the rest were subjected to both mRNA and protein isolation.

Clinical sample analysis. Authorization was obtained to analyse a database of 100 metastatic colorectal cancer (CRC) patients treated with irinotecan and cetuximab inside a phase II translational trial[39] and 40 localized patients from a single cohort prospective study[40] that relapsed during the study follow-up. Site of metastasis was extracted and tabulated by primary site (colon versus rectum) with basic descriptive statistics.

Mass spectrometry analysis. Proteins were digested with trypsin following standard protocols. Briefly, 50 µg of sample was reduced with 2 mM dithiothreitol. After 1 h at 25 °C, iodoacetamide was added to a final concentration of 7 mM and the samples were incubated for 30 min in the darkness. The reaction was stopped by adding 2 mM dithiothreitol. Then, proteins were digested with trypsin and incubated at 37 °C overnight. Digestions were stopped by adding formic acid to a final concentration of 1%. The resulting peptide mixtures were diluted in 1% FA and loaded in a nano-LC–MS/MS system. The nano-LC–MS/MS set up was as follows. Samples were loaded to a 180 µm ×2 cm C18 Symmetry trap column (Waters) at a flow rate of 15 µl min^{-1} using a nanoAcquity Ultra Performance LCTM chromatographic system (Waters). Peptides were separated using a C18 analytical column (BEH130TM 75 µm × 10 cm, 1.7 µm, Waters) with a 90 min run, comprising three consecutive steps with linear gradients from 1 to 35% B in 60 min, from 35 to 50% B in 5 min, and from 50% to 85% B in 3 min, followed by isocratic elution at 85% B in 10 min and stabilization to initial conditions ($A = 0.1\%$ FA in water, $B = 0.1\%$ FA in CH_3CN). The column outlet was directly connected to an Advion TriVersa NanoMate (Advion) fitted to an LTQ-FT Ultra mass spectrometer (Thermo). Spray voltage in the NanoMate source was set to 1.70 kV. Capillary voltage and tube lens on the LTQ-FT were tuned to 40 V and 120 V. The spectrometer was working in positive polarity mode. At least two blank runs before each analysis were performed to ensure the absence of cross-contamination from previous samples. To select the PTHLH-targeted ions, the mass spectrometer was operated in a data-dependent acquisition (DDA) mode. Survey MS scans were acquired in the FT with the resolution (defined at 400 m/z) set to 100,000. Up to six of the most intense ions per scan were fragmented and detected in the linear ion trap. The ion count target value was 1,000,000 for the survey scan and 50,000 for the MS/MS scan. Target ions already selected for MS/MS were dynamically excluded for 30 s. A database search was performed with Proteome Discoverer software v1.3 (Thermo) using the Sequest search engine and the SwissProt database (human release 12_03) where PTHLH peptide was added. Search parameters included trypsin enzyme specificity, allowing for two missed cleavage sites, carbamidomethyl in cysteine as a static modification and methionine oxidation as dynamic modifications. Peptide mass tolerance was 10 ppm and the MS/MS tolerance was 0.8 Da. Peptides with a q value lower than 0.1 were considered as positive identifications with a high confidence level. One peptide ion was selected for targeted MS/MS analysis: SDQDLR (m/z 366.21). The presence of PTHLH in the samples was determined by using the same nano-LC–MS/MS system described above. The spectrometric analysis was performed in a targeted mode, acquiring a full MS/MS scan of the precursor ion SDQDLR (m/z 366.21). The quantification was performed with Xcalibur software versus 2.0SR2 (Thermo Scientific) by using extracted ion chromatograms of the optimum MS/MS transitions in terms of sensitivity (SDQDLR, 366.22 → 531.38).

Sample size calculation. An assessment of the number of animals required for each procedure was performed using Statistical Power Analysis and taking into consideration the appropriate statistical tests, significance level of 5% and statistical power of 80%. An estimate of variance was inferred from previous experiments, especially considering the variability of tumour xenograft growth.

Method of randomization. A method of randomization was used in the experiment shown in Fig. 3c. Parental cells were implanted directly into the liver in nude mice (one implant per mouse) and, when the liver tumour signal reached a certain photon flux threshold ($>1\times10^8$ photons s^{-1}), mice were randomly allocated to daily systemic treatment with either vehicle or PH-797804.

Group allocation. For the results obtained in Figs 5e, 6c and 7c,d and Supplementary Figs 1a, 3d,e, 4b,e,f and 7a,d the investigator was not aware of group allocation when assessing the outcome.

Data sets analysed. GSE17538 is a metacohort composed of 177 colon cancer patients treated at H. Lee Moffitt Cancer Center (Tampa, USA) plus 55 colon cancer patients treated at Vanderbilt University Medical Center (Vanderbilt, USA; ref. 41). Note that this cohort did not include rectal cancers. GSE14333 contains a pool of 290 CRC patients treated at two different hospitals: Peter MacCallum Cancer Center (Australia) and H. Lee Moffitt Cancer Center (USA; ref. 42). We combined both cohorts for a total of 340 CRC expression data sets from which we used 267 (stages I, II and III). Note that the GSE17538 and GSE14333 cohorts were partially overlapping owing to patients treated at H. Lee Moffitt Cancer Center being duplicated in both data sets. Duplicated cases were included only once in the final selection. To remove biases due to the data having been collected in different hospitals, we computed z-scores (that is, subtracted the mean and divided by the standard deviation) for each gene and hospital separately before merging them into a meta-cohort.

Accession number of data set generated for this study (Fig. 2a): GSE33350.

31. Ponomarev, V. *et al.* A novel triple-modality reporter gene for whole-body fluorescent, bioluminescent, and nuclear noninvasive imaging. *Eur. J. Nucl. Med. Mol. Imaging* **31,** 740–751 (2004).
32. Giavazzi, R., Campbell, D. E., Jessup, J. M., Cleary, K. & Fidler, I. J. Metastatic behavior of tumor cells isolated from primary and metastatic human colorectal carcinomas implanted into different sites in nude mice. *Cancer Res.* **46,** 1928–1933 (1986).
33. Céspedes, M. V. *et al.* Orthotopic microinjection of human colon cancer cells in nude mice induces tumor foci in all clinically relevant metastatic sites. *Am. J. Pathol.* **170,** 1077–1085 (2007).
34. Gentleman, R. C. *et al.* Bioconductor: open software development for computational biology and bioinformatics. *Genome Biol.* **5,** R80 (2004).
35. Rossell, D., Guerra, R. & Scott, C. Semi-parametric differential, expression analysis via partial mixture estimation. *Stat. Appl. Genet. Mol. Biol.* **7,** Article15 (2008).
36. Mallick, B. K., Gold, D. & Baladandayuthapani, V. *Bayesan Analysis of Gene Expression Data* (Wiley, 2009).
37. Benjamini, Y. & Hochberg, Y. Controlling the false discovery rate: a practical and powerful approach to multiple testing. *J. Roy. Stat. Soc. Ser. B* **57,** 289–300 (1995).
38. Alonso, G., Ambrosino, C., Jones, M. & Nebreda, A. R. Differential activation of p38 mitogen-activated protein kinase isoforms depending on signal strength. *J. Biol. Chem.* **275,** 40641–40648 (2000).
39. Garcia-Albeniz, X. *et al.* Serum matrilysin correlates with poor survival independently of KRAS and BRAF status in refractory advanced colorectal cancer patients treated with irinotecan plus cetuximab. *Tumour Biol.* **32,** 417–424 (2011).
40. Martínez-Fernandez, A. *et al.* Serum matrilysin levels predict outcome in curatively resected colorectal cancer patients. *Ann. Surg. Oncol.* **16,** 1412–1420 (2009).
41. Smith, J. J. *et al.* Experimentally derived metastasis gene expression profile predicts recurrence and death in patients with colon cancer. *Gastroenterology* **138,** 958–968 (2010).
42. Jorissen, R. N. *et al.* Metastasis-associated gene expression changes predict poor outcomes in patients with dukes stage B and C colorectal cancer. *Clin. Cancer Res.* **15,** 7642–7651 (2009).

DOI: 10.1038/ncb2977

nature cell biology

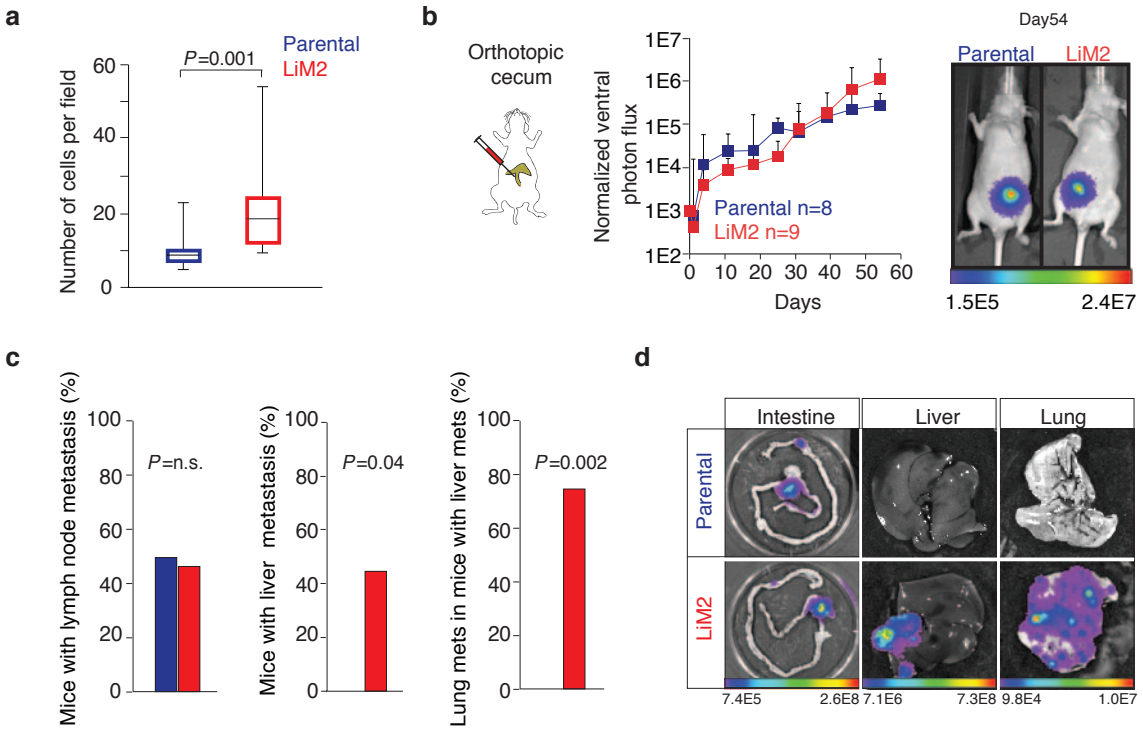

Supplementary Figure 1 Characterization of liver and lung metastatic potential of SW620 parental and LiM2 cells. **(a)** Invasion capacity of SW620 parental and LiM2 cells was measured using matrigel-coated Boyden chambers. Results represent values of three independent experiments where each cell line was seeded in six Boyden chambers and five fields per chamber were analyzed and average for each chamber obtained (n=18 chambers per group). Statistical significance was calculated using two-tailed Mann Whitney test; the box extends from 25 to 75 percentile where black line within the box represents median, whiskers extend from 10 to 90 percentile. **(b)** *In vivo* proliferation of parental and LiM2 cells ($0.5x10^5$) injected into cecum of nude mice. Bioluminescent images were taken at day 54. n =8 (Parental) and n=9 (LiM2) number of mice used for each cell line. Statistical analysis was done using two-tailed Mann Whitney test and no statistically significant differences were found. **(c)** Percentage of lymph node and liver metastasis as well as lung metastasis in mice that developed liver metastasis upon intracecum injections of parental and LiM2 cells determined post-mortem. Number of mice (n) used is defined in (b). Statistical significance was calculated using one-sided Fisher's exact test. **(d)** Representative bioluminescent images of intestine, liver and lung from mice injected intracecum with SW620 parental and LiM2 cells. Data is presented as average plus s.d.

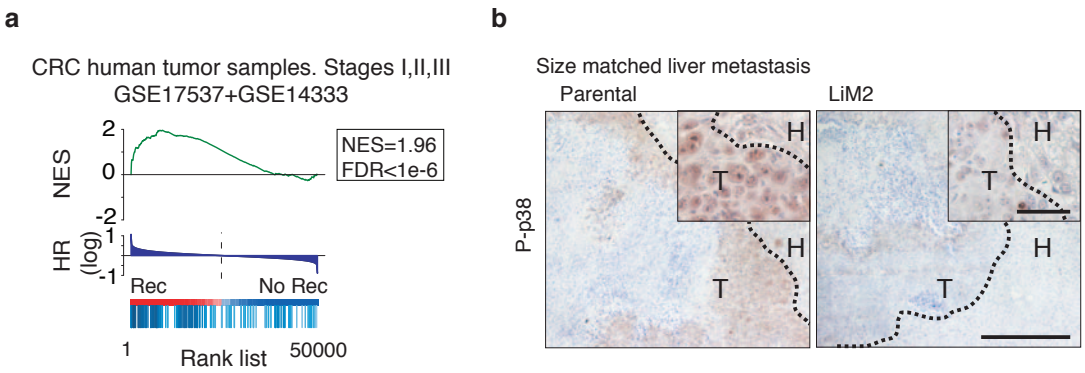

Supplementary Figure 2 Gene set enrichment analyses (GSEA) of the CCM downregulated gene set and phosphorylated p38 MAPK levels in liver metastatic lesions formed by LiM2 cells. **(a)** GSEA analysis of the CCM downregulated gene set in human colon cancer dataset (pooled GSE17537 and GSE14333 expression set). NES-normalized enrichment score; FDR-false discovery rate. **(b)** SW620 parental and LiM2 cells were injected intraliver and 40 days later mice were sacrificed. Size matched liver lesions were selected for immunohistochemistry staining with anti- phospho-p38 (P-p38) antibodies. Representative IHC staining is shown where n=6 animals per group were used. Scale bar 500 μm; inset scale bar 50 μm; H-healthy tissue; T-tumor.

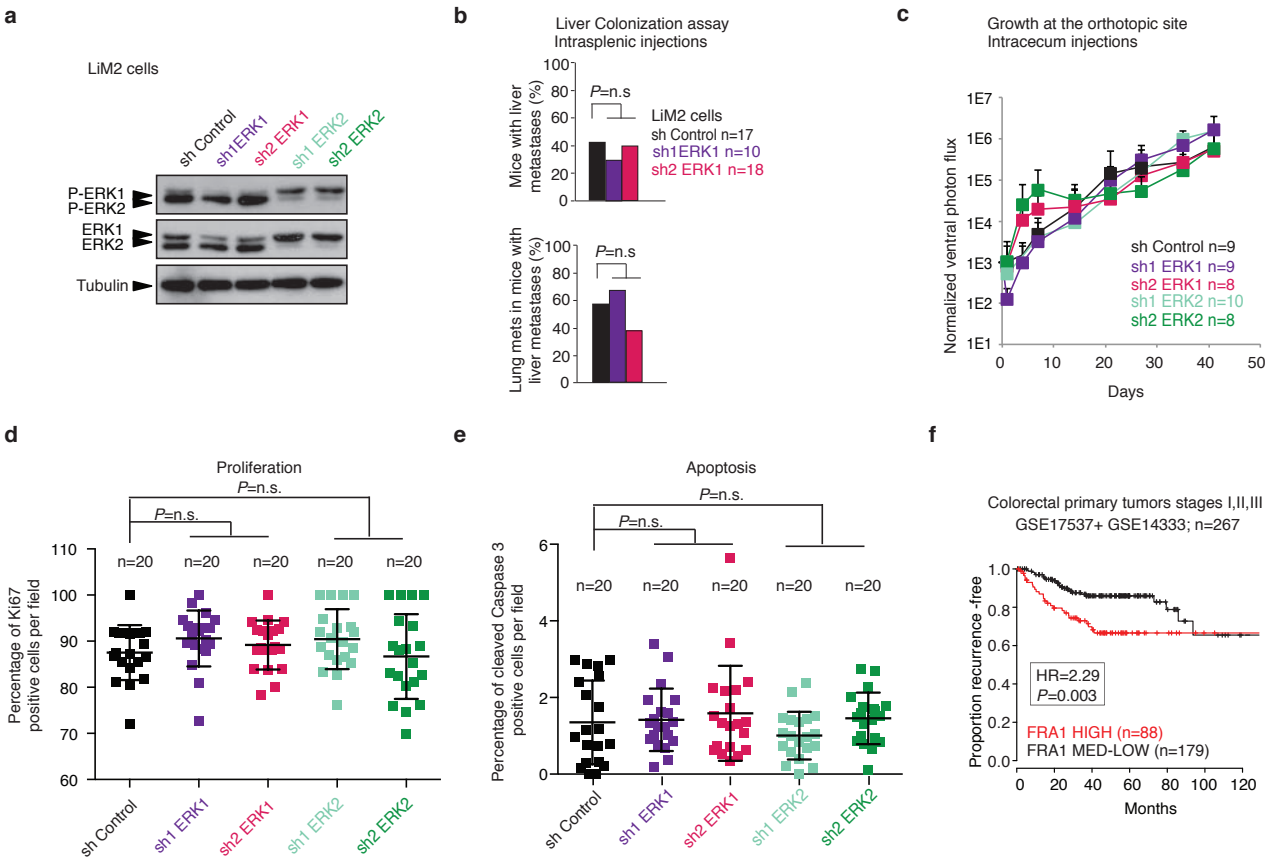

Supplementary Figure 3 ERK1 and ERK2 influence on primary tumors and metastasis. **(a)** ERK1 and ERK2 downregulation was confirmed by Western blotting (representative Western blots from three independent experiments are shown). **(b)** Percentage of mice intrasplenically injected with LiM2 cells expressing the indicated shRNAs that developed liver metastases (up) or lung metastasis (bottom). n= 17 (shControl), n=10 (sh1 ERK1) and n=18 (sh2 ERK1) number of mice used per group pooled from two independent experiments. Statistical analysis was done using two-sided Fisher's exact test. n.s.- not significant. **(c)** LiM2 cells expressing the indicated shRNAs were injected orthotopically into mice cecum and growth rates by photon flux quantification were determined. n=9 (shControl), n=9 (sh1 ERK1), n=8 (sh2 ERK1), n=10 (sh1 ERK2), n=8 (sh2 ERK2) number of mice used per group. Data is presented as average plus s.d. Statistical analysis was done using one-way ANOVA and no statistical differences were found. **(d and e)** Size matched lesions from (c) were selected for immunohistochemistry Ki-67 (d) and cleaved caspase-3 staining (e). n=20 total fields per group analyzed where five different fields from size matched lesions per mouse were quantified. Number of mice used in each group was 4. Statistical analysis was done using two-tailed Mann Whitney test. All values are presented in the graphs together with average ±s.d. **(f)** Kaplan-Meier curves representing association of proportion of recurrence-free patients with relative *FRA1* gene expression levels in human primary colon cancer dataset (pooled GSE17537 and GSE14333; n=267). HR-hazard ratio. Statistical analysis was done using Cox proportional hazard's model.

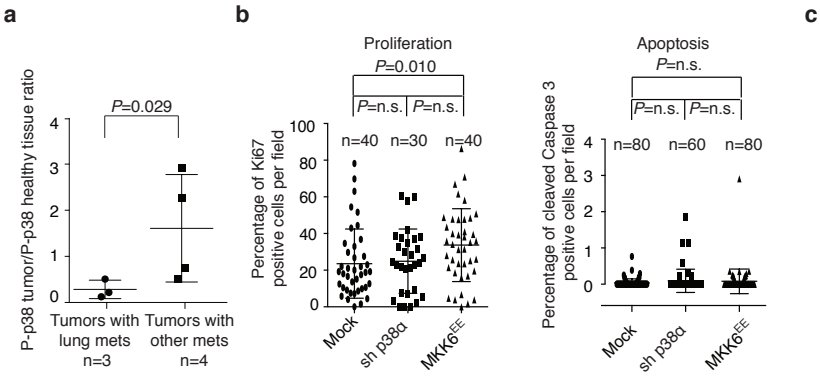

c

Group	Metastasis		
	mice with liver mets (%)	area (mm^2) liver	area (mm^2) lung
Mock	44.4	0.09±0.02	0.03±0.01 #
$MKK6^{EE}$	55.5	0.08±0.07	0.04±0.01 †
sh p38α	16.7	0.04±0.02	0.13±0.02 #†

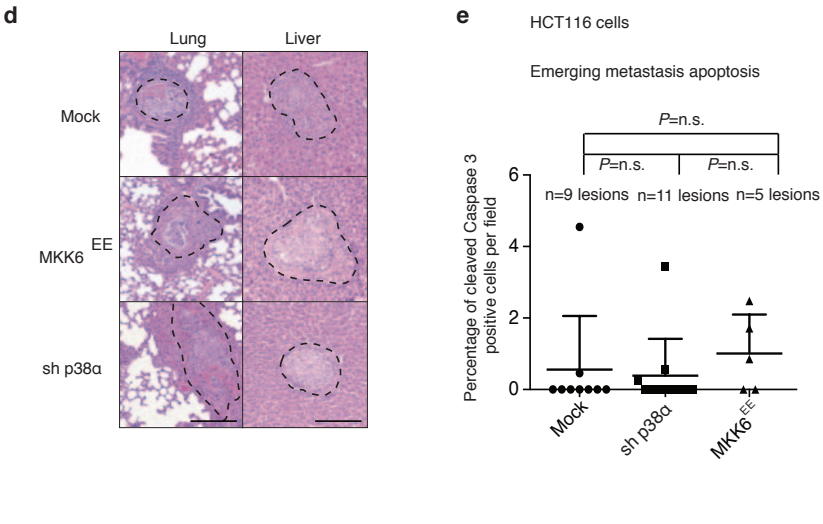

Supplementary Figure 4 Lung metastasis in colon cancer associates with low levels of phopsho-p38 MAPK in primary tumors. **(a)** Association of lung metastasis with levels of phosphorylated p38 (P-p38) protein in samples of 7 primary CRC tumor samples that developed metastasis. P-p38 levels were normalized to p38 total amount of protein and P-p38 expressed in the respective healthy mucosa samples. n=3 tumors with lung mets and n=4 tumors with other mets. Statistical analysis was done using one-tailed Mann Whitney test. **(b)** HCT116 cells expressing p38α shRNAs or constitutively active $MKK6^{EE}$ were injected orthotopically into mice cecum and size matched lesions were selected for Ki-67 and cleaved caspase-3 staining. Five different fields per lesion and mouse for Ki67 staining and ten different fields /lesion/mouse for cleaved caspase-3 staining were scored. n=40 (Mock), n=30 (sh p38 α) and n=40 ($MKK6^{EE}$) total number of fields per group analyzed for Ki67 staining. n=80 (Mock), n=60 (sh p38 α) and n=80 ($MKK6^{EE}$) total number of fields per group analyzed for cleaved caspase-3 staining. **(c)** HCTT116 cells expressing p38α shRNAs or constitutively active $MKK6^{EE}$ were injected orthotopically into mice cecum and the percentage of mice that developed liver metastasis, the area of liver and lung metastasis were determined. #, † indicate the groups which statistically significant. # P=0.001; † P=0.017. Values for area represent mean ± s.e.m. n=41 (Mock), n=14 (sh p38 α) and n=61 ($MKK6^{EE}$) number of lung lesions analyzed. **(d)** Representative H&E staining of lung and liver histological sections from (c). Dashed lines delineate metastasis. Scale bar 200 μm. **(e)** Emerging lung metastatic lesions from HCTT116 cells expressing p38α shRNAs or constitutively active $MKK6^{EE}$ injected orthotopically into mice cecum were selected for cleaved caspase-3 staining. n=9 (Mock), n=11 (sh p38 α) and n=5 ($MKK6^{EE}$) total number of lesions analyzed per group. **(f)** Emerging lung metastatic lesions from SW620 parental and LiM2 cells were selected for cleaved caspase-3 staining. n=6 (Parental) and n=9 (LiM2) total number of lesions analyzed per group. Scale bar 50 μm. For (b),(c), (e) and (f) two-tailed Mann Whitney test was used for statistical analysis; n.s.- not significant. In panels (a), (b), and (f) all values are presented in the graphs together with average ±s.d. In panel (e) all values are presented in the graph together with average plus s.d.

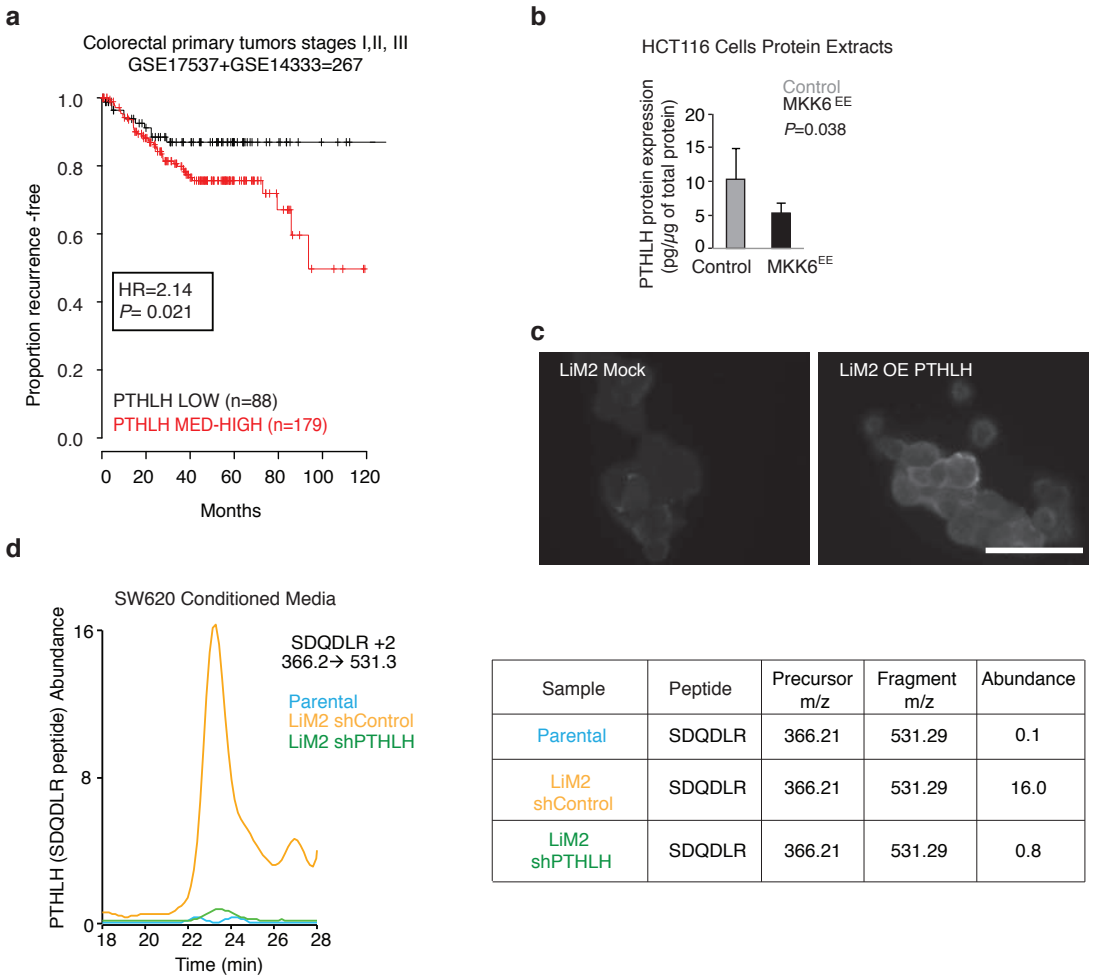

Sample	Peptide	Precursor m/z	Fragment m/z	Abundance
Parental	SDQDLR	366.21	531.29	0.1
LiM2 shControl	SDQDLR	366.21	531.29	16.0
LiM2 shPTHLH	SDQDLR	366.21	531.29	0.8

Supplementary Figure 5 *PTHLH* gene expression is associated with poor clinical outcome in patients with colon cancer. **(a)** Kaplan-Meier curves representing association of proportion of recurrence-free patients with relative *PTHLH* gene expression levels in human primary colon cancer dataset (pooled GSE17537 and GSE14333; n=267). HR-hazard ratio. Statistical analysis was done using Cox proportional hazard's model. **(b and c)** ELISA analysis of PTHLH levels in HCTT116 cells (n=3 values from independent experiments) expressing constitutively active MKK6EE (b) or immunofluorescence analysis of PTHLH levels (representative images from two independent experiments) in SW620 cells expressing PTHLH (c). Statistical analysis was done using one-tailed Student's t test in (b) and graphs represent average plus s.d. Scale bar in (c) 50μM. **(d)** Detection of PTHLH by mass-spec analysis in conditioned medium from SW620 parental, LiM2 shControl and LiM2 shPTHLH cell lines.

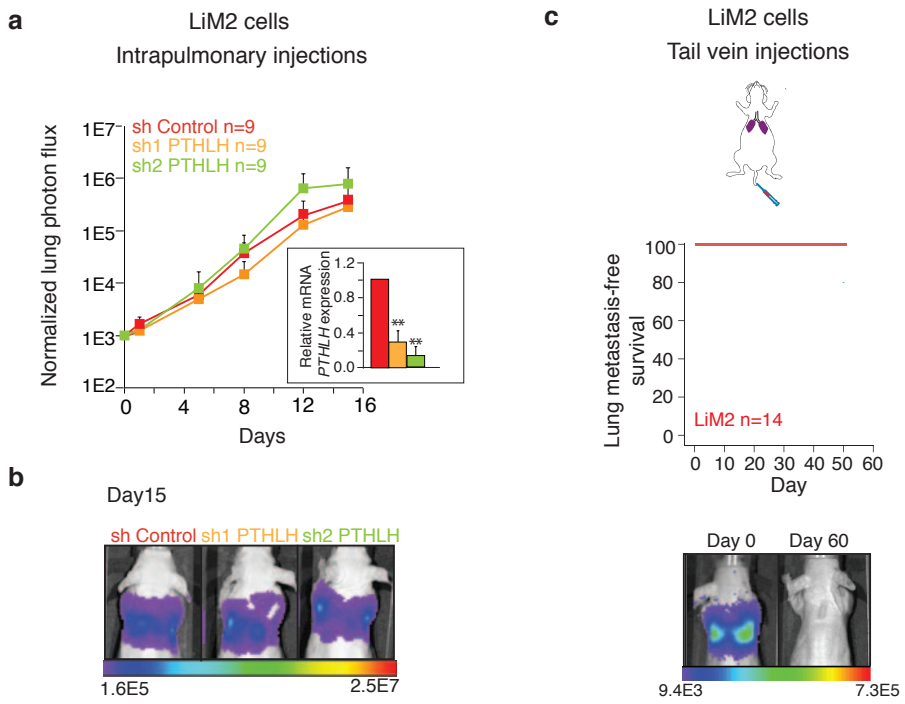

Supplementary Figure 6 *PTHLH* does not affect the growth of LiM2 cells in the lung. **(a)** Photon flux of dorsal upper back area of mice injected intrapulmonary with LiM2 cells expressing two different shRNA against *PTHLH.* Normalization was done to values of day 0. n=9 (sh Control), n=9 (sh1 PTHLH) and n=9 (sh2 PTHLH) number of mice used per group. Inset represents qRT-PCR analysis of *PTHLH* expression levels in LiM2 cells infected with lentivirus expressing shRNA against *PTHLH* or the control shRNA in three independent experiments (n=3). Statistical analysis for main graph was done using two-tailed Mann Whitney test and no statistically significant differences were found. Statistics for the graph presented in inset was done using two-tailed Student's t test. ** $P<0.001$. Values represented in the main graph as well as in inset represent average plus s.d. **(b)** Representative bioluminescent images of mice injected intrapulmonary with LiM2 cells expressing two different shRNAs against *PTHLH.* **(c)** Lung metastasis-free survival of mice (n = 14) upon tail vein injection of LiM2 cells. Representative bioluminescent images are shown.

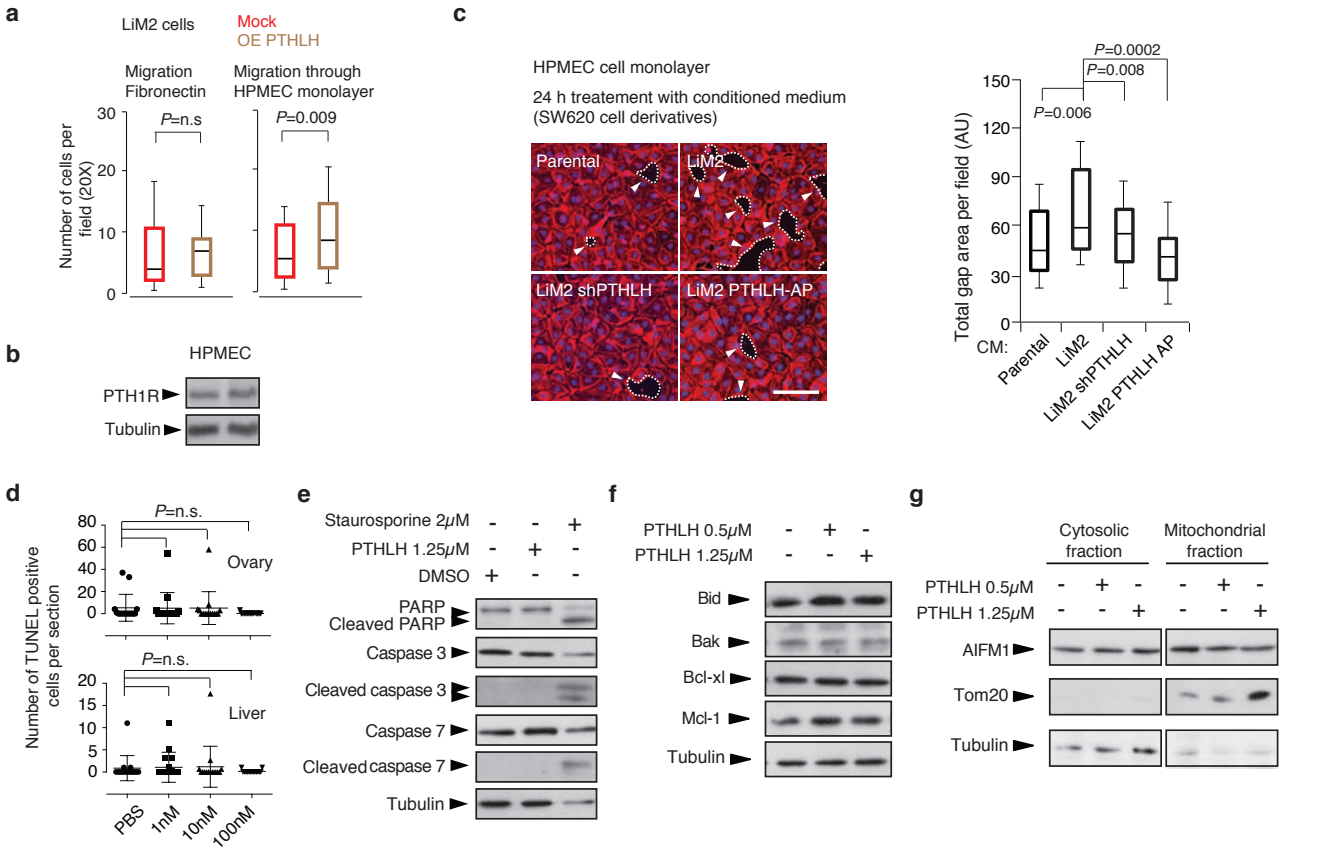

Supplementary Figure 7 Effect of PTHLH on endothelial cells of the lung. **(a)** Migration of LiM2 cells mock infected or infected with a retrovirus that expresses PTHLH was scored in Boyden chambers covered with fibronectin or with fibronectin and HPMEC monolayer. Each cell line was seeded in triplicate and 5 fields per chamber were counted. Results represent three independent experiments for migration through fibronectin and four independent experiments for migration through fibronectin and HPMEC monolayer. n=45 total number of fields analyzed per group for migration through fibronectin and n=60 total number of fields analyzed per group for migration through fibronectin and HPMEC monolayer. Statistical analysis was done using two-tailed Mann Whitney test **(b)** Western blot analysis of PTH1R expression levels in HPMEC cells (representative images from two independent experiments). Tubulin was used as a loading control. **(c)** HPMEC cells were grown until reaching tight confluence and then were treated for 24 h with conditioned medium from SW620 parental, LiM2, LiM2 shPTHLH and LiM2 treated cells with PTHLH-Antagonist Peptide (AP). Phalloidin staining was performed and total gap area per field was determined. Results represent values of three independent experiments where each sample was seeded in duplicate and for each coverslip at least 5 fields were analyzed. n=40,40,40 and 30 total number of fields analyzed per group respectively. Statistical analysis was done using two-tailed Student's t test; scale bar 100 μm. **(d)** Average number of TUNEL-positive cells in ovary or liver 4 h post tail vein injection of recombinant PTHLH (1-34). Three 30 μm distant sections per animal were counted. PBS, 1 nM, 10 nM, and 100 nM rPTHLH (5 mice per group). n=15 total number of sections analyzed per group. Statistical analysis was done using two-tailed Mann Whitney test; n.s.-not significant. All values are presented in the graphs together with average ±s.d. **(e)** Western blot analysis of total and cleaved PARP, Caspases-3 and Caspases-7 in HPMEC cells treated for 20 h with PTHLH or Staurosporine. Tubulin was used as a loading control. **(f)** Western blot analysis of pro-apoptotic and anti-apoptotic protein levels in HPMEC cells upon 4 h treatment with the indicated doses of recombinant PTHLH. Tubulin was used as a loading control. **(g)** HPMEC cells were treated for 4 h with the indicated doses of recombinant PTHLH and the cytosolic and mitochondrial fractions were isolated and subjected to western blot analysis for AIFM1 protein expression levels. Tom 20 was used as a loading control of mitochondria and tubulin as a loading control of cytosol. In panels (a) and (c) the box extends from 25 to 75 percentile where black line within the box represents median, the whiskers extend from 10 to 90 percentile. Western blot images in (e), (f) and (g) are representative from at least two independent experiments.

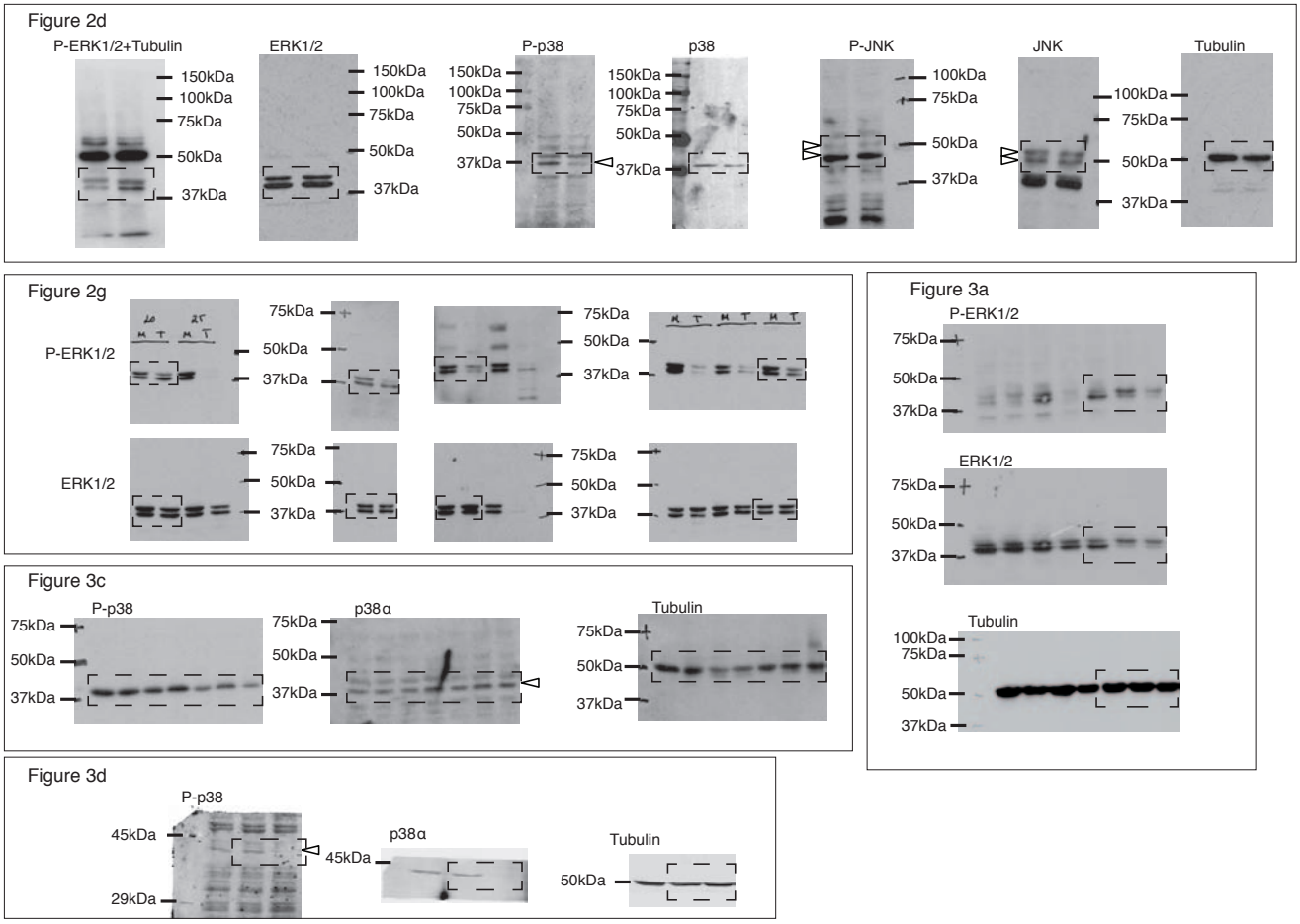

Supplementary Figure 8 Full scans

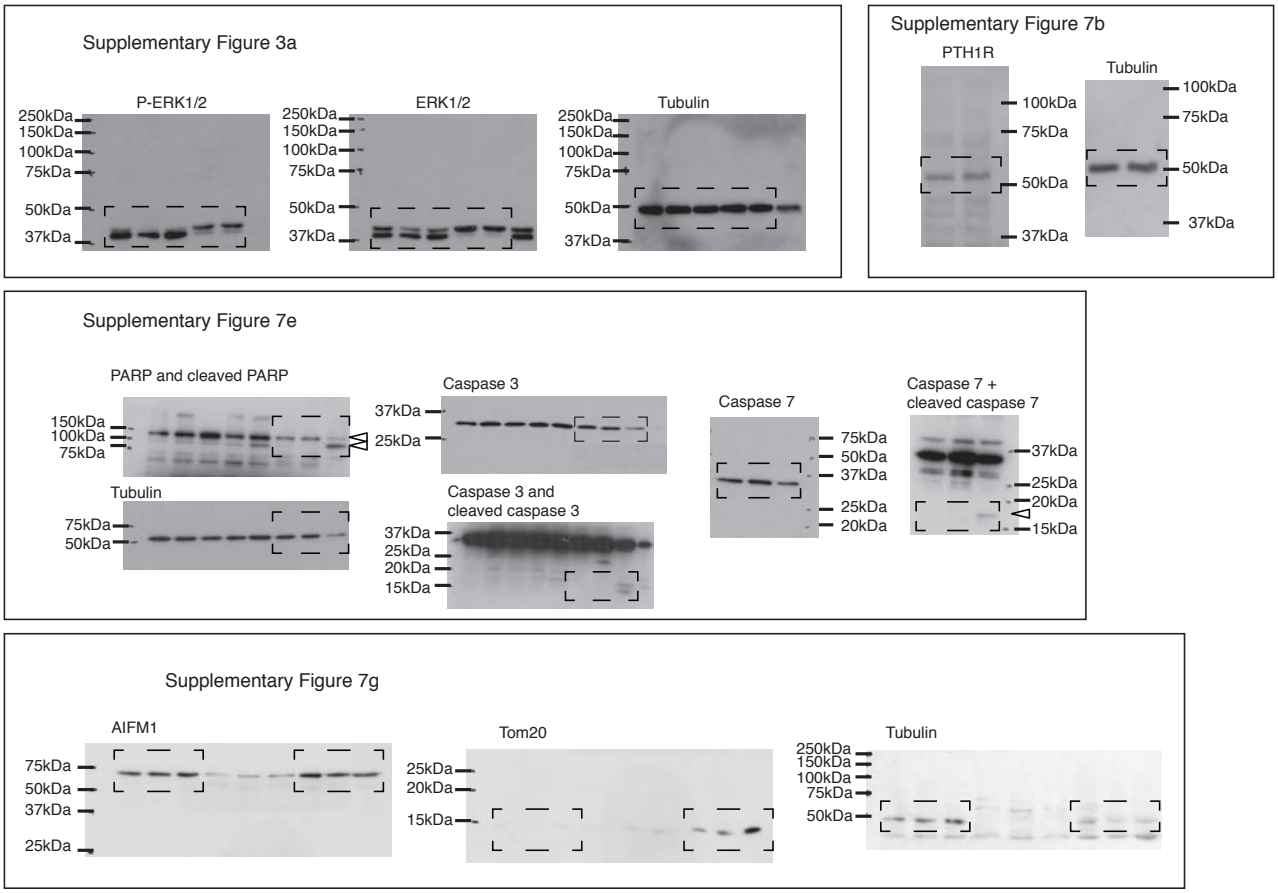

Supplementary Figure 8 continued Full scans

Supplementary Video Legend

Supplementary Video 1 PTHLH treatment increases intracellular Ca2+ levels. Cells were treated for 15 min with Fluo4-AM calcium indicator and then imaged for 9 min. First two minutes of imaging were used for determining the basal Ca2+ levels. At min 2, control media was added to cells and at min 5 media with 1.25μM recombinant PTHLH.

Supplementary Table Legends

Supplementary Table 1 Genes differentially expressed between Parental and LiM2 cells. Comparative genome-wide expression analysis of genes that were overexpressed or underexpressed at least 2.5-fold in the highly liver metastatic derivative LiM2 compared to parental cells

Supplementary Table 2 BGSEA for KEGG gene sets (Parental vs. LiM2). By using BGSEA we identified pathway-specific gene expression signatures (KEGG gene sets) that were differentially represented in the gene expression profiles of parental and LiM2 cells.

Supplementary Table 3 Frequency of liver and lung metastasis in a pooled analysis of patients with metastatic colon and rectal cancers. Frequency of liver and lung metastasis in a pooled analysis of patients with metastatic colon and rectal cancers with clinical annotation for the site of metastasis.

Supplementary Table 4 Genes differentially expressed in LiM2 cells compared to Parental that correlated significantly with MKK6 expression in CRC primary tumors. Genes differentially expressed in LiM2 cells compared to Parental (fc>1.7) that correlated significantly ($p<0.05$) with MKK6 expression in Stage II and III CRC primary tumors.

Supplementary Table 1. Genes differentially expressed between Parental and LiM2 cells (cut off 2.5)

Accession	Entrezid	Symbol	Fold change	ProbDE	LiM2 upregulated (1) LiM2 downregulated (-1)
7968678	341640	FREM2	24.08653858	0.999999949	1
8044225	27233	SULT1C4	26.52948714	0.999999928	1
7971150	10186	LHFP	10.82175184	0.999999913	1
8150529	27121	DKK4	9.067136049	0.999999864	1
7996819	1001	CDH3	8.893116512	0.999999697	1
8120654	56479	KCNQ5	6.617315074	0.999999694	1
8151369	157869	C8orf84	8.235975632	0.999999669	1
8123246	6581	SLC22A3	-13.20478963	0.999999575	-1
8149142	1670	DEFA5	21.4552802	0.999999502	1
7955963	118430	MUCL1	17.42689016	0.999999479	1
7943892	4684	NCAM1	-6.896299997	0.999999179	-1
8018652	114804	RNF157	-5.115656414	0.999999012	-1
7985159	1381	CRABP1	-10.74399738	0.99999859	-1
8054451	10913	EDAR	9.789151555	0.999998519	1
8149465	26281	FGF20	17.05711611	0.999998482	1
8149927	1191	CLU	5.789090398	0.999998422	1
8162502	2203	FBP1	5.443603034	0.999998393	1
7989199	8854	ALDH1A2	4.239215443	0.999998251	1
7962455	4753	NELL2	8.873481898	0.999998119	1
7932243	221061	FAM171A1	3.696377047	0.999998079	1
8044154	926	CD8B	5.892235369	0.999997984	1
7940409	921	CD5	5.735089339	0.999997852	1
7963427	3852	KRT5	10.01237522	0.999997749	1
8121850	23493	HEY2	8.748918888	0.999997527	1
8138381	10551	AGR2	8.528661076	0.999997501	1
7990714	1136	CHRNA3	5.375162024	0.99999743	1
8040365	28951	TRIB2	3.575833149	0.999997282	1
8068651	5121	PCP4	-5.787313903	0.999997275	-1
8107823	171019	ADAMTS19	6.278995307	0.999997225	1
8169145	139221	MUM1L1	6.060861226	0.999996884	1
8102232	51176	LEF1	7.6912546	0.999996553	1
8081590	90102	PHLDB2	8.145721728	0.999996409	1
7944769	57476	GRAMD1B	-5.451589415	0.99999604	-1
8073088	60489	APOBEC3G	5.317387373	0.99999597	1
8113130	79772	MCTP1	6.63524134	0.999995795	1
8117054	10486	CAP2	-4.231752363	0.999995599	-1
7953200	894	CCND2	5.053642341	0.99999558	1
8078066	152273	FGD5	-5.030668514	0.999995406	-1
8020455	2627	GATA6	-3.908156132	0.99999537	-1
8115147	972	CD74	3.183285686	0.999995365	1
7913237	55450	CAMK2N1	-5.705441	0.999995365	-1
8148040	114569	MAL2	10.90406283	0.999995127	1
8020141	147495	APCDD1	3.628691314	0.999994847	1
7925929	8644	AKR1C3	-4.030067133	0.999994826	-1
7948332	9404	LPXN	3.336534706	0.999994727	1
7977046	7127	TNFAIP2	4.242035576	0.999993157	1
7965403	4060	LUM	-6.128287931	0.999993055	-1

Supplementary Table 2. BGSEA for KEGG gene sets (Parental vs. LiM2)

set	KEGGterm	probEnriched
4010	MAPK signaling pathway	1
4514	Cell adhesion molecules (CAMs)	1
910	Nitrogen metabolism	1
120	Primary bile acid biosynthesis	1
532	Chondroitin sulfate biosynthesis	1
561	Glycerolipid metabolism	1
4360	Axon guidance	1
4512	ECM-receptor interaction	1
4950	Maturity onset diabetes of the young	1
5200	Pathways in cancer	1
534	Heparan sulfate biosynthesis	1
4510	Focal adhesion	1
600	Sphingolipid metabolism	1
3320	PPAR signaling pathway	1
4520	Adherens junction	1
4660	T cell receptor signaling pathway	1
4670	Leukocyte transendothelial migration	1
5218	Melanoma	1
5410	Hypertrophic cardiomyopathy (HCM)	0.99
51	Fructose and mannose metabolism	0.99
4810	Regulation of actin cytoskeleton	0.99
5412	Arrhythmogenic right ventricular cardiomyopathy (ARVC)	0.99
4310	Wnt signaling pathway	0.99
4920	Adipocytokine signaling pathway	0.98
4350	TGF-beta signaling pathway	0.98
5222	Small cell lung cancer	0.98
4020	Calcium signaling pathway	0.98
510	N-Glycan biosynthesis	0.98
2010	ABC transporters	0.97
4666	Fc gamma R-mediated phagocytosis	0.97
564	Glycerophospholipid metabolism	0.97
4060	Cytokine-cytokine receptor interaction	0.97
4070	Phosphatidylinositol signaling system	0.97
790	Folate biosynthesis	0.96
512	O-Glycan biosynthesis	0.96
5212	Pancreatic cancer	0.95
361	gamma-Hexachlorocyclohexane degradation	0.95
360	Phenylalanine metabolism	0.95

Supplementary Table 3. Frequency of liver and lung metastasis in a pooled analysis of patients with metastatic colon and rectal cancers

	Patients with only liver metastasis (%)	Patients with only lung metastasis (%)	Patients with liver and lung metastasis (%)	Total number of patients*
Colon cancer	40 (42.6)	3 (3.2)	23 (24.5)	94
Rectal cancer	11 (23.9)	12 (26)	13 (28.3)	46

* Some of the patients developed metastasis is sites other than liver and lung.

Pooled analysis of patients from references [1 and 2 of supplementary information].

Supplementary Table 4. Genes differentially expressed in LiM2 cells compared to Parental (fc>1.7) that correlated significantly (p<0.05) with *MKK6* expression in Stage II and III CRC primary tumors

Entrezid	Symbol	Probeid
29974	A1CF	220951_s_at
257629	ANKS4B	239087_at
10123	**ARL4C**	202207_at
81563	C1orf21	223127_s_at
814	CAMK4	210349_at
50515	**CHST11**	226372_at
119467	CLRN3	229777_at
1644	DDC	214347_s_at
2918	GRM8	216255_s_at
3174	HNF4G	207456_at
5654	**HTRA1**	201185_at
10186	**LHFP**	218656_s_at
5744	**PTHLH**	211756_at
54502	RBM47	229439_s_at
6038	RNASE4	205158_at
6515	**SLC2A3**	202499_s_at
54843	SYTL2	220613_s_at
7113	TMPRSS2	1570433_at
28951	**TRIB2**	202478_at
128553	TSHZ2	244521_at
7103	TSPAN8	203824_at

In Bold, highlighted genes whose change of expression in SW620 cells liver metastatic derivatives compared to parental is concordant to that found in patients CRC primary tumors that correlate with *MKK6* expression.

5

Discussion

We used two diverse and complementary approaches to shed light on the biology that drives the clinical behavior of CRC.

In the first place, we have used a modern epidemiology approach combining a prospective cohort of healthy individuals where we identified incident cases of CRC with genotyping techniques and histological characterization of the tumors. The use of a prospectively collected detailed data on CRC risk factors over a long-term follow-up allowed us to account for the main potential confounders of our association. We found that in this study, involving 1509 cases of CRC and 2307 controls nested in the two prospective cohorts, the CRC-susceptibility locus *SMAD7* intronic rs4939827 was associated with a lower risk of CRCs with pT1 and pT2 stage but not pT3 and pT4 stage. Among patients diagnosed with CRC, those with at least one G allele had 1.5 - fold higher odds of having a pT3 or pT4 tumor compared with a pT1 or pT2 tumor. This finding may explain in part observed associations of the G allele of rs4939827 with lower overall risk of incident CRC (23), but worsened survival after diagnosis (25, 112).

The seemingly contrary associations of this SNP in SMAD7 with decreased risk of incident disease shown in GWAS studies (17, 22) but poorer outcomes in patients with established disease may be due to SMAD7's known involvement in modulating the TGFβ type 1 pathway.

The *SMAD7* gene codes for an intracellular protein that interacts with the TGFβ type 1 receptor, and promotes its degradation in the proteasome therefore inhibiting TGFβ1-induced phosphorylation of SMAD2/SMAD3 (113). SMAD7 overexpression has been reported to be associated with the development of lung, pancreatic and skin

cancer and at the same time it can delay hepatocellular carcinoma growth and inhibit metastasis from melanoma and breast cancer (114). *SMAD7* also exerts its function via TGFβ-independent pathways. Specifically, it downregulates CDC25A (a phosphatase that regulates cell cycle) at a postranscriptional level (115). In normal epithelium, TGFβ1 functions as a tumor suppressor through induction of cell arrest and inhibition of cell proliferation. However, once cells are resistant to TGFβ1-mediated proliferative inhibition (*i.e.* in established tumors), TGFβ1 appears to promote metastasis by enhancing angiogenesis and extracellular matrix disruption and inhibiting infiltrating tumor immune cells.

We also found an association of rs4939827 with *RUNX3* methylation status in the tumors, which supports a role of rs4939827 in the TGFβ1 pathway. *RUNX3* is a Runt domain transcription factor 3 involved in TGFβ1 signaling by interaction with SMAD transcription factors and it is considered a suppressor of solid tumors. The RUNX3 promoter is commonly aberrantly methylated in a CpG island in CRC (116, 117, 118), leading to gene inactivation. RUNX3 is a downstream target of the TGFβ pathway. Specifically, RUNX3 is involved in mediating TGFβ-induced apoptosis. RUNX3 antagonizes the oncogenic Wnt pathway in CRC carcinogenesis by binding directly to the T-cell factor 4 (TCF4) and forming a ternary complex with β-catenin that negatively regulates the transcriptional activity of Wnt target genes (119). RUNX3 also acts as a downstream target of the bone morphogenetic proteins (proteins that belong to the TGFβ superfamily with a wide range of functions, including proliferation and apoptosis) and exerts its tumor suppressor effect by inhibiting c-Myc (120). *RUNX3* SNPs are associated with survival after a diagnosis of CRC (121). Differential methylation of *RUNX3* according to rs4939827 could help explain the worsened survival among individuals with CRC who have a variant G allele (121). TGFβ and Wnt signaling are involved in the induction of epithelial-mesenchymal transition, a process that mediates invasion and metastasis in CRC. However, our mediation analysis does not suggest that the association between rs4939827 on risk of CRC according to pT stage is primarily related to *RUNX3*. Nonetheless, the mediation analysis should be interpreted in the context of some limitations (111), including the assumption of a lack of other, strong unmeasured confounders.

We also examined several other molecular markers besides *RUNX3* and did not observe relevant differences in the association with rs4939827. *BRAF* status did appear

to be differentially associated with rs4939827 (uncorrected p value=0.02), despite the lack of a significant p value for heterogeneity after correction for multiple comparisons. Given that an interplay between TGFβ and *BRAF* mutations is biologically plausible (122) and that *BRAF* mutations are relative rare and strongly associated with CRC prognosis (123, 124), we cannot rule out that in a larger sample size such heterogeneity might have been more evident. A previous study that also studied the heterogeneity in associations of rs4939827 with *CIMP* status, MSI, *KRAS* or *p53* mutational status did not find any relevant association (121).

In the second place, we used a *bench* approach based on cell lines and animal models merged with publically available clinical data to investigate mechanisms of metastasis in CRC, taking advantadge of high-throughput gene expression technology. Research on biology of metastasis has progressed in the last decade, throwing light on many of the processes involved: angiogenesis, the role of the stroma, EMT and mesenchimal-to-epithelial transition, intravasation, circulation, extravasation, survival upon arrival to the distant organ, stemness, the role of metastatic niches and celullar latency (71, 81).

Here we describe a novel "metastasis from metastasis" mechanism of CRC spread. Liver is the predominant site of CRC; nevertheless, a small set of patients with *KRAS* mutant tumors can also present lung metastasis with an enrichment of *KRAS* mutations (125). We provide evidence for a distinct mechanism that relies on different signalling pathways whose hierarchical modulation enhances the ability of departing tumour cells to consecutively seed the liver and the lungs.

After enriching the liver metastatic capacity of a *mutant* KRAS cell line, colaterally the lung metastatic capacity was also enhanced. Through mRNA expression and pathway analysis we identified a high activity of ERK1/2 and low levels of p38 as plausible mediators. Reinforcing these findings, a low ERK/p38 signal ratio was found in fresh tumor biopsies from CRC patients with liver metastasis as compared with patients without metastasis after two years of follow-up from primary tumor surgery. This is in line with previous studies that have shown that ERK signaling favors circulating tumor cells colonization and growth (126). Notably, we propose that p38 inhibition is required for lung colonization exclusively and that this is mediated by the cytokine PTHLH. Loss of p38 induces PHTLH which in turn induces caspase-independent endothelial cell death allowing extravasation of circulating tumor cells into the lung.

Our study confronts previous evidence claiming "distant metastasis do not metastasize" (127). The study of Holzel *et.al.* argues, using breast cancer data from a national tumor registry and analyzing the relationship of metastasis-free survival or overall survival with primary tumor size and lymph node involvement, that all the metastasis happen before primary tumor retrieval (127). They do not provide any experimental evidence to support their claim. Metastatic cancer cells need to gain a number of functions in order to be able to generate overt metastases (*i.e.* angiogenesis, stroma activation, invasion, EMT, intravasation, circulation, extravasation, survival on the distant organ, stemness, immune evasion, cellular latency, reactivation, specialized cooption, recirculation (81)). It seems unlikely that cells that have gained these functions and have been able to colonize a distant organ cannot repeat the process to colonize a second one. Experimental evidence shows that metastatic cells can seed the primary tumor with more efficiency than their corresponding parental lines (49).

Our results indicate that genetic changes that allow cancer cells to efficiently metastatize to the liver must be followed by additional genetic alterations that allow secondary metastases from the liver to the lung, emphasizing the concept of "metastases from metastases". We illustrate the systemic contribution of PTHLH released from tumor cells in supporting distant metastatic processes by triggering vascular permeability. The expression of PTHLH is higher in CRC tissue than in normal colorectal mucosa or polyps (128), and our findings emphasize the ability of PTHLH to trigger caspase-independent cell death at the lung vasculature as a novel contributor to the hierarchical process of metastasis in CRC. Previous studies have implicated PTHLH in breast and squamous cell carcinoma tumour progression to bone metastasis through its activity in the bone remodelling process (129, 130, 131).

The observation that liver and lung colonization are linked to tumour-specific or circulating cell-specific factors may help create new therapeutic opportunities and also opens new questions that can help understand the biology of the evolution of CRC. Based on our results, Bragado *et al.* hypothesized that, given that TGFβ2 and BMPs can induce dormancy post extravasation by establishing a low ERK/p38 signaling ratio (126, 132), our cell line with higher metastatic capacity might have regained sensitivity to dormancy signals via p38 activation. This opens new research opportunities and enrich the research field on metastasis of CRC.

6

Conclusions

- Patients with the rs4939827 CRC-susceptibility locus diagnosed with CRC tend to develop tumors with greater invasiveness (as measured by the pT stage).
- The variant rs4939827 is differentially associated with RUNX3 methylation status, supporting an effect of rs4939827 or causal variants tagged by this SNP on carcinogenesis mediated through the TGFβ pathway. Taken together, these results could explain, at least in part, the lower risk of CRC associated with the G allele of rs4939827 yet poorer survival.
- ERK2 activation provides colon cancer cells with the ability to seed and colonize the liver.
- Reduced p38 MAPK signalling endows cancer cells with the ability to form lung metastasis from previously established liver lesions. Downregulation of p38 MAPK signalling results in increased expression of the cytokine PTHLH, which contributes to colon cancer cell extravasation to the lung by inducing caspase-independent death in endothelial cells of the lung microvasculature.

References

[1] http://globocan.iarc.fr/ (last accessed 08/24/14), editor. *GLOBOCAN 2012*. International Agency for Research on Cancer (World Health Organization), 06 2012. 1

[2] P Lichtenstein, N V Holm, P K Verkasalo, A Iliadou, J Kaprio, M Koskenvuo, E Pukkala, A Skytthe, and K Hemminki. **Environmental and heritable factors in the causation of cancer–analyses of cohorts of twins from Sweden, Denmark, and Finland**. *N Engl J Med*, **343**(2):78–85, Jul 2000. 1

[3] Paul R Burton, Martin D Tobin, and John L Hopper. **Key concepts in genetic epidemiology**. *Lancet*, **366**(9489):941–51, 2005. 3

[4] Teri A Manolio, Francis S Collins, Nancy J Cox, David B Goldstein, Lucia A Hindorff, David J Hunter, Mark I McCarthy, Erin M Ramos, Lon R Cardon, Aravinda Chakravarti, Judy H Cho, Alan E Guttmacher, Augustine Kong, Leonid Kruglyak, Elaine Mardis, Charles N Rotimi, Montgomery Slatkin, David Valle, Alice S Whittemore, Michael Boehnke, Andrew G Clark, Evan E Eichler, Greg Gibson, Jonathan L Haines, Trudy F C Mackay, Steven A McCarroll, and Peter M Visscher. **Finding the missing heritability of complex diseases**. *Nature*, **461**(7265):747–53, Oct 2009. 3

[5] R S Houlston, J Cheadle, S E Dobbins, A Tenesa, A M Jones, K Howarth, S L Spain, P Broderick, E Domingo, S Farrington, J G Prendergast, A M Pittman, E Theodoratou, C G Smith, B Olver, A Walther, R A Barnetson, M Churchman, E E Jaeger, S Penegar, E Barclay, L Martin, M Gorman, R Mager, E Johnstone, R Midgley, I Niittymaki, S Tuupanen, J Colley, S Idziaszczyk, H J Thomas, A M Lucassen, D G Evans, E R Maher, T Maughan, A Dimas, E Dermitzakis, J B Cazier, L A Aaltonen, P Pharoah, D J Kerr, L G Carvajal-Carmona, H Campbell, M G Dunlop, and I P Tomlinson. **Meta-analysis of three genome-wide association studies identifies susceptibility loci for colorectal cancer at 1q41, 3q26.2, 12q13.13 and 20q13.33**. *Nat Genet*, **42**(11):973–977, 2010. 4

[6] Ulrike Peters, Shuo Jiao, Fredrick R Schumacher, Carolyn M Hutter, Aaron K Aragaki, John A Baron, Sonja I Berndt, Stéphane Bézieau, Hermann Brenner, Katja Butterbach, Bette J Caan, Peter T Campbell, Christopher S Carlson, Graham Casey, Andrew T Chan, Jenny Chang-Claude, Stephen J Chanock, Lin S Chen, Gerhard A Coetzee, Simon G Coetzee, David V Conti, Keith R Curtis, David Duggan, Todd Edwards, Charles S Fuchs, Steven Gallinger, Edward L Giovannucci, Stephanie M Gogarten, Stephen B Gruber, Robert W Haile, Tabitha A Harrison, Richard B Hayes, Brian E Henderson, Michael Hoffmeister, John L Hopper, Thomas J Hudson, David J Hunter, Rebecca D Jackson, Sun Ha Jee, Mark A Jenkins, Wei-Hua Jia, Laurence N Kolonel, Charles Kooperberg, Sébastien Küry, Andrea Z Lacroix, Cathy C Laurie, Cecelia A Laurie, Loic Le Marchand, Mathieu Lemire, David Levine, Noralane M Lindor, Yan Liu, Jing Ma, Karen W Makar, Keitaro Matsuo, Polly A Newcomb, John D Potter, Ross L Prentice, Conghui Qu, Thomas Rohan, Stephanie A Rosse, Robert E Schoen, Daniela Seminara, Martha Shrubsole, Xiao-Ou Shu, Martha L Slattery, Darin Taverna, Stephen N Thibodeau, Cornelia M Ulrich, Emily White, Yongbing Xiang, Brent W Zanke, Yi-Xin Zeng, Ben Zhang, Wei Zheng, Li Hsu, and Colon Cancer Family Registry and the Genetics and Epidemiology of Colorectal Cancer Consortium. **Identification of Genetic Susceptibility Loci for Colorectal Tumors in a Genome-Wide Meta-analysis**. *Gastroenterology*, **144**(4):799–807.e24, Apr 2013. 4, 5

[7] Stephanie L Stenzel, Fredrick R Schumacher, Christopher K Edlund, David V Conti, Leon Raskin, Flavio Lejbkowicz, Mila Pinchev, Hedy S Rennert, Mark A Jenkins, John L Hopper, Daniel D Buchanan, Noralane M Lindor, Loic Le Marchand, Steven Gallinger, Robert W Haile, Polly A Newcomb, Shu-Chen Huang, Gad Rennert, Graham Casey, and Stephen B Gruber. **A novel colorectal cancer risk locus at 4q32.2 identified from an international genome-wide association study**. *Carcinogenesis*, Jul 2014. 4

[8] Wei-Hua Jia, Ben Zhang, Keitaro Matsuo, Aesun Shin, Yong-Bing Xiang, Sun Ha Jee, Dong-Hyun Kim, Zefang Ren, Qiuyin Cai, Jirong Long, Jiajun Shi, Wanqing Wen, Gong Yang, Ryan J Delahanty, Genetics and Epidemiology of Colorectal Cancer Consortium (GECCO), Colon Cancer Family Registry (CCFR), Bu-Tian Ji, Zhi-Zhong Pan, Fumihiko Matsuda, Yu-Tang Gao, Jae Hwan Oh, Yoon-Ok Ahn, Eun Jung Park, Hong-Lan Li, Ji Won Park, Jaeseong Jo, Jin-Young Jeong, Satoyo Hosono, Graham Casey, Ulrike Peters, Xiao-Ou Shu, Yi-Xin Zeng, and Wei Zheng. **Genome-wide association analyses in East Asians identify new susceptibility loci for colorectal cancer**. *Nat Genet*, **45**(2):191–6, Feb 2013. 4

[9] Malcolm G Dunlop, Sara E Dobbins, Susan Mary Farrington, Angela M Jones, Claire Palles, Nicola Whiffin, Albert Tenesa, Sarah Spain, Peter Broderick, Li-Yin Ooi, Enric Domingo, Claire Smillie, Marc Henrion, Matthew Frampton, Lynn Martin, Graeme Grimes, Maggie Gorman, Colin Semple, Yusanne P Ma, Ella Barclay, James Prendergast, Jean-Baptiste Cazier, Bianca Olver, Steven Penegar, Steven Lubbe, Ian Chander, Luis G Carvajal-Carmona, Stephane Ballereau, Amy Lloyd, Jayaram Vijayakrishnan, Lina Zgaga, Igor Rudan, Evropi Theodoratou, Colorectal Tumour Gene Identification (CORGI) Consortium, John M Starr, Ian Deary, Iva Kirac, Dujo Kovacević, Lauri A Aaltonen, Laura Renkonen-Sinisalo, Jukka-Pekka Mecklin, Koichi Matsuda, Yusuke Nakamura, Yukinori Okada, Steven Gallinger, David J Duggan, David Conti, Polly Newcomb, John Hopper, Mark A Jenkins, Fredrick Schumacher, Graham Casey, Douglas Easton, Mitul Shah, Paul Pharoah, Annika Lindblom, Tao Liu, Swedish Low-Risk Colorectal Cancer Study Group, Christopher G Smith, Hannah West, Jeremy P Cheadle, COIN Collaborative Group, Rachel Midgley, David J Kerr, Harry Campbell, Ian P Tomlinson, and Richard S Houlston. **Common variation near CDKN1A, POLD3 and**

REFERENCES

SHROOM2 influences colorectal cancer risk. *Nat Genet*, **44**(7):770–6, Jul 2012. 4

[10] R Cui, Y Okada, S G Jang, J L Ku, J G Park, Y Kamatani, N Hosono, T Tsunoda, V Kumar, C Tanikawa, N Kamatani, R Yamada, M Kubo, Y Nakamura, and K Matsuda. **Common variant in 6q26-q27 is associated with distal colon cancer in an Asian population.** *Gut*, **60**(6):799–805, June 2011. 4

[11] Ian P M Tomlinson, Emily Webb, Luis Carvajal-Carmona, Peter Broderick, Kimberley Howarth, Alan M Pittman, Sarah Spain, Steven Lubbe, Axel Walther, Kate Sullivan, Emma Jaeger, Sarah Fielding, Andrew Rowan, Jayaram Vijayakrishnan, Enric Domingo, Ian Chandler, Zoe Kemp, Mobshra Qureshi, Susan M Farrington, Albert Tenesa, James G D Prendergast, Rebecca A Barnetson, Steven Penegar, Ella Barclay, Wendy Wood, Lynn Martin, Maggie Gorman, Huw Thomas, Julian Peto, D Timothy Bishop, Richard Gray, Eamonn R Maher, Anneke Lucassen, David Kerr, D Gareth R Evans, Clemens Schafmayer, Stephan Buch, Henry Völzke, Jochen Hampe, Stefan Schreiber, Ulrich John, Thibaud Koessler, Paul Pharoah, Tom van Wezel, Hans Morreau, Juul T Wijnen, John L Hopper, Melissa C Southey, Graham G Giles, Gianluca Severi, Sergi Castellví-Bel, Clara Ruiz-Ponte, Angel Carracedo, Antoni Castells, Asta Försti, Kari Hemminki, Pavel Vodicka, Alessio Naccarati, Lara Lipton, Judy W C Ho, K K Cheng, Pak C Sham, J Luk, Jose A G Agúndez, Jose M Ladero, Miguel de la Hoya, Trinidad Caldés, Iina Niittymäki, Sari Tuupanen, Auli Karhu, Lauri Aaltonen, Jean-Baptiste Cazier, Harry Campbell, Malcolm G Dunlop, and Richard S Houlston. **A genome-wide association study identifies colorectal cancer susceptibility loci on chromosomes 10p14 and 8q23.3.** *Nature genetics*, **40**(5):623–30, May 2008. 4, 5

[12] Brent W Zanke, Celia M T Greenwood, Jagadish Rangrej, Rafal Kustra, Albert Tenesa, Susan M Farrington, James Prendergast, Sylviane Olschwang, Theodore Chiang, Edgar Crowdy, Vincent Ferretti, Philippe Laflamme, Saravanan Sundararajan, Stéphanie Roumy, Jean-François Olivier, Frédérick Robidoux, Robert Sladek, Alexandre Montpetit, Peter Campbell, Stephane Bezieau, Anne Marie O'Shea, George Zogopoulos, Michelle Cotterchio, Polly Newcomb, John McLaughlin, Ban Younghusband, Roger Green, Jane Green, Mary E M Porteous, Harry Campbell, Helene Blanche, Mourad Sahbatou, Emmanuel Tubacher, Catherine Bonaiti-Pellié, Bruno Buecher, Elio Riboli, Sebastien Kury, Stephen J Chanock, John Potter, Gilles Thomas, Steven Gallinger, Thomas J Hudson, and Malcolm G Dunlop. **Genome-wide association scan identifies a colorectal cancer susceptibility locus on chromosome 8q24**. *Nat Genet*, **39**(8):989–94, Aug 2007. 4

[13] Stephen B Gruber, Victor Moreno, Laura S Rozek, Hedy S Rennerts, Flavio Lejbkowicz, Joseph D Bonner, Joel K Greenson, Thomas J Giordano, Eric R Fearson, and Gad Rennert. **Genetic variation in 8q24 associated with risk of colorectal cancer**. *Cancer Biol Ther*, **6**(7):1143–7, Jul 2007. 4

[14] Christopher A Haiman, Loïc Le Marchand, Jennifer Yamamato, Daniel O Stram, Xin Sheng, Laurence N Kolonel, Anna H Wu, David Reich, and Brian E Henderson. **A common genetic risk factor for colorectal and prostate cancer**. *Nat Genet*, **39**(8):954–6, Aug 2007. 4

[15] Ian Tomlinson, Emily Webb, Luis Carvajal-Carmona, Peter Broderick, Zoe Kemp, Sarah Spain, Steven Penegar, Ian Chandler, Maggie Gorman, Wendy Wood, Ella Barclay, Steven Lubbe, Lynn Martin, Gabrielle Sellick, Emma Jaeger, Richard Hubner, Ruth Wild, Andrew Rowan, Sarah Fielding, Kimberley Howarth, CORGI Consortium, Andrew Silver, Wendy Atkin, Kenneth Muir, Richard Logan, David Kerr, Elaine Johnstone, Oliver Sieber, Richard Gray, Huw Thomas, Julian Peto, Jean-Baptiste Cazier, and Richard Houlston. **A genome-wide association scan of tag SNPs identifies a susceptibility variant for colorectal cancer at 8q24.21**. *Nat Genet*, **39**(8):984–8, Aug 2007. 4

[16] Carolyn M Hutter, Martha L Slattery, David J Duggan, Jill Muehling, Karen Curtin, Li Hsu, Shirley A A Beresford, Aleksandar Rajkovic, Gloria E Sarto, James R Marshall, Nazik Hammad, Robert Wallace, Karen W Makar, Ross L Prentice, Bette J Caan, John D Potter, and Ulrike Peters. **Characterization of the association between 8q24 and colon cancer: gene-environment exploration and meta-analysis.** *BMC cancer*, **10**:670, January 2010. 4

[17] Albert Tenesa, Susan M Farrington, James G D Prendergast, Mary E Porteous, Marion Walker, Naila Haq, Rebecca A Barnetson, Evropi Theodoratou, Roseanne Cetnarskyj, Nicola Cartwright, Colin Semple, Andrew J Clark, Fiona J L Reid, Lorna A Smith, Kostas Kavoussanakis, Thibaud Koessler, Paul D P Pharoah, Stephan Buch, Clemens Schafmayer, Jürgen Tepel, Stefan Schreiber, Henry Völzke, Carsten O Schmidt, Jochen Hampe, Jenny Chang-Claude, Michael Hoffmeister, Hermann Brenner, Stefan Wilkening, Federico Canzian, Gabriel Capella, Victor Moreno, Ian J Deary, John M Starr, Ian P M Tomlinson, Zoe Kemp, Kimberley Howarth, Luis Carvajal-Carmona, Emily Webb, Peter Broderick, Jayaram Vijayakrishnan, Richard S Houlston, Gad Rennert, Dennis Ballinger, Laura Rozek, Stephen B Gruber, Koichi Matsuda, Tomohide Kidokoro, Yusuke Nakamura, Brent W Zanke, Celia M T Greenwood, Jagadish Rangrej, Rafal Kustra, Alexandre Montpetit, Thomas J Hudson, Steven Gallinger, Harry Campbell, and Malcolm G Dunlop. **Genome-wide association scan identifies a colorectal cancer susceptibility locus on 11q23 and replicates risk loci at 8q24 and 18q21.** *Nature genetics*, **40**(5):631–7, May 2008. 4, 5, 61

[18] Jonathan D Kocarnik, Carolyn M Hutter, Martha L Slattery, Sonja I Berndt, Li Hsu, David J Duggan, Jill Muehling, Bette J Caan, Shirley A A Beresford, Aleksandar Rajkovic, Gloria E Sarto, James R Marshall, Nazik Hammad, Robert B Wallace, Karen W Makar, Ross L Prentice, John D Potter, Richard B Hayes, and Ulrike Peters. **Characterization of 9p24 risk locus and colorectal adenoma and cancer: gene-environment interaction and meta-analysis.** *Cancer epidemiology, biomarkers & prevention*, **19**(12):3131–9, December 2010. 4

[19] Richard S Houlston, Emily Webb, Peter Broderick, Alan M Pittman, Maria Chiara Di Bernardo, Steven Lubbe, Ian Chandler, Jayaram Vijayakrishnan, Kate Sullivan, Steven Penegar, Luis Carvajal-Carmona, Kimberley Howarth, Emma Jaeger, Sarah L Spain, Axel

Walther, Ella Barclay, Lynn Martin, Maggie Gorman, Enric Domingo, Ana S Teixeira, David Kerr, Jean-Baptiste Cazier, Iina Niittymäki, Sari Tuupanen, Auli Karhu, Lauri A Aaltonen, Ian P M Tomlinson, Susan M Farrington, Albert Tenesa, James G D Prendergast, Rebecca A Barnetson, Roseanne Cetnarskyj, Mary E Porteous, Paul D P Pharoah, Thibaud Koessler, Jochen Hampe, Stephan Buch, Clemens Schafmayer, Jurgen Tepel, Stefan Schreiber, Henry Völzke, Jenny Chang-Claude, Michael Hoffmeister, Hermann Brenner, Brent W Zanke, Alexandre Montpetit, Thomas J Hudson, Steven Gallinger, Harry Campbell, and Malcolm G Dunlop. **Meta-analysis of genome-wide association data identifies four new susceptibility loci for colorectal cancer.** *Nature genetics*, **40**(12):1426–35, December 2008. 4

[20] Ian P M Tomlinson, Luis G Carvajal-Carmona, Sara E Dobbins, Albert Tenesa, Angela M Jones, Kimberley Howarth, Claire Palles, Peter Broderick, Emma E M Jaeger, Susan Farrington, Annabelle Lewis, James G D Prendergast, Alan M Pittman, Evropi Theodoratou, Bianca Olver, Marion Walker, Steven Penegar, Ella Barclay, Nicola Whiffin, Lynn Martin, Stephane Ballereau, Amy Lloyd, Maggie Gorman, Steven Lubbe, Bryan Howie, Jonathan Marchini, Clara Ruiz-Ponte, Ceres Fernandez-Rozadilla, Antoni Castells, Angel Carracedo, Sergi Castellvi-Bel, David Duggan, David Conti, Jean-Baptiste Cazier, Harry Campbell, Oliver Sieber, Lara Lipton, Peter Gibbs, Nicholas G Martin, Grant W Montgomery, Joanne Young, Paul N Baird, Steven Gallinger, Polly Newcomb, John Hopper, Mark A Jenkins, Lauri A Aaltonen, David J Kerr, Jeremy Cheadle, Paul Pharoah, Graham Casey, Richard S Houlston, and Malcolm G Dunlop. **Multiple Common Susceptibility Variants near BMP Pathway Loci GREM1, BMP4, and BMP2 Explain Part of the Missing Heritability of Colorectal Cancer.** *PLoS genetics*, **7**(6):e1002105, June 2011. 4

[21] Emma Jaeger, Emily Webb, Kimberley Howarth, Luis Carvajal-Carmona, Andrew Rowan, Peter Broderick, Axel Walther, Sarah Spain, Alan Pittman, Zoe Kemp, Kate Sullivan, Karl Heinimann, Steven Lubbe, Enric Domingo, Ella Barclay, Lynn Martin, Maggie Gorman, Ian Chandler, Jayaram Vijayakrishnan, Wendy Wood, Elli Papaemmanuil, Steven Penegar, Mobshra Qureshi, CORGI Consortium, Susan Farrington, Albert Tenesa, Jean-Baptiste Cazier, David Kerr, Richard Gray, Julian Peto, Malcolm Dunlop, Harry Campbell, Huw Thomas, Richard Houlston, and Ian Tomlinson. **Common genetic variants at the CRAC1 (HMPS) locus on chromosome 15q13.3 influence colorectal cancer risk**. *Nat Genet*, **40**(1):26–8, Jan 2008. 4

[22] Peter Broderick, Luis Carvajal-Carmona, Alan M Pittman, Emily Webb, Kimberley Howarth, Andrew Rowan, Steven Lubbe, Sarah Spain, Kate Sullivan, Sarah Fielding, Emma Jaeger, Jayaram Vijayakrishnan, Zoe Kemp, Maggie Gorman, Ian Chandler, Elli Papaemmanuil, Steven Penegar, Wendy Wood, Gabrielle Sellick, Mobshra Qureshi, Ana Teixeira, Enric Domingo, Ella Barclay, Lynn Martin, Oliver Sieber, David Kerr, Richard Gray, Julian Peto, Jean-Baptiste Cazier, Ian Tomlinson, and Richard S Houlston. **A genome-wide association study shows that common alleles of SMAD7 influence colorectal cancer risk.** *Nature genetics*, **39**(11):1315–7, November 2007. 4, 5, 61

[23] Ulrike Peters, Carolyn M Hutter, Li Hsu, Fredrick R Schumacher, David V Conti, Christopher S Carlson, Christopher K Edlund, Robert W Haile, Steven Gallinger, Brent W Zanke, Mathieu Lemire, Jagadish Rangrej, Raakhee Vijayaraghavan, Andrew T Chan, Aditi Hazra, David J Hunter, Jing Ma, Charles S Fuchs, Edward L Giovannucci, Peter Kraft, Yan Liu, Lin Chen, Shuo Jiao, Karen W Makar, Darin Taverna, Stephen B Gruber, Gad Rennert, Victor Moreno, Cornelia M Ulrich, Michael O Woods, Roger C Green, Patrick S Parfrey, Ross L Prentice, Charles Kooperberg, Rebecca D Jackson, Andrea Z Lacroix, Bette J Caan, Richard B Hayes, Sonja I Berndt, Stephen J Chanock, Robert E Schoen, Jenny Chang-Claude, Michael Hoffmeister, Hermann Brenner, Bernd Frank, Stéphane Bézieau, Sébastien Küry, Martha L Slattery, John L Hopper, Mark A Jenkins, Loic Le Marchand, Noralane M Lindor, Polly A Newcomb, Daniela Seminara, Thomas J Hudson, David J Duggan, John D Potter, and Graham Casey. **Meta-analysis of new genome-wide association studies of colorectal cancer risk.** *Human Genetics*, **131**(2):217–34, February 2012. 3, 4, 5, 21, 61

[24] Peter ten Dijke and Caroline S Hill. **New insights into TGF-beta-Smad signalling**. *Trends Biochem Sci*, **29**(5):265–73, May 2004. 3

[25] Amanda I Phipps, Polly A Newcomb, Xabier Garcia-Albeniz, Carolyn M Hutter, Emily White, Charles S Fuchs, Aditi Hazra, Shuji Ogino, Hongmei Nan, Jing Ma, Peter T Campbell, Jane C Figueiredo, Ulrike Peters, and Andrew T Chan. **Association between colorectal cancer susceptibility Loci and survival time after diagnosis with colorectal cancer.** *Gastroenterology*, **143**(1):51–54.e4, July 2012. 3, 21, 61

[26] Lauri Aaltonen, Louise Johns, Heikki Järvinen, Jukka-Pekka Mecklin, and Richard Houlston. **Explaining the familial colorectal cancer risk associated with mismatch repair (MMR)-deficient and MMR-stable tumors**. *Clin Cancer Res*, **13**(1):356–61, Jan 2007. 6

[27] Yvonne M C Hendriks, Andrea E de Jong, Hans Morreau, Carli M J Tops, Hans F Vasen, Juul Th Wijnen, Martijn H Breuning, and Annette H J T Bröcker-Vriends. **Diagnostic approach and management of Lynch syndrome (hereditary nonpolyposis colorectal carcinoma): a guide for clinicians**. *CA Cancer J Clin*, **56**(4):213–25, 2006. 6

[28] Jan J Koornstra, Marian Je Mourits, Rolf H Sijmons, Annemarie M Leliveld, Harry Hollema, and Jan H Kleibeuker. **Management of extracolonic tumours in patients with Lynch syndrome**. *Lancet Oncol*, **10**(4):400–8, Apr 2009. 6

[29] Polymnia Galiatsatos and William D Foulkes. **Familial adenomatous polyposis**. *Am J Gastroenterol*, **101**(2):385–98, Feb 2006. 6

[30] Malcolm G Dunlop and Susan M Farrington. **MUTYH-associated polyposis and colorectal cancer**. *Surg Oncol Clin N Am*, **18**(4):599–610, Oct 2009. 6

[31] A. Walther, E. Johnstone, C. Swanton, R. Midgley, I. Tomlinson, and D. Kerr. **Genetic prognostic and predictive markers in colorectal cancer**. *Nat Rev Cancer*, **9**(7):489–99, 2009. 6

REFERENCES

[32] L N Spirio, W Samowitz, J Robertson, M Robertson, R W Burt, M Leppert, and R White. **Alleles of APC modulate the frequency and classes of mutations that lead to colon polyps**. *Nat Genet*, **20**(4):385–8, Dec 1998. 7

[33] M. Bienz and H. Clevers. **Linking colorectal cancer to Wnt signaling.** *Cell*, **103**(2):311–320, Oct 2000. 7

[34] G. C. Blobe, W. P. Schiemann, and H. F. Lodish. **Role of transforming growth factor beta in human disease.** *N Engl J Med*, **342**(18):1350–1358, May 2000. 7

[35] Rebecca L. Elliott and Gerard C. Blobe. **Role of transforming growth factor Beta in human cancer.** *J Clin Oncol*, **23**(9):2078–2093, Mar 2005. 7

[36] Klaudia Giehl. **Oncogenic Ras in tumour progression and metastasis**. *Biol Chem*, **386**(3):193–205, Mar 2005. 7

[37] E Miranda, A Destro, A Malesci, E Balladore, P Bianchi, E Baryshnikova, G Franchi, E Morenghi, L Laghi, L Gennari, and M Roncalli. **Genetic and epigenetic changes in primary metastatic and nonmetastatic colorectal cancer**. *Br J Cancer*, **95**(8):1101–7, Oct 2006. 8

[38] C. S. Karapetis, S. Khambata-Ford, D. J. Jonker, C. J. O'Callaghan, D. Tu, N. C. Tebbutt, R. J. Simes, H. Chalchal, J. D. Shapiro, S. Robitaille, T. J. Price, L. Shepherd, H. J. Au, C. Langer, M. J. Moore, and J. R. Zalcberg. **K-ras mutations and benefit from cetuximab in advanced colorectal cancer**. *N Engl J Med*, **359**(17):1757–65, 2008. 8

[39] A. C. Chiang and J. Massague. **Molecular basis of metastasis**. *N Engl J Med*, **359**(26):2814–23, 2008. 8

[40] D. X. Nguyen, P. D. Bos, and J. Massague. **Metastasis: from dissemination to organ-specific colonization**. *Nat Rev Cancer*, **9**(4):274–84, 2009. 8

[41] Gaorav P Gupta, Don X Nguyen, Anne C Chiang, Paula D Bos, Juliet Y Kim, Roger R Gomis, Katia Manova-Todorova, and Joan Massagué. **Mediators of vascular remodelling co-opted for sequential steps in lung metastasis**. *Nature*, **446**(7137):765–70, Apr 2007. 8, 10

[42] Jacques Pouysségur, Frédéric Dayan, and Nathalie M Mazure. **Hypoxia signalling in cancer and approaches to enforce tumour regression**. *Nature*, **441**(7092):437–43, May 2006. 9

[43] Evanthia T Roussos, John S Condeelis, and Antonia Patsialou. **Chemotaxis in cancer**. *Nat Rev Cancer*, **11**(8):573–87, Aug 2011. 9

[44] Sun-Jin Kim, Jang-Seong Kim, Eun Sung Park, Ju-Seog Lee, Qingtang Lin, Robert R Langley, Marva Maya, Junqin He, Seung-Wook Kim, Zhang Weihua, Krishnakumar Balasubramanian, Dominic Fan, Gordon B Mills, Mien-Chie Hung, and Isaiah J Fidler. **Astrocytes upregulate survival genes in tumor cells and induce protection from chemotherapy**. *Neoplasia*, **13**(3):286–98, Mar 2011. 9

[45] Fei Xing, Aya Kobayashi, Hiroshi Okuda, Misako Watabe, Sudha K Pai, Puspa R Pandey, Shigeru Hirota, Andrew Wilber, Yin-Yuan Mo, Brian E Moore, Wen Liu, Koji Fukuda, Megumi Iiizumi, Sambad Sharma, Yin Liu, Kerui Wu, Elizabeth Peralta, and Kounosuke Watabe. **Reactive astrocytes promote the metastatic growth of breast cancer stem-like cells by activating Notch signalling in brain**. *EMBO Mol Med*, **5**(3):384–96, Mar 2013. 9

[46] Theresa A Guise. **Breaking down bone: new insight into site-specific mechanisms of breast cancer osteolysis mediated by metalloproteinases**. *Genes Dev*, **23**(18):2117–23, Sep 2009. 9

[47] X. H. Zhang, Q. Wang, W. Gerald, C. A. Hudis, L. Norton, M. Smid, J. A. Foekens, and J. Massague. **Latent bone metastasis in breast cancer tied to Src-dependent survival signals**. *Cancer Cell*, **16**(1):67–78, 2009. Zhang, Xiang H-F Wang, Qiongqing Gerald, William Hudis, Clifford A Norton, Larry Smid, Marcel Foekens, John A Massague, Joan U54 CA126518/CA/NCI NIH HHS/United States U54 CA126518-030002/CA/NCI NIH HHS/United States Howard Hughes Medical Institute/United States Research Support, N.I.H., Extramural Research Support, Non-U.S. Gov't United States Cancer cell Cancer Cell. 2009 Jul 7;16(1):67-78. 9, 11

[48] Thordur Oskarsson, Swarnali Acharyya, Xiang H-F Zhang, Sakari Vanharanta, Sohail F Tavazoie, Patrick G Morris, Robert J Downey, Katia Manova-Todorova, Edi Brogi, and Joan Massagué. **Breast cancer cells produce tenascin C as a metastatic niche component to colonize the lungs**. *Nat Med*, **17**(7):867–74, Jul 2011. 9

[49] Mi-Young Kim, Thordur Oskarsson, Swarnali Acharyya, Don X Nguyen, Xiang H-F Zhang, Larry Norton, and Joan Massagué. **Tumor self-seeding by circulating cancer cells**. *Cell*, **139**(7):1315–26, Dec 2009. 9, 64

[50] Alexandre Calon, Elisa Espinet, Sergio Palomo-Ponce, Daniele V F Tauriello, Mar Iglesias, María Virtudes Céspedes, Marta Sevillano, Peter Jung, Xiang H-F Zhang, Daniel Byrom, Antoni Riera, David Rossell, Ramón Mangues, Joan Massagué, Elena Sancho, and Eduard Batlle. **Dependency of Colorectal Cancer on a TGF-B-Driven Program in Stromal Cells for Metastasis Initiation**. *Cancer Cell*, **22**(5):571–84, Nov 2012. 9

[51] Louis Vermeulen, Felipe De Sousa E Melo, Maartje van der Heijden, Kate Cameron, Joan H de Jong, Tijana Borovski, Jurriaan B Tuynman, Matilde Todaro, Christian Merz, Hans Rodermond, Martin R Sprick, Kristel Kemper, Dick J Richel, Giorgio Stassi, and Jan Paul Medema. **Wnt activity defines colon cancer stem cells and is regulated by the microenvironment**. *Nat Cell Biol*, **12**(5):468–76, May 2010. 9

[52] Jing Yang and Robert A Weinberg. **Epithelial-mesenchymal transition: at the crossroads of development and tumor metastasis**. *Dev Cell*, **14**(6):818–29, Jun 2008. 9

[53] Muh-Hwa Yang, Min-Zu Wu, Shih-Hwa Chiou, Po-Min Chen, Shyue-Yih Chang, Chung-Ji Liu, Shu-Chun Teng, and Kou-Juey Wu. **Direct regulation of TWIST by HIF-1alpha promotes metastasis**. *Nat Cell Biol*, **10**(3):295–305, Mar 2008. 9

[54] Sendurai A Mani, Wenjun Guo, Mai-Jing Liao, Elinor Ng Eaton, Ayyakkannu Ayyanan, Alicia Y Zhou, Mary Brooks, Ferenc Reinhard, Cheng Cheng Zhang, Michail Shipitsin, Lauren L Campbell, Kornelia Polyak, Cathrin Brisken, Jing Yang, and Robert A Weinberg. **The epithelial-mesenchymal transition generates cells with properties of stem cells**. *Cell*, **133**(4):704–15, May 2008. 10

[55] Jing Yang, Sendurai A Mani, Joana Liu Donaher, Sridhar Ramaswamy, Raphael A Itzykson, Christophe Come, Pierre Savagner, Inna Gitelman, Andrea Richardson, and Robert A Weinberg. **Twist, a master regulator of morphogenesis, plays an essential role in tumor metastasis**. *Cell*, **117**(7):927–39, Jun 2004. 10

[56] Oscar H Ocaña, Rebeca Córcoles, Angels Fabra, Gema Moreno-Bueno, Hervé Acloque, Sonia Vega, Alejandro Barrallo-Gimeno, Amparo Cano, and M Angela Nieto. **Metastatic colonization requires the repression of the epithelial-mesenchymal transition inducer Prrx1**. *Cancer Cell*, **22**(6):709–24, Dec 2012. 10

[57] Manav Korpal, Brian J Ell, Francesca M Buffa, Toni Ibrahim, Mario A Blanco, Toni Celià-Terrassa, Laura Mercatali, Zia Khan, Hani Goodarzi, Yuling Hua, Yong Wei, Guohong Hu, Benjamin A Garcia, Jiannis Ragoussis, Dino Amadori, Adrian L Harris, and Yibin Kang. **Direct targeting of Sec23a by miR-200s influences cancer cell secretome and promotes metastatic colonization**. *Nat Med*, **17**(9):1101–8, Sep 2011. 10

[58] Irène Baccelli, Andreas Schneeweiss, Sabine Riethdorf, Albrecht Stenzinger, Anja Schillert, Vanessa Vogel, Corinna Klein, Massimo Saini, Tobias Bäuerle, Markus Wallwiener, Tim Holland-Letz, Thomas Höfner, Martin Sprick, Martina Scharpff, Frederik Marmé, Hans Peter Sinn, Klaus Pantel, Wilko Weichert, and Andreas Trumpp. **Identification of a population of blood circulating tumor cells from breast cancer patients that initiates metastasis in a xenograft assay.** *Nat Biotechnol*, **31**(6):539–544, Jun 2013. 10

[59] Jeffrey B. Wyckoff, Yarong Wang, Elaine Y. Lin, Jiufeng Li, Sumanta Goswami, E Richard Stanley, Jeffrey E. Segall, Jeffrey W. Pollard, and John Condeelis. **Direct visualization of macrophage-assisted tumor cell intravasation in mammary tumors.** *Cancer Res*, **67**(6):2649–2656, Mar 2007. 10

[60] Elsa Quintana, Elena Piskounova, Mark Shackleton, Daniel Weinberg, Ugur Eskiocak, Douglas R. Fullen, Timothy M. Johnson, and Sean J. Morrison. **Human melanoma metastasis in NSG mice correlates with clinical outcome in patients.** *Sci Transl Med*, **4**(159):159ra149, Nov 2012. 10

[61] Shinichi Yachida, Siân Jones, Ivana Bozic, Tibor Antal, Rebecca Leary, Baojin Fu, Mihoko Kamiyama, Ralph H. Hruban, James R. Eshleman, Martin A. Nowak, Victor E. Velculescu, Kenneth W. Kinzler, Bert Vogelstein, and Christine A. Iacobuzio-Donahue. **Distant metastasis occurs late during the genetic evolution of pancreatic cancer.** *Nature*, **467**(7319):1114–1117, Oct 2010. 10

[62] Paula D. Bos, Xiang H-F. Zhang, Cristina Nadal, Weiping Shu, Roger R. Gomis, Don X. Nguyen, Andy J. Minn, Marc J. van de Vijver, William L. Gerald, John A. Foekens, and Joan Massagué. **Genes that mediate breast cancer metastasis to the brain.** *Nature*, **459**(7249):1005–1009, Jun 2009. 10

[63] David Padua, Xiang H-F. Zhang, Qiongqing Wang, William L. Gerald, Roger R. Gomis, and Joan Massagué. **TGFbeta primes breast tumors for lung metastasis seeding through angiopoietin-like 4.** *Cell*, **133**(1):66–77, Apr 2008. 10

[64] Sara Weis, Jianhua Cui, Leo Barnes, and David Cheresh. **Endothelial barrier disruption by VEGF-mediated Src activity potentiates tumor cell extravasation and metastasis.** *J Cell Biol*, **167**(2):223–229, Oct 2004. 10

[65] Monika Julia Wolf, Alexandra Hoos, Judith Bauer, Steffen Boettcher, Markus Knust, Achim Weber, Nicole Simonavicius, Christoph Schneider, Matthias Lang, Michael Stürzl, Roland S. Croner, Andreas Konrad, Markus G. Manz, Holger Moch, Adriano Aguzzi, Geert van Loo, Manolis Pasparakis, Marco Prinz, Lubor Borsig, and Mathias Heikenwalder. **Endothelial CCR2 signaling induced by colon carcinoma cells enables extravasation via the JAK2-Stat5 and p38MAPK pathway.** *Cancer Cell*, **22**(1):91–105, Jul 2012. 10

[66] Qing Chen, Xiang H-F. Zhang, and Joan Massagué. **Macrophage binding to receptor VCAM-1 transmits survival signals in breast cancer cells that invade the lungs.** *Cancer Cell*, **20**(4):538–549, Oct 2011. 11

[67] A. Merlos-Suarez, F. M. Barriga, P. Jung, M. Iglesias, M. V. Cespedes, D. Rossell, M. Sevillano, X. Hernando-Momblona, V. da Silva-Diz, P. Munoz, H. Clevers, E. Sancho, R. Mangues, and E. Batlle. **The intestinal stem cell signature identifies colorectal cancer stem cells and predicts disease relapse**. *Cell Stem Cell*, **8**(5):511–24, 2011. 11

[68] Roberta Pang, Wai Lun Law, Andrew C Y Chu, Jensen T Poon, Colin S C Lam, Ariel K M Chow, Lui Ng, Leonard W H Cheung, Xiao R Lan, Hui Y Lan, Victoria P Y Tan, Thomas C Yau, Ronnie T Poon, and Benjamin C Y Wong. **A subpopulation of CD26+ cancer stem cells with metastatic capacity in human colorectal cancer**. *Cell Stem Cell*, **6**(6):603–15, Jun 2010. 11

[69] Sebastian M Dieter, Claudia R Ball, Christopher M Hoffmann, Ali Nowrouzi, Friederike Herbst, Oksana Zavidij, Ulrich Abel, Anne Arens, Wilko Weichert, Karsten Brand, Moritz Koch, Jürgen Weitz, Manfred Schmidt, Christof von Kalle, and Hanno Glimm. **Distinct types of tumor-initiating cells form human colon cancer tumors and metastases**. *Cell Stem Cell*, **9**(4):357–65, Oct 2011. 11

[70] Antonija Kreso, Catherine A O'Brien, Peter van Galen, Olga I Gan, Faiyaz Notta, Andrew M K Brown, Karen Ng, Jing Ma, Erno Wienholds, Cyrille Dunant, Aaron Pollett, Steven Gallinger, John McPherson, Charles G Mullighan, Darryl Shibata, and John E Dick. **Variable clonal repopulation dynamics influence chemotherapy response in colorectal cancer**. *Science*, **339**(6119):543–8, Feb 2013. 11

[71] Thordur Oskarsson, Eduard Batlle, and Joan Massagué. **Metastatic stem cells: sources, niches, and vital pathways.** *Cell Stem Cell*, **14**(3):306–321, Mar 2014. 11, 12, 63

REFERENCES

[72] Hans Clevers. **The intestinal crypt, a prototype stem cell compartment.** *Cell*, **154**(2):274–284, Jul 2013. 12

[73] Ya-Chieh Hsu and Elaine Fuchs. **A family business: stem cell progeny join the niche to regulate homeostasis.** *Nat Rev Mol Cell Biol*, **13**(2):103–114, Feb 2012. 12

[74] Yusuke Shiozawa, Elisabeth A. Pedersen, Aaron M. Havens, Younghun Jung, Anjali Mishra, Jeena Joseph, Jin Koo Kim, Lalit R. Patel, Chi Ying, Anne M. Ziegler, Michael J. Pienta, Junhui Song, Jingcheng Wang, Robert D. Loberg, Paul H. Krebsbach, Kenneth J. Pienta, and Russell S. Taichman. **Human prostate cancer metastases target the hematopoietic stem cell niche to establish footholds in mouse bone marrow.** *J Clin Invest*, **121**(4):1298–1312, Apr 2011. 12

[75] Nikki Charles and Eric C. Holland. **The perivascular niche microenvironment in brain tumor progression.** *Cell Cycle*, **9**(15):3012–3021, Aug 2010. 12

[76] Yvonne Kienast, Louisa von Baumgarten, Martin Fuhrmann, Wolfgang E F. Klinkert, Roland Goldbrunner, Jochen Herms, and Frank Winkler. **Real-time imaging reveals the single steps of brain metastasis formation.** *Nat Med*, **16**(1):116–122, Jan 2010. 12

[77] Manuel Valiente, Anna C. Obenauf, Xin Jin, Qing Chen, Xiang H-F. Zhang, Derek J. Lee, Jamie E. Chaft, Mark G. Kris, Jason T. Huse, Edi Brogi, and Joan Massagué. **Serpins promote cancer cell survival and vascular co-option in brain metastasis.** *Cell*, **156**(5):1002–1016, Feb 2014. 12

[78] Jia Lu, Xiangcang Ye, Fan Fan, Ling Xia, Rajat Bhattacharya, Seth Bellister, Federico Tozzi, Eric Sceusi, Yunfei Zhou, Isamu Tachibana, Dipen M. Maru, David H. Hawke, Janusz Rak, Sendurai A. Mani, Patrick Zweidler-McKay, and Lee M. Ellis. **Endothelial cells promote the colorectal cancer stem cell phenotype through a soluble form of Jagged-1.** *Cancer Cell*, **23**(2):171–185, Feb 2013. 12

[79] Ilaria Malanchi, Hector Peinado, Deepika Kassen, Thomas Hussenet, Daniel Metzger, Pierre Chambon, Marcel Huber, Daniel Hohl, Amparo Cano, Walter Birchmeier, and Joerg Huelsken. **Cutaneous cancer stem cell maintenance is dependent on beta-catenin signalling.** *Nature*, **452**(7187):650–653, Apr 2008. 12

[80] A. J. Minn, G. P. Gupta, P. M. Siegel, P. D. Bos, W. Shu, D. D. Giri, A. Viale, A. B. Olshen, W. L. Gerald, and J. Massague. **Genes that mediate breast cancer metastasis to lung**. *Nature*, **436**(7050):518–24, 2005. 12

[81] Sakari Vanharanta and Joan Massagué. **Origins of metastatic traits.** *Cancer Cell*, **24**(4):410–421, Oct 2013. 12, 63, 64

[82] Dalit Barkan, Jeffrey E. Green, and Ann F. Chambers. **Extracellular matrix: a gatekeeper in the transition from dormancy to metastatic growth.** *Eur J Cancer*, **46**(7):1181–1188, May 2010. 12

[83] Paul E. Goss and Ann F. Chambers. **Does tumour dormancy offer a therapeutic target?** *Nat Rev Cancer*, **10**(12):871–877, Dec 2010. 12

[84] Julio A. Aguirre-Ghiso, Liliana Ossowski, and Sarah K. Rosenbaum. **Green fluorescent protein tagging of extracellular signal-regulated kinase and p38 pathways reveals novel dynamics of pathway activation during primary and metastatic growth.** *Cancer Res*, **64**(20):7336–7345, Oct 2004. 12

[85] Hua Gao, Goutam Chakraborty, Ai Ping Lee-Lim, Qianxing Mo, Markus Decker, Alin Vonica, Ronglai Shen, Edi Brogi, Ali H. Brivanlou, and Filippo G. Giancotti. **The BMP inhibitor Coco reactivates breast cancer cells at lung metastatic sites.** *Cell*, **150**(4):764–779, Aug 2012. 12

[86] SB Edge, DR Byrd, C C Compton, and AG Fritz. *AJCC Cancer Staging Manual*. Springer, 2009. 13

[87] A B Benson, M A Choti, A M Cohen, J H Doroshow, C Fuchs, K Kiel, E W Martin, C McGinn, N J Petrelli, J A Posey, J M Skibber, A Venook, and T J Yeatman. **NCCN Practice Guidelines for Colorectal Cancer.** *Oncology (Williston Park, N.Y.)*, **14**(11A):203–12, November 2000. 13

[88] Paul F Engstrom, Al B Benson, and Leonard Saltz. **Colon cancer. Clinical practice guidelines in oncology.** *Journal of the National Comprehensive Cancer Network : JNCCN*, **1**(1):40–53, January 2003. 13

[89] R Labianca, B Nordlinger, G D Beretta, S Mosconi, M Mandalà, A Cervantes, and D Arnold. **Early colon cancer: ESMO Clinical Practice Guidelines for diagnosis, treatment and follow-up.** *Annals of oncology*, **24 Suppl 6**(April 2002):vi64–72, October 2013. 13

[90] Hye Young Kim, Soon Jin Lee, Gilsun Lee, Limwha Song, Su-A Kim, Jin Yong Kim, Dong Kyung Chang, Poong-Lyul Rhee, Jae J Kim, Jong Chul Rhee, Ho-Kyung Chun, and Young-Ho Kim. **Should Preoperative Chest CT Be Recommended to All Colon Cancer Patients?** *Annals of surgery*, February 2013. 13

[91] T. Andre, C. Boni, M. Navarro, J. Tabernero, T. Hickish, C. Topham, A. Bonetti, P. Clingan, J. Bridgewater, F. Rivera, and A. de Gramont. **Improved overall survival with oxaliplatin, fluorouracil, and leucovorin as adjuvant treatment in stage II or III colon cancer in the MOSAIC trial**. *J Clin Oncol*, **27**(19):3109–16, 2009. 13, 14

[92] Quasar Collaborative Group, Richard Gray, Jennifer Barnwell, Christopher McConkey, Robert K Hills, Norman S Williams, and David J Kerr. **Adjuvant chemotherapy versus observation in patients with colorectal cancer: a randomised study**. *Lancet*, **370**(9604):2020–9, Dec 2007. 13

[93] (IMPACT) investigators. **Efficacy of adjuvant fluorouracil and folinic acid in colon cancer. International Multicentre Pooled Analysis of Colon Cancer Trials .** *Lancet*, **345**(8955):939–944, Apr 1995. 13

[94] Sharlene Gill, Charles L. Loprinzi, Daniel J. Sargent, Stephan D. Thomé, Steven R. Alberts, Daniel G. Haller, Jacqueline Benedetti, Guido Francini, Lois E. Shepherd, Jean Francois Seitz, Roberto Labianca, Wei Chen, Stephen S. Cha, Michael P. Heldebrant, and Richard M. Goldberg. **Pooled analysis of fluorouracil-based adjuvant therapy for stage II and III colon cancer: who benefits and by how much?** *J Clin Oncol*, **22**(10):1797–1806, May 2004. 13

[95] Al B Benson, 3rd, Deborah Schrag, Mark R. Somerfield, Alfred M. Cohen, Alvaro T. Figueredo, Patrick J. Flynn, Monika K. Krzyzanowska, Jean Maroun, Pamela McAllister, Eric Van Cutsem, Melissa Brouwers, Manya Charette, and Daniel G. Haller. **American Society of Clinical Oncology recommendations on adjuvant chemotherapy for stage II colon cancer.** *J Clin Oncol*, **22**(16):3408–3419, Aug 2004. 13

[96] Greg Yothers, Michael J O'Connell, Carmen J Allegra, J Philip Kuebler, Linda H Colangelo, Nicholas J Petrelli, and Norman Wolmark. **Oxaliplatin as adjuvant therapy for colon cancer: updated results of NSABP C-07 trial, including survival and subset analyses**. *J Clin Oncol*, **29**(28):3768–74, Oct 2011. 13, 14

[97] L. B. Saltz, S. Clarke, E. Diaz-Rubio, W. Scheithauer, A. Figer, R. Wong, S. Koski, M. Lichinitser, T. S. Yang, F. Rivera, F. Couture, F. Sirzen, and J. Cassidy. **Bevacizumab in combination with oxaliplatin-based chemotherapy as first-line therapy in metastatic colorectal cancer: a randomized phase III study**. *J Clin Oncol*, **26**(12):2013–9, 2008. 14

[98] V Alonso-Orduna, M Marmol, P Escudero, A Salud, MJ Safont, JC Mendez, A Garcia Giron, M Martin, C Fernandez-Martos, X. Garcia-Albeniz, J Feliu, and J Maurel. **A validation of current prognostic scores in metastatic colorectal cancer (mCRC) and a new prognostic score (A GEMCAD study)**. *Annals of Oncology*, **25**(s4):167–209, 2014. 14

[99] Eric Van Cutsem, Claus-Henning Köhne, Erika Hitre, Jerzy Zaluski, Chung-Rong Chang Chien, Anatoly Makhson, Geert D'Haens, Tamás Pintér, Robert Lim, György Bodoky, Jae Kyung Roh, Gunnar Folprecht, Paul Ruff, Christopher Stroh, Sabine Tejpar, Michael Schlichting, Johannes Nippgen, and Philippe Rougier. **Cetuximab and chemotherapy as initial treatment for metastatic colorectal cancer**. *N Engl J Med*, **360**(14):1408–17, Apr 2009. 14

[100] Jean-Yves Douillard, Kelly S. Oliner, Salvatore Siena, Josep Tabernero, Ronald Burkes, Mario Barugel, Yves Humblet, Gyorgy Bodoky, David Cunningham, Jacek Jassem, Fernando Rivera, Ilona Kocákova, Paul Ruff, Maria Błasi?ska-Morawiec, Martin Šmakal, Jean Luc Canon, Mark Rother, Richard Williams, Alan Rong, Jeffrey Wiezorek, Roger Sidhu, and Scott D. Patterson. **Panitumumab-FOLFOX4 treatment and RAS mutations in colorectal cancer.** *N Engl J Med*, **369**(11):1023–1034, Sep 2013. 14

[101] R. G. Amado, M. Wolf, M. Peeters, E. Van Cutsem, S. Siena, D. J. Freeman, T. Juan, R. Sikorski, S. Suggs, R. Radinsky, S. D. Patterson, and D. D. Chang. **Wild-type KRAS is required for panitumumab efficacy in patients with metastatic colorectal cancer**. *J Clin Oncol*, **26**(10):1626–34, 2008. 14

[102] Axel Grothey, Eric Van Cutsem, Alberto Sobrero, Salvatore Siena, Alfredo Falcone, Marc Ychou, Yves Humblet, Olivier Bouché, Laurent Mineur, Carlo Barone, Antoine Adenis, Josep Tabernero, Takayuki Yoshino, Heinz-Josef Lenz, Richard M. Goldberg, Daniel J. Sargent, Frank Cihon, Lisa Cupit, Andrea Wagner, Dirk Laurent, and C. O. R. R. E. C. T Study Group . **Regorafenib monotherapy for previously treated metastatic colorectal cancer (CORRECT): an international, multicentre, randomised, placebo-controlled, phase 3 trial.** *Lancet*, **381**(9863):303–312, Jan 2013. 14

[103] Eric Van Cutsem, Josep Tabernero, Radek Lakomy, Hans Prenen, Jana Prausová, Teresa Macarulla, Paul Ruff, Guy A. van Hazel, Vladimir Moiseyenko, David Ferry, Joe McKendrick, Jonathan Polikoff, Alexia Tellier, Rémi Castan, and Carmen Allegra. **Addition of aflibercept to fluorouracil, leucovorin, and irinotecan improves survival in a phase III randomized trial in patients with metastatic colorectal cancer previously treated with an oxaliplatin-based regimen.** *J Clin Oncol*, **30**(28):3499–3506, Oct 2012. 14

[104] Niall C Tebbutt, Kate Wilson, Val J Gebski, Michelle M Cummins, Diana Zannino, Guy A van Hazel, Bridget Robinson, Adam Broad, Vinod Ganju, Stephen P Ackland, Garry Forgeson, David Cunningham, Mark P Saunders, Martin R Stockler, Yujo Chua, John R Zalcberg, R John Simes, and Timothy J Price. **Capecitabine, bevacizumab, and mitomycin in first-line treatment of metastatic colorectal cancer: results of the Australasian Gastrointestinal Trials Group Randomized Phase III MAX Study**. *J Clin Oncol*, **28**(19):3191–8, Jul 2010. 14

[105] Rolf Sauer, Heinz Becker, Werner Hohenberger, Claus Rödel, Christian Wittekind, Rainer Fietkau, Peter Martus, Jörg Tschmelitsch, Eva Hager, Clemens F. Hess, Johann-H. Karstens, Torsten Liersch, Heinz Schmidberger, Rudolf Raab, and German Rectal Cancer Study Group . **Preoperative versus postoperative chemoradiotherapy for rectal cancer.** *N Engl J Med*, **351**(17):1731–1740, Oct 2004. 14

[106] C Fernandez-Martos and X Garcia-Albeniz. **Should upfront chemotherapy precede preoperative chemoradiation and surgery?** In V Valentini, HJ Schmoll, and CJH Van de Velde, editors, *Multidisciplinary management of rectal cancer: questions and answers*, pages 193–204. Heidelberg:Springer, 2012. 14

[107] A. L. Martling, T. Holm, L. E. Rutqvist, B. J. Moran, R. J. Heald, and B. Cedemark. **Effect of a surgical training programme on outcome of rectal cancer in the County of Stockholm. Stockholm Colorectal Cancer Study Group, Basingstoke Bowel Cancer Research Project.** *Lancet*, **356**(9224):93–96, Jul 2000. 14

[108] Xabier García-Albéniz, Rosa Gallego, Ralf Dieter Hofheinz, Gloria Fernández-Esparrach, Juan Ramón Ayuso-Colella, Josep Antoni Bombí, Carles Conill, Miriam Cuatrecasas, Salvadora Delgado, Angels Ginés, Rosa Miquel, Mario Pagés, Estela Pineda, Verónica Pereira, Aarón Sosa, Oscar Reig, Iván Victoria, Luis Feliz, Antonio María de Lacy, Antoni Castells, Iris Burkholder, Andreas Hochhaus, and Joan Maurel. **Adjuvant therapy sparing in rectal cancer achieving complete response after chemoradiation**. *World J Gastroenterol*, **20**(42):15820–9, Nov 2014. 15

REFERENCES

[109] **National Comprehensive Cancer Network. Colon Cancer (Version 1.2012)**. 15

[110] Tyler J Vanderweele and Stijn Vansteelandt. **Odds ratios for mediation analysis for a dichotomous outcome.** *American journal of epidemiology*, **172**(12):1339–48, December 2010. 22, 23

[111] Linda Valeri and Tyler J Vanderweele. **Mediation analysis allowing for exposure-mediator interactions and causal interpretation: theoretical assumptions and implementation with SAS and SPSS macros**. *Psychol Methods*, **18**(2):137–50, Jun 2013. 22, 62

[112] M.N. Passarelli, A.E. Coghill, C.M. Hutter, Yingye Zheng, K.W. Makar, J.D. Potter, and P.A. Newcomb. **Common colorectal cancer risk variants in SMAD7 are associated with survival among prediagnostic nonsteroidal anti-inflammatory drug users: A population-based study of postmenopausal women**. *Genes, Chromosomes and Cancer*, **50**(July):875–886, 2011. 61

[113] A Nakao, M Afrakhte, A Morén, T Nakayama, J L Christian, R Heuchel, S Itoh, M Kawabata, N E Heldin, C H Heldin, and P ten Dijke. **Identification of Smad7, a TGFbeta-inducible antagonist of TGF-beta signalling**. *Nature*, **389**(6651):631–5, Oct 1997. 61

[114] Marco A Briones-Orta, Angeles C Tecalco-Cruz, Marcela Sosa-Garrocho, Cassandre Caligaris, and Marina Macías-Silva. **Inhibitory Smad7: emerging roles in health and disease**. *Curr Mol Pharmacol*, **4**(2):141–53, Jun 2011. 62

[115] C Stolfi, V De Simone, A Colantoni, E Franzè, E Ribichini, M C Fantini, R Caruso, I Monteleone, G S Sica, P Sileri, T T MacDonald, F Pallone, and G Monteleone. **A functional role for Smad7 in sustaining colon cancer cell growth and survival**. *Cell Death Dis*, **5**:e1073, 2014. 62

[116] Terje Ahlquist, Guro E Lind, Vera L Costa, Gunn I Meling, Morten Vatn, Geir S Hoff, Torleiv O Rognum, Rolf I Skotheim, Espen Thiis-Evensen, and Ragnhild A Lothe. **Gene methylation profiles of normal mucosa, and benign and malignant colorectal tumors identify early onset markers.** *Molecular cancer*, **7**:94, January 2008. 62

[117] R Soong, N Shah, B K Peh, P Y Chong, S S Ng, N Zeps, D Joseph, M Salto-Tellez, B Iacopetta, and Y Ito. **The expression of RUNX3 in colorectal cancer is associated with disease stage and patient outcome.** *British journal of cancer*, **100**(5):676–9, March 2009. 62

[118] Manish M Subramaniam, Jason Y Chan, Richie Soong, Kosei Ito, Khay G Yeoh, Reuben Wong, Thomas Guenther, Olivia Will, Chee L Chen, Marian P Kumarasinghe, Yoshiaki Ito, and Manuel Salto-Tellez. **RUNX3 inactivation in colorectal polyps arising through different pathways of colonic carcinogenesis.** *The American journal of gastroenterology*, **104**(2):426–36, February 2009. 62

[119] Kosei Ito, Anthony Chee-Beng Lim, Manuel Salto-Tellez, Lena Motoda, Motomi Osato, Linda Shyue Huey Chuang, Cecilia Wei Lin Lee, Dominic Chih-Cheng Voon, Jason Kin Wai Koo, Huajing Wang, Hiroshi Fukamachi, and Yoshiaki Ito. **RUNX3 attenuates beta-catenin/T cell factors in intestinal tumorigenesis.** *Cancer cell*, **14**(3):226–37, September 2008. 62

[120] Cecilia Wei Lin Lee, Kosei Ito, and Yoshiaki Ito. **Role of RUNX3 in bone morphogenetic protein signaling in colorectal cancer**. *Cancer Res*, **70**(10):4243–52, May 2010. 62

[121] Martha L Slattery, Abbie Lundgreen, Jennifer S Herrick, Roger K Wolff, and Bette J Caan. **Genetic variation in the transforming growth factor-beta signaling pathway and survival after diagnosis with colon and rectal cancer.** *Cancer*, **117**(18):4175–83, September 2011. 62, 63

[122] Y M Fleming, G J Ferguson, L C Spender, J Larsson, S Karlsson, B W Ozanne, R Grosse, and G J Inman. **TGF-beta-mediated activation of RhoA signalling is required for efficient (V12)HaRas and (V600E)BRAF transformation.** *Oncogene*, **28**(7):983–93, February 2009. 63

[123] Xabier Garcia-Albeniz, Carles Pericay, Virginia Alonso-Espinaco, Vicente Alonso, Pilar Escudero, Carlos Fernández-Martos, Rosa Gallego, Pere Gascón, Sergi Castellví-Bel, and Joan Maurel. **Serum matrilysin correlates with poor survival independently of KRAS and BRAF status in refractory advanced colorectal cancer patients treated with irinotecan plus cetuximab.** *Tumour Biol*, **32**(2):417–424, Apr 2011. 63

[124] Timothy J Price, Jennifer E Hardingham, Chee K Lee, Andrew Weickhardt, Amanda R Townsend, Joseph W Wrin, Ann Chua, Aravind Shivasami, Michelle M Cummins, Carmel Murone, and Niall C Tebbutt. **Impact of KRAS and BRAF Gene Mutation Status on Outcomes From the Phase III AGITG MAX Trial of Capecitabine Alone or in Combination With Bevacizumab and Mitomycin in Advanced Colorectal Cancer**. *J Clin Oncol*, Jun 2011. 63

[125] Jeanne Tie, Lara Lipton, Jayesh Desai, Peter Gibbs, Robert N. Jorissen, Michael Christie, Katharine J. Drummond, Benjamin N J. Thomson, Valery Usatoff, Peter M. Evans, Adrian W. Pick, Simon Knight, Peter W G. Carne, Roger Berry, Adrian Polglase, Paul McMurrick, Qi Zhao, Dana Busam, Robert L. Strausberg, Enric Domingo, Ian P M. Tomlinson, Rachel Midgley, David Kerr, and Oliver M. Sieber. **KRAS mutation is associated with lung metastasis in patients with curatively resected colorectal cancer.** *Clin Cancer Res*, **17**(5):1122–1130, Mar 2011. 63

[126] Paloma Bragado, Yeriel Estrada, Falguni Parikh, Sarah Krause, Carla Capobianco, Hernan G. Farina, Denis M. Schewe, and Julio A. Aguirre-Ghiso. **TGF-β2 dictates disseminated tumour cell fate in target organs through TGF-β-RIII and p38α/β signalling.** *Nat Cell Biol*, **15**(11):1351–1361, Nov 2013. 63, 64

[127] Dieter Hölzel, Renate Eckel, Rebecca T. Emeny, and Jutta Engel. **Distant metastases do not metastasize.** *Cancer Metastasis Rev*, **29**(4):737–750, Dec 2010. 64

[128] S. Malakouti, F. K. Asadi, S. C. Kukreja, H. A. Abcarian, and J. R. Cintron. **Parathyroid hormone-related protein expression in the human colon: immunohistochemical evaluation.** *Am Surg*, **62**(7):540–4; discussion 544–5, Jul 1996. 64

[129] Wolfgang E. Gallwitz, Theresa A. Guise, and Gregory R. Mundy. **Guanosine nucleotides inhibit different syndromes of PTHrP excess caused by human cancers in vivo.** *J Clin Invest*, **110**(10):1559–1572, Nov 2002. 64

[130] Yuki Takayama, Taisuke Mori, Takeshi Nomura, Takahiko Shibahara, and Michiie Sakamoto. **Parathyroid-related protein plays a critical role in bone invasion by oral squamous cell carcinoma.** *Int J Oncol*, **36**(6):1387–1394, Jun 2010. 64

[131] T. A. Guise. **Molecular mechanisms of osteolytic bone metastases.** *Cancer*, **88**(12 Suppl):2892–2898, Jun 2000. 64

[132] Aya Kobayashi, Hiroshi Okuda, Fei Xing, Puspa R. Pandey, Misako Watabe, Shigeru Hirota, Sudha K. Pai, Wen Liu, Koji Fukuda, Christopher Chambers, Andrew Wilber, and Kounosuke Watabe. **Bone morphogenetic protein 7 in dormancy and metastasis of prostate cancer stem-like cells in bone.** *J Exp Med*, **208**(13):2641–2655, Dec 2011. 64